Published for SISSA by Springer

Received: March 23, 2021
Accepted: July 6, 2021
Published: July 22, 2021

Search for supersymmetry in events with four or more charged leptons in 139 fb^{-1} of $\sqrt{s} = 13$ TeV pp collisions with the ATLAS detector

The ATLAS collaboration

E-mail: atlas.publications@cern.ch

Abstract: A search for supersymmetry in events with four or more charged leptons (electrons, muons and τ-leptons) is presented. The analysis uses a data sample corresponding to 139 fb^{-1} of proton-proton collisions delivered by the Large Hadron Collider at $\sqrt{s} = 13$ TeV and recorded by the ATLAS detector. Four-lepton signal regions with up to two hadronically decaying τ-leptons are designed to target several supersymmetric models, while a general five-lepton signal region targets any new physics phenomena leading to a final state with five charged leptons. Data yields are consistent with Standard Model expectations and results are used to set upper limits on contributions from processes beyond the Standard Model. Exclusion limits are set at the 95% confidence level in simplified models of general gauge-mediated supersymmetry, excluding higgsino masses up to 540 GeV. In R-parity-violating simplified models with decays of the lightest supersymmetric particle to charged leptons, lower limits of 1.6 TeV, 1.2 TeV, and 2.5 TeV are placed on wino, slepton and gluino masses, respectively.

Keywords: Hadron-Hadron scattering (experiments), Supersymmetry, Beyond Standard Model

ArXiv ePrint: 2103.11684

https://doi.org/10.1007/JHEP07(2021)167

Contents

JHEP07(2021)167

1 Introduction

Standard Model (SM) processes rarely produce events with four or more charged leptons, while many new theories, such as supersymmetry (SUSY) [1–6], predict events which would regularly decay to these multilepton final states. This paper presents a search for new phenomena in final states with at least four isolated, charged leptons (electrons, muons or τ-leptons) where up to two hadronically decaying τ-leptons are considered. Here, electrons and muons are referred to as 'light leptons' and include those from leptonic τ decays. The full proton-proton dataset delivered by the LHC and collected by the ATLAS experiment during the 2015–2018 data-taking period is used in the analysis, corresponding to an integrated luminosity of 139 fb^{-1} [7] at a centre-of-mass energy of 13 TeV. Several SUSY signal models are used to optimise the search, but the search itself is generally model-agnostic,

using selections on either the presence of, or absence of, Z bosons in the event, and loose requirements on either the effective mass or the missing transverse momentum. Results are presented in terms of limits on SUSY models.

Previous searches for SUSY particles using signatures with three or more leptons were carried out at the Tevatron collider [8–13], and at the LHC by the ATLAS experiment [14–19] and the CMS experiment [20–25]. Searching for new physics using a four or more lepton final state may offer more sensitivity to some beyond the SM scenarios than using lower lepton multiplicities, as the very low SM background can allow for a looser selection and a more inclusive approach to be adopted. This analysis closely follows the ATLAS analyses on the datasets at 7 TeV [14] and 8 TeV [17], and on the partial dataset at 13 TeV [18]. Previous results are extended here by analysing the full ATLAS 13 TeV dataset, expanding the search with an additional channel selecting at least five leptons, and using data to constrain major sources of SM background.

2 Targeted models

SUSY is a space-time symmetry that postulates the existence of a new superpartner for every SM particle, with spin differing by one half-unit from its SM partner: each SM fermion (boson) is associated with a SUSY boson (fermion). The new SUSY particles (sparticles) would have the same quantum numbers as their SM counterparts except for spin and provide a potential solution to the hierarchy problem [26–29]. The scalar superpartners of the SM fermions are the charged sleptons, $\tilde{\ell}$, the sneutrinos, $\tilde{\nu}$, and the squarks, $\tilde{q}$, while the gluons have fermionic superpartners called gluinos ($\tilde{g}$). The bino, wino and higgsino fields are fermionic superpartners of the $\mathrm{SU}(2) \times \mathrm{U}(1)$ gauge fields of the SM, and the two complex scalar doublets of a minimally extended Higgs sector, respectively. They mix to give mass eigenstates that are referred to as charginos $\tilde{\chi}_i^{\pm}$ $(i = 1, 2)$ and neutralinos $\tilde{\chi}_j^0$ $(j = 1, 2, 3, 4)$, numbered in order of increasing mass.

SUSY processes can result in proton decay at a rate that is in conflict with the stringent experimental constraints on the proton lifetime if they do not conserve both lepton number (L) and baryon number (B) [30]. This conflict can be avoided by imposing the conservation of R-parity [31], defined as $(-1)^{3(B-L)+2S}$, where S is spin, or by explicitly conserving either B or L in R-parity-violating (RPV) scenarios [32, 33]. In R-parity-conserving (RPC) models, the lightest SUSY particle (LSP) is stable and a viable dark-matter candidate [34, 35], and leptons can originate from unstable weakly interacting sparticles decaying to the LSP. In RPV models, the LSP is unstable and decays into SM particles, including charged leptons and neutrinos when violating L but not B. Both the RPC and RPV SUSY scenarios can therefore result in signatures with high lepton multiplicities and substantial missing transverse momentum, selections on which can be used to suppress SM background processes effectively.

RPC and RPV SUSY models are used for signal region optimisation and to interpret the results of this analysis; each requires a different approach for signal selection, as discussed in section 5. In all SUSY scenarios considered here, the light CP-even Higgs boson, h, of the minimal supersymmetric extension of the SM [36, 37] Higgs sector is assumed

JHEP07(2021)167

to be practically identical to the SM Higgs boson [38], with mass and couplings compatible with the LHC measurements [39–42]. In addition, the decoupling limit is used, which is defined by $m_A \gg m_Z$, while the CP-odd (A), the neutral CP-even (H), and the two charged ($H^{\pm}$) Higgs bosons are considered to be very heavy and thus considerably beyond the kinematic reach of the LHC.

2.1 RPC SUSY scenarios

Naturalness [43, 44] motivates light higgsino states ($\tilde{\chi}_1^0$, $\tilde{\chi}_2^0$ and $\tilde{\chi}_1^{\pm}$); however, searching for higgsinos can be experimentally challenging. The sparticles in the higgsino system are close in mass, thus decays of the $\tilde{\chi}_2^0/\tilde{\chi}_1^{\pm}$ to a $\tilde{\chi}_1^0$ LSP result in low-momentum decay products that are difficult to reconstruct efficiently. The LEP experiments searched for higgsino $\tilde{\chi}_1^{\pm}$ in approximately mass-degenerate scenarios and excluded chargino masses below 103.5 GeV (reduced to 92 GeV for small chargino-LSP mass differences between 0.1 GeV and 3 GeV) [45, 46]. More recently, the ATLAS and CMS experiments have searched for higgsino production [47, 48], excluding higgsino $\tilde{\chi}_2^0$ up to masses of ∼240 GeV and down to $\tilde{\chi}_2^0$-LSP mass differences of 1.5 GeV.

General gauge-mediated (GGM) SUSY models [49] offer an opportunity to study light higgsinos without relying on the reconstruction of experimentally challenging, low-momentum final states. In the Planck-scale-mediated SUSY breaking scenario, the gravitino $\tilde{G}$ is the fermionic superpartner of the graviton and its mass is comparable to the masses of the other SUSY particles, $m \sim 100$ GeV [50, 51]. In contrast, GGM models predict that the $\tilde{G}$ is nearly massless and can be produced at the LHC via the decays of the higgsinos, e.g. $\tilde{\chi}_1^0 \to Z/h + \tilde{G}$. The leptonic decays of the Z/h from the two $\tilde{\chi}_1^0$ decays can be reconstructed and are targeted in this analysis, giving an opportunity to study four-lepton signatures with one or more Z boson candidates.

Simplified RPC SUSY models [52–54] inspired by GGM are considered here, where an almost mass-degenerate higgsino system $\tilde{\chi}_1^{\pm}$, $\tilde{\chi}_1^0$, $\tilde{\chi}_2^0$ and an LSP $\tilde{G}$ with mass 1 MeV are the only SUSY particles within the reach of the LHC. The $\tilde{\chi}_1^{\pm}$ and $\tilde{\chi}_2^0$ masses are set to 1 GeV above the $\tilde{\chi}_1^0$ mass to ensure they decay promptly, and because they have only a weak coupling to the $\tilde{G}$, the $\tilde{\chi}_1^{\pm}$ and $\tilde{\chi}_2^0$ always decay to the $\tilde{\chi}_1^0$ via virtual Z/W bosons. The virtual Z/W in turn decay to very soft final states that are not reconstructed, while the $\tilde{\chi}_1^0$ decays promptly to a gravitino plus a Z or h boson, $\tilde{\chi}_1^0 \to Z/h + \tilde{G}$. A higgsino system offers four production processes at the LHC: $\tilde{\chi}_1^+\tilde{\chi}_1^-$, $\tilde{\chi}_1^{\pm}\tilde{\chi}_1^0$, $\tilde{\chi}_1^{\pm}\tilde{\chi}_2^0$ and $\tilde{\chi}_1^0\tilde{\chi}_2^0$, all of which are considered in these GGM models, as shown in figure 1. The $\tilde{\chi}_1^0$ mass and $\tilde{\chi}_1^0 \to Z\tilde{G}$ branching ratio are the two free parameters of the simplified GGM higgsino scenarios.

2.2 RPV SUSY scenarios

In generic SUSY models with minimal particle content, the superpotential includes terms that violate conservation of L and B:

$$\frac{1}{2}\lambda_{ijk}L_iL_j\bar{E}_k + \lambda'_{ijk}L_iQ_j\bar{D}_k + \frac{1}{2}\lambda''_{ijk}\bar{U}_i\bar{D}_j\bar{D}_k + \kappa_iL_iH_2,$$

where L_i and Q_i indicate the lepton and quark SU(2)-doublet superfields, respectively, and $\bar{E}_i$, $\bar{U}_i$ and $\bar{D}_i$ are the corresponding singlet superfields. Quark and lepton generations are

JHEP07(2021)167

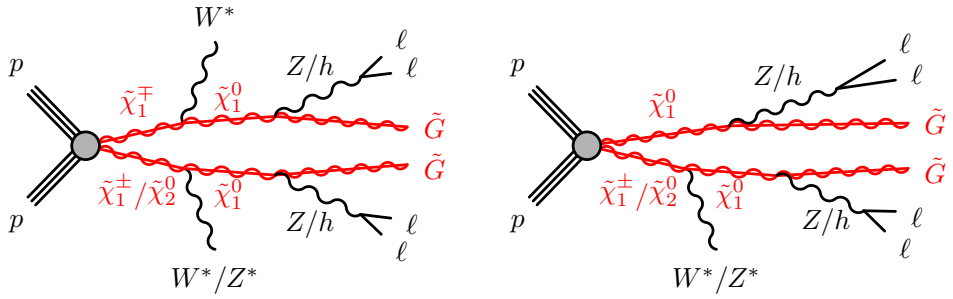

Figure 1. Diagrams of the processes in the SUSY RPC GGM higgsino models. The W^*/Z^* produced in the $\tilde{\chi}_1^{\pm}/\tilde{\chi}_2^0$ decays are off-shell ($m \sim 1\,\text{GeV}$) and their decay products are usually not reconstructed. The Higgs boson may decay into leptons and possible additional products via intermediate $\tau\tau$, WW or ZZ states.

referred to by the indices i, j and k, while the Higgs field that couples to up-type quarks is represented by the Higgs SU(2)-doublet superfield H_2. The λ, λ' and λ'' parameters are three sets of new Yukawa couplings, while the κ_i parameters have dimensions of mass.

Simplified models of RPV SUSY scenarios are considered here, with a bino neutralino ($\tilde{\chi}_1^0$) LSP which decays via an RPV interaction. The lepton-number-violating superpotential term $\frac{1}{2}\lambda_{ijk}L_iL_j\bar{E}_k$ mediates the LSP decay into two charged leptons and a neutrino,

$$\tilde{\chi}_1^0 \to \ell_k^{\pm}\ell_{i/j}^{\mp}\nu_{j/i}, \tag{2.1}$$

through a virtual slepton or sneutrino, with the allowed lepton flavours depending on the indices of the associated λ_{ijk} couplings [55]. The complex conjugate of the decay in eq. (2.1) is also allowed. Thus, when two $\tilde{\chi}_1^0$ are present in a signal process, every signal event contains a minimum of four charged leptons and two neutrinos, giving an opportunity to study four-lepton SUSY signatures.

In principle, the nine[1] λ_{ijk} RPV couplings allow the $\tilde{\chi}_1^0$ to decay to every possible combination of charged-lepton pairs, where the branching ratio for each combination differs for each λ_{ijk}. For example, for $\lambda_{121} \neq 0$ the branching ratios for $\tilde{\chi}_1^0 \to e\mu\nu$, $\tilde{\chi}_1^0 \to ee\nu$ and $\tilde{\chi}_1^0 \to \mu\mu\nu$ are 50%, 50% and 0% respectively, whereas for $\lambda_{122} \neq 0$ the corresponding branching ratios are 50%, 0% and 50%. It was shown in ref. [17] that the four-charged-lepton search sensitivity is comparable in the cases of $\lambda_{121} \neq 0$ or $\lambda_{122} \neq 0$, and for $\lambda_{133} \neq 0$ or $\lambda_{233} \neq 0$. Since the analysis reported here uses similar techniques for these cases, the number of L-violating RPV scenarios studied is reduced by making no distinction between the electron and muon decay modes of the $\tilde{\chi}_1^0$. Two extremes of the λ_{ijk} RPV couplings are considered:

- $LL\bar{E}12k$ ($k \in 1, 2$) scenarios, where $\lambda_{12k} \neq 0$ and only decays to electrons and muons are included,
- $LL\bar{E}i33$ ($i \in 1, 2$) scenarios, where $\lambda_{i33} \neq 0$ and only decays to τ-leptons and either electrons or muons are included,

[1]The 27 λ_{ijk} RPV couplings are reduced to 9 by the antisymmetry requirement $\lambda_{ijk} = -\lambda_{jik}$ and the $i \neq j$ requirement for the generation of the L terms in the superpotential.

JHEP07(2021)167

Scenario	$\tilde{\chi}_1^0$ branching ratios					
	$e^+e^-\nu$	$e^\pm\mu^\mp\nu$	$\mu^+\mu^-\nu$	$e^\pm\tau^\mp\nu$	$\tau^+\tau^-\nu$	$\mu^\pm\tau^\mp\nu$
$LL\bar{E}12k$	1/4	1/2	1/4	0	0	0
$LL\bar{E}i33$	0	0	0	1/4	1/2	1/4

Table 1. Decay modes and branching ratios for the $\tilde{\chi}_1^0$ LSP in the RPV models, where ν denotes neutrinos or antineutrinos of any lepton generation.

with all other RPV couplings assumed to be zero. The branching ratios for the $\tilde{\chi}_1^0$ decay in the $LL\bar{E}12k$ and $LL\bar{E}i33$ scenarios are shown in Table 1. The sensitivity to $\lambda_{ijk} \neq 0$ couplings not considered here (e.g. $\lambda_{123} \neq 0$) is expected to be between that achieved in the $LL\bar{E}12k$ and $LL\bar{E}i33$ scenarios.

Pure-bino $\tilde{\chi}_1^0\tilde{\chi}_1^0$ production has a vanishingly small cross-section at the LHC, thus models that include one or more next-to-lightest SUSY particles (NLSP) are considered in order to obtain a reasonably large cross-section. The choice of NLSP in the RPV SUSY scenarios determines the production cross-section, and can impact the signal acceptance to a lesser extent as intermediate decay products may also decay to leptons. In all cases considered here, the NLSP is pair-produced in an RPC interaction and decays to the $\tilde{\chi}_1^0$ LSP (which itself undergoes an RPV decay). Three different possibilities are considered for the NLSP in the $LL\bar{E}12k$ and $LL\bar{E}i33$ scenarios:

- **wino NLSP**: mass-degenerate wino charginos and neutralinos are produced in association ($\tilde{\chi}_1^+\tilde{\chi}_1^-$ or $\tilde{\chi}_1^\pm\tilde{\chi}_2^0$). The charginos decay via $\tilde{\chi}_1^\pm \to W^{(*)}\tilde{\chi}_1^0$ with 100% branching fraction, while the neutralinos decay via $\tilde{\chi}_2^0 \to Z^{(*)}\tilde{\chi}_1^0$ or $h\tilde{\chi}_1^0$ with 50% branching fraction each, as shown in figure 2a.

- **$\tilde{\ell}_L/\tilde{\nu}$ NLSP**: mass-degenerate sleptons and sneutrinos of all three generations are produced in association ($\tilde{\ell}_L\tilde{\ell}_L$, $\tilde{\nu}\tilde{\nu}$, $\tilde{\ell}_L\tilde{\nu}$, where the subscript L refers to the chirality of the partner lepton). The sleptons decay via $\tilde{\ell}_L \to \ell\tilde{\chi}_1^0$ and sneutrinos decay via $\tilde{\nu} \to \nu\tilde{\chi}_1^0$, both with 100% branching fraction, as seen in figure 2b.

- **$\tilde{g}$ NLSP**: gluino pair-production, where the gluino decays with 100% branching fraction via $\tilde{g} \to q\bar{q}\tilde{\chi}_1^0$ ($q = u, d, s, c, b$ only, with equal branching fractions), as seen in figure 2c. Decays to top quarks are not considered here, as this would introduce a significant change in signature for scenarios with mass difference $m(\tilde{g}) - m(\tilde{\chi}_1^0)$ above and below $\sim 350\,\text{GeV}$.

For the RPV models, the LSP mass is restricted to the range $10\,\text{GeV} \leq m(\text{LSP}) \leq m(\text{NLSP}) - 10\,\text{GeV}$ to ensure that both the RPC cascade decay and the RPV LSP decay are prompt. Non-prompt decays of the $\tilde{\chi}_1^0$ in similar models were previously studied in refs. [56, 57].

JHEP07(2021)167

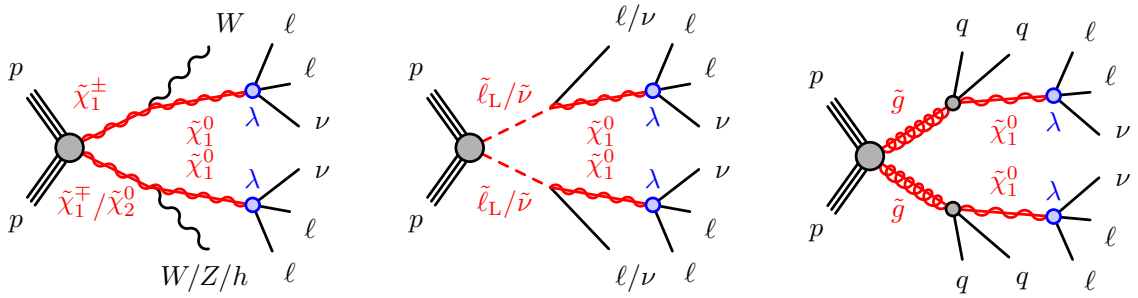

(a) wino NLSP. **(b)** $\tilde{\ell}_L/\tilde{\nu}$ NLSP. **(c)** $\tilde{g}$ NLSP.

Figure 2. Diagrams of the benchmark SUSY models of RPC NLSP pair production of a (a) wino, (b) slepton/sneutrino and (c) gluino, followed by the RPV decay of the $\tilde{\chi}_1^0$ LSP. The LSP is assumed to decay as $\tilde{\chi}_1^0 \to \ell\ell\nu$ with 100% branching ratio.

3 ATLAS detector

The ATLAS experiment [58–60] at the LHC is a multipurpose particle detector with a forward-backward symmetric cylindrical geometry and a near 4π coverage in solid angle.[2] It consists of an inner tracking detector (ID) surrounded by a thin superconducting solenoid providing a 2 T axial magnetic field, electromagnetic and hadron calorimeters, and a muon spectrometer (MS). The ID covers the pseudorapidity range $|\eta| < 2.5$. It consists of silicon pixel, silicon microstrip, and transition radiation tracking detectors. Lead/liquid-argon (LAr) sampling calorimeters provide electromagnetic (EM) energy measurements with high granularity. Hadronic calorimetry is provided by the steel/scintillator-tile calorimeter, which covers the central pseudorapidity range ($|\eta| < 1.7$). The endcap and forward regions are instrumented with LAr calorimeters for EM and hadronic energy measurements up to $|\eta| = 4.9$. The MS surrounds the calorimeters and is based on three large air-core toroidal superconducting magnets with eight coils each. The field integral of the toroids ranges between 2.0 and 6.0 T m across most of the detector. The MS includes a system of precision tracking chambers covering the region $|\eta| < 2.7$ and fast detectors for triggering. A two-level trigger system is used to select events. The first-level trigger is implemented in hardware and uses a subset of the detector information to accept events at a rate below 100 kHz. This is followed by a software-based trigger that reduces the accepted event rate to 1 kHz on average, depending on the data-taking conditions.

4 Data and simulated event samples

This analysis uses the full $\sqrt{s} = 13$ TeV pp dataset collected by the ATLAS experiment during the 2015–2018 data-taking period. The average number of multiple pp collisions

[2] ATLAS uses a right-handed coordinate system with its origin at the nominal interaction point (IP) in the centre of the detector and the z-axis along the beam pipe. The x-axis points from the IP to the centre of the LHC ring, and the y-axis points upwards. Cylindrical coordinates (r, ϕ) are used in the transverse plane, ϕ being the azimuthal angle around the z-axis. The pseudorapidity is defined in terms of the polar angle θ as $\eta = -\ln\tan(\theta/2)$. Angular distance is measured in units of $\Delta R \equiv \sqrt{(\Delta\eta)^2 + (\Delta\phi)^2}$.

JHEP07(2021)167

Trigger	Offline p_{T} threshold [GeV]		
	2015	2016	2017–2018
Single e (isolated)	25	27	27
Single e	61	61	61
Single μ (isolated)	21	25 or 27	27
Single μ	41	41 or 51	51
Double e	13, 13	18, 18	(18, 18) or (25, 25)
Double μ (symmetric)	11, 11	(11, 11) or (15, 15)	15, 15
(asymmetric)	19, 9	(21, 9) or (23, 9)	23, 9
Double $e\mu$	8(e), 25(μ)	8(e), 25(μ)	8(e), 25(μ)
	18(e), 15(μ)	18(e), 15(μ)	18(e), 15(μ)
		27(e), 9(μ)	27(e), 9(μ)
Triple $e\mu\mu$, $ee\mu$		13(e), 11(2μ)	13(e), 11(2μ)
		13(2e), 11(μ)	13(2e), 11(μ)

Table 2. The triggers used in the analysis of 2015–2018 data. The offline p_{T} thresholds are required only for reconstructed charged leptons responsible for triggering the event. Trigger thresholds increase across the years due to the increase in beam luminosity, and "or" denotes a move to a higher-threshold trigger during data-taking.

in the same or nearby bunch crossings (pile-up) increased from 14 in 2015 to $\sim$ 38 in 2018. After the application of beam, detector and data-quality requirements [61], the total integrated luminosity considered in this analysis corresponds to 139.0 ± 2.4 fb^{-1} [7]. Events recorded during stable data-taking conditions are used in the analysis if the reconstructed primary vertex has at least two tracks with transverse momentum $p_{\mathrm{T}} > 500$ MeV associated with it. The primary vertex of an event is identified as the vertex with the highest Σp_{T}^2 of associated tracks.

Events are selected using the single-lepton, dilepton, or trilepton triggers [62, 63] listed in table 2, where the trigger efficiencies are in the plateau region above the offline p_{T} thresholds. Dilepton (trilepton) triggers are used only when the leptons in the event fail p_{T}-threshold requirements for the single-lepton (single-lepton and dilepton) triggers. The trigger efficiency for events with four (three) electrons/muons in signal SUSY scenarios is typically >99% (>96%). For signal SUSY events with only two light leptons, the trigger efficiency is typically > 95% for events with at least one electron and decreases to $\sim$ 90% for events with only two muons.

Monte Carlo (MC) generators were used to simulate SM processes and new physics signals. The SM processes considered are those that can lead to signatures with at least four reconstructed charged leptons. Details of the signal and background MC simulation samples used in this analysis, as well as the order of the cross-section calculations in perturbative quantum chromodynamics used for yield normalisation, are shown in table 3.

The SUSY signal processes were generated from leading-order (LO) matrix elements with up to two extra partons. Jet-parton matching followed the CKKW-L prescription [64],

JHEP07(2021)167

with a matching scale set to one quarter of the mass of the pair-produced SUSY particles. Signal cross-sections were calculated to next-to-leading order in the strong coupling constant, adding the resummation of soft gluon emission at next-to-leading-logarithm accuracy (NLO+NLL) [65–72]. The nominal signal cross-section and its uncertainty were taken from an envelope of cross-section predictions using different parton distribution function (PDF) sets and factorisation and renormalisation scales, as described in ref. [73].

The dominant irreducible background processes that can produce four prompt and isolated charged leptons are ZZ, $t\bar{t}Z$, VVV and Higgs production (where $V = W$, Z, and includes off-shell Z/γ contributions). For simulated ZZ production, the matrix elements contain all diagrams with four electroweak vertices, and they were calculated for up to one extra parton at NLO, and up to three extra partons at LO. The production of top quark pairs with an additional Z boson was simulated with matrix elements calculated at NLO precision. Simulated triboson (VVV) production includes the processes ZZZ, WZZ and WWZ with four to six charged leptons, and was generated at NLO with additional LO matrix elements for up to two extra partons. The simulation of Higgs processes includes Higgs production via gluon-gluon fusion (ggF) and vector-boson fusion (VBF), and associated production with a boson (WH, ZH) or a top-antitop pair ($t\bar{t}H$). Other irreducible background processes with small cross-sections are grouped into a category labelled 'Other', which contains the tWZ, $t\bar{t}WW$, $t\bar{t}ZZ$, $t\bar{t}WZ$, $t\bar{t}WH$, $t\bar{t}HH$, $t\bar{t}tW$ and $t\bar{t}t\bar{t}$ processes.

Top quark pair production and Z+jets are the dominant SM processes that may produce one or more non-prompt or misidentified leptons among the four charged leptons. Processes such as W+jets, WW, WZ, and $t\bar{t}W$ also contribute to a four or more charged lepton signature, but at very small rates either due to a small production cross-section, or they require a higher multiplicity of non-prompt or misidentified leptons. MC simulation of these processes is used as part of the estimation of the reducible background, as described in section 7.2. Further information about the MC simulations of the reducible backgrounds can be found in refs. [74, 75].

For all MC simulation samples, the propagation of particles through the ATLAS detector was modelled with Geant4 [76] using the full ATLAS detector simulation [77], except for the SUSY signal samples, which use a fast simulation based on a parameterisation of the response of the electromagnetic and hadronic calorimeters [78] and full simulation elsewhere. The effect of pile-up is incorporated into the simulation by overlaying additional inelastic pp events onto hard-scatter events. These were generated with Pythia 8 [79] with a set of tuned parameters called the A3 tune [80] and the MSTW2008LO PDF set [81]. Simulated events are reconstructed in the same manner as data, and are weighted to match the distribution of the expected mean number of interactions per bunch crossing in data. The simulated MC samples are corrected to account for differences from the data in the triggering efficiencies, lepton reconstruction efficiencies, b-quark jet identification efficiencies, and the energy and momentum measurements of leptons and jets.

JHEP07(2021)167

Process	Generator(s)	Cross-section calculation	Tune	PDF set
ZZ, WZ, WW	Sherpa 2.2.2 [82]	NLO [83]	Sherpa default	NNPDF30NNLO [84]
VVV	Sherpa 2.2.1	NLO [83]	Sherpa default	NNPDF30NNLO
H via ggF, VBF, VH	Powheg-Box v2 [85–87] + Pythia 8.212 [79]	NNNLO+NNLL [88–94]	AZNLO [95]	CTEQ6L1 [96]
$t\bar{t}H$	Powheg-Box v2 + Pythia 8.230	NLO [88]	A14 [97]	NNPDF23LO [98]
$t\bar{t}Z$, $t\bar{t}W$	MadGraph5_aMC@NLO 2.3.3 [99] + Pythia 8.210	NLO [100]	A14	NNPDF23LO
$t\bar{t}WW$	MadGraph5_aMC@NLO 2.2.2 + Pythia 8.186	NLO [100]	A14	NNPDF23LO
$t\bar{t}WZ$, tWZ	MadGraph5_aMC@NLO 2.3.3 + Pythia 8.212	NLO [100]	A14	NNPDF23LO
$t\bar{t}ZZ$, $t\bar{t}WZ$, $t\bar{t}WH$, $t\bar{t}HH$	MadGraph5_aMC@NLO 2.6.7 + Pythia 8.240	NLO [100]	A14	NNPDF23LO
$t\bar{t}tW$, $t\bar{t}t\bar{t}$	MadGraph5_aMC@NLO 2.2.2 + Pythia 8.186	NLO [99]	A14	NNPDF23LO
$t\bar{t}$	Powheg-Box v2 + Pythia 8.230	NNLO+NNLL [101–107]	A14	NNPDF23LO
Z+jets, W+jets	Powheg-Box v1 + Pythia 8.186	NNLO [108]	AZNLO	CTEQ6L1
SUSY signal	MadGraph5_aMC@NLO 2.2.2 + Pythia 8.230	NLO+NLL [65–72]	A14	NNPDF23LO

Table 3. Summary of the simulated SM background and signal samples used in this analysis, where $V = W, Z$, and includes off-shell contributions. "Tune" refers to the set of parameter values used by the generator.

5 Event reconstruction

This analysis uses reconstructed electrons, muons, τ-leptons, and jets, which are classified as 'preselected' or 'signal' using various kinematic and quality criteria. Preselected objects must satisfy a loose set of criteria and pass the overlap removal procedure, which resolves ambiguities among reconstructed objects. Signal leptons are those preselected leptons that satisfy a more stringent set of criteria; those failing the signal lepton requirements are used as part of the background estimation in section 7.2. The p_{T} thresholds for leptons are nominally low; however, p_{T} thresholds are higher for the one, two, or three leptons responsible for triggering the event via the single-lepton, dilepton, or trilepton triggers listed in table 2.

The missing transverse momentum, $E_{\mathrm{T}}^{\mathrm{miss}}$, is the magnitude of the negative vector sum of the transverse momenta of all preselected objects (electrons, photons, muons, and jets, including all jets with $|\eta| < 4.5$) and an additional soft term [109]. Hadronically decaying τ-leptons are included in the $E_{\mathrm{T}}^{\mathrm{miss}}$ as jets. The soft term is constructed from the tracks matched to the primary vertex, but not associated with identified physics objects. By using tracks, it cannot account for the neutral component of calorimeter energy deposits; however, this allows the soft term to be nearly independent of pile-up [110].

Preselected electrons are reconstructed using calibrated clusters of energy deposits in the electromagnetic calorimeter that are matched to a track in the ID, and must have $p_{\mathrm{T}} > 4.5\,\mathrm{GeV}$ and $|\eta| < 2.47$. They must also satisfy the tracking- and calorimeter-based 'loose and B-layer' criteria of the likelihood-based identification algorithm [111]. Preselected muons are reconstructed by combining tracks in the ID with tracks in the MS, and must have $p_{\mathrm{T}} > 3\,\mathrm{GeV}$ and $|\eta| < 2.7$. They must also satisfy 'medium' identification requirements [112], which are based on the number of hits in the different ID and MS subsystems, and on the significance of the charge-to-momentum ratio. The cosmic-ray muon background is suppressed by rejecting events containing one or more muons that have a transverse impact parameter $|d_0| > 0.2\,\mathrm{mm}$, or a longitudinal impact parameter $|z_0| > 1\,\mathrm{mm}$, both relative to the primary vertex. Preselected electrons and muons must point back to the primary vertex, with $|z_0 \sin\theta|$ required to be less than 0.5 mm.

JHEP07(2021)167

Jets are reconstructed from three-dimensional calorimeter energy clusters using the anti-k_t algorithm [113] with a radius parameter of $R = 0.4$. The jets are calibrated following ref. [114] and must have $p_{\mathrm{T}} > 20\,\mathrm{GeV}$ and $|\eta| < 2.8$. Events with large calorimeter noise or non-collision backgrounds are suppressed by rejecting events with jets that fail to satisfy the quality criteria described in ref. [115]. A multivariate technique based on quantities related to reconstructed secondary vertices is used to identify jets with $|\eta| < 2.5$ that originate from b-quarks (referred to as 'b-tagging'). The b-tagging algorithm [116] used here correctly identifies b-quark jets in simulated $t\bar{t}$ samples with an efficiency of 85% and a rejection factor of 25 for light-flavour jets.

Leptonically decaying τ-leptons are reconstructed as electrons and muons as described above. Hadronically decaying τ-leptons are denoted by τ_{had}, and their visible decay products are reconstructed as jets, as described above, with $p_{\mathrm{T}} > 10\,\mathrm{GeV}$ and $|\eta| < 2.47$. In this analysis, kinematic variables built with τ_{had} candidates use only their visible decay products. The τ_{had} reconstruction algorithm [117] uses the electromagnetic and hadronic shower shapes in the calorimeters, as well as information about the tracks within $\Delta R = 0.2$ of the jet direction. Since τ-leptons mostly decay into either one or three charged hadrons together with a neutrino (and often additional neutral hadrons), τ_{had} candidates are required to have one or three associated tracks, referred to as 'prongs'. The preselected τ_{had} candidates must have $p_{\mathrm{T}} > 20\,\mathrm{GeV}$, $|\eta| < 1.37$ or $1.52 < |\eta| < 2.47$, total charge of their constituent tracks equal to ± 1, and the τ_{had} energy scale is corrected using an η- and p_{T}-dependent calibration. A recurrent neural network (RNN) uses discriminating track and cluster variables to optimise τ_{had} identification, where 'loose', 'medium' and 'tight' working points are defined [118]. The RNN-based identification is used to define signal τ_{had} candidates, but not preselected τ_{had} candidates. Transition radiation tracker and calorimeter information is used to suppress electrons misidentified as preselected τ_{had} candidates.

To avoid double counting of identified physics objects, preselected charged leptons and jets must survive an overlap removal procedure, applied in the following order:

1. Any τ_{had} within $\Delta R = 0.2$ of an electron or muon is removed.
2. Any electron sharing an ID track with a muon is removed.
3. Any jet within $\Delta R = 0.2$ of an electron is removed.
4. Any electron within $\Delta R = 0.4$ of a jet is removed (to suppress electrons from semileptonic decays of c- and b-hadrons).
5. Any jet with fewer than three associated tracks is removed either if a muon is within $\Delta R = 0.2$ or if the muon can be matched to a track associated with the jet.
6. Any muon within $\Delta R = 0.4$ of a jet is removed (to suppress muons from semileptonic decays of c- and b-hadrons).
7. Any jet within $\Delta R = 0.4$ of a preselected τ_{had} passing 'medium' RNN-based identification requirements is removed.

To suppress low-mass particle decays, if surviving electrons and muons form an opposite-sign (OS) pair with $m_{\mathrm{OS}} < 4\,\mathrm{GeV}$, or form a same-flavour, opposite-sign (SFOS) pair in the $\Upsilon(1S)$–$\Upsilon(3S)$ mass range $8.4 < m_{\mathrm{SFOS}} < 10.4\,\mathrm{GeV}$, both leptons are discarded. Finally, to suppress leptons from a decay chain with multiple heavy flavour quarks undergoing leptonic decay, e.g. $b \to Wc(\to Ws)$ where $W \to \ell\bar{\nu}$, if two leptons are found within $\Delta R = 0.6$ of one another and one of them has $p_{\mathrm{T}} < 30\,\mathrm{GeV}$, both leptons are discarded.

JHEP07(2021)167

Reconstructed charged leptons may be 'real', defined to be prompt and genuinely isolated leptons (including those from leptonic τ decays), or 'fake/non-prompt', defined to be non-prompt or non-isolated leptons that could originate from semileptonic decays of b- and c-hadrons, from in-flight decays of light mesons, from misidentification of particles within light-flavour or gluon-initiated jets, or from photon conversions. To suppress fake/non-prompt leptons, preselected objects surviving overlap removal are required to satisfy additional identification criteria and are referred to as *signal leptons/jets*. Signal electrons must have $p_{\mathrm{T}} > 7\,\mathrm{GeV}$ and signal muons must have $p_{\mathrm{T}} > 5\,\mathrm{GeV}$. Signal electrons must also satisfy 'medium' likelihood-based identification criteria [111], while signal τ_{had} must satisfy the 'medium' RNN-based identification criteria [118]. Signal electrons and muons must pass p_{T}-dependent isolation requirements imposed to reduce the contributions from semileptonic decays of hadrons and jets misidentified as prompt leptons. The 'Loose' isolation working point is used for electrons and muons, as described in refs. [111] and [112], including updates to improve the performance under conditions with higher pile-up encountered during 2017 and 2018 data-taking. To improve the identification of closely spaced charged leptons (e.g. from boosted decays), contributions to the isolation energy and p_{T} sums from nearby electrons and muons passing all other signal lepton requirements are removed. To further suppress electrons and muons originating from secondary vertices, the transverse impact parameter normalised to its uncertainty must be small, $|d_0|/\sigma_{d_0} < 5\,(3)$ for electrons (muons). To reduce pile-up effects, signal jets with $p_{\mathrm{T}} < 120\,\mathrm{GeV}$ and $|\eta| < 2.5$ must satisfy additional criteria using the 'medium' working point of the jet-vertex-tagging algorithm described in ref. [119].

6 Signal regions

The search strategy for the SUSY scenarios considered here selects events with at least four signal leptons (e, μ, τ_{had}) and the events are classified according to the number of light signal leptons ($L = e, \mu$) and signal τ_{had} (T) required as follows: $4L0T$, with at least four light leptons and no τ_{had} multiplicity requirement; $3L1T$, with exactly three light leptons and at least one τ_{had}; or $2L2T$, with exactly two light leptons and at least two τ_{had}. A general region, $5L0T$, with at least five light leptons and no τ_{had} multiplicity requirement is also considered. The signal region (SR) definitions are summarised in table 4.

To target the RPC GGM scenarios, events with $4L0T$ are selected and these must have two pairs of SFOS leptons that are both consistent with a leptonic Z boson decay. The SFOS pair with mass closer to the Z boson mass is labelled as the first Z candidate, while the other SFOS pair is labelled as the second Z candidate. The first (second) Z candidate must have an invariant mass $m(LL)$ in the range 81.2–101.2 GeV (61.2–101.2 GeV). The peak of the first Z candidate is narrower due to the ordering of the Z candidates, so that widening the low-mass side of the $m(LL)$ window used for the selection of a second Z candidate increases the GGM signal acceptance. GGM scenarios with branching ratio $\mathcal{B}(\tilde{\chi}_1^0 \to \tilde{G}h) > 0$ will have a significant $h \to b\bar{b}$ component, but the four-lepton analysis is not sensitive to these decays, so b-tagged jets are vetoed to suppress the $t\bar{t}Z$ and $t\bar{t}$ SM backgrounds. Two SRs are defined with $4L0T$, no b-tagged jets, a first- and second-

JHEP07(2021)167

Z requirement, and different selections on $E_{\mathrm{T}}^{\mathrm{miss}}$: a loose signal region ($\texttt{SR0-ZZ}_{\mathrm{bveto}}^{\mathrm{loose}}$) with $E_{\mathrm{T}}^{\mathrm{miss}} > 100\,\mathrm{GeV}$, and a tighter signal region ($\texttt{SR0-ZZ}_{\mathrm{bveto}}^{\mathrm{tight}}$) with $E_{\mathrm{T}}^{\mathrm{miss}} > 200\,\mathrm{GeV}$, optimised for the low-mass and high-mass higgsino GGM scenarios, respectively. Two further SRs that showed an excess in the 13 TeV partial dataset analysis in ref. [18] are also examined here, and are defined with $4L0T$, no requirement on b-tagged jets, with a first- and second-Z requirement, and with different selections on $E_{\mathrm{T}}^{\mathrm{miss}}$: a loose signal region ($\texttt{SR0-ZZ}^{\mathrm{loose}}$, labelled SR0C in ref. [18]) with $E_{\mathrm{T}}^{\mathrm{miss}} > 50\,\mathrm{GeV}$, and a tighter signal region ($\texttt{SR0-ZZ}^{\mathrm{tight}}$, labelled SR0D in ref. [18]) with $E_{\mathrm{T}}^{\mathrm{miss}} > 100\,\mathrm{GeV}$. The two newly defined regions, $\texttt{SR0-ZZ}_{\mathrm{bveto}}^{\mathrm{loose}}$ and $\texttt{SR0-ZZ}_{\mathrm{bveto}}^{\mathrm{tight}}$, are subsets of these two regions, $\texttt{SR0-ZZ}^{\mathrm{loose}}$ and $\texttt{SR0-ZZ}^{\mathrm{tight}}$.

For the RPV scenarios, events with $4L0T$ are used to target the $LL\bar{E}12k$ models, and events with $4L0T$, $3L1T$, and $2L2T$ are used to target the $LL\bar{E}i33$ models. To suppress SM backgrounds with a Z boson, a Z veto is required, which rejects events where any SFOS lepton pair combination has an invariant mass close to the Z boson mass, in the range 81.2–101.2 GeV. The Z veto is extended to three- and four-lepton invariant mass combinations to suppress events where a photon radiated from a $Z \to \ell\ell$ decay converts to a second SFOS lepton pair; any event with an $\ell^+\ell^-\ell'^{\pm}$ or $\ell^+\ell^-\ell'^+\ell'^-$ system with invariant mass in the range 81.2–101.2 GeV is rejected (the flavour of ℓ and ℓ' may be different). A small number of four-lepton events will satisfy neither the Z requirement described above for the GGM scenarios nor the Z veto; however, these are assumed to come from $Z \to \ell^+\ell^-\gamma$ and $Z \to \ell^+\ell^-\ell^+\ell^-$ decays, which are not considered to be signal-like.

The gluino and wino RPV models can produce b-quarks ($\tilde{g} \to b\bar{b}\tilde{\chi}_1^0$, or $\tilde{\chi}_2^0 \to \tilde{\chi}_1^0 h, h \to b\bar{b}$) and these decay chains are an important component of the signal for high $\Delta m(\mathrm{NLSP}, \tilde{\chi}_1^0) = m(\mathrm{NLSP}) - m(\tilde{\chi}_1^0)$. A veto on the presence of b-tagged jets is required for some signal regions to minimise heavy-flavour SM backgrounds, and at least one b-tagged jet is required for other signal regions to improve sensitivity to high $\Delta m(\mathrm{NLSP}, \tilde{\chi}_1^0)$ gluino and wino RPV scenarios.

In order to separate the RPV SUSY signal from the SM background, the effective mass of the event, m_{eff}, is used, defined as the scalar sum of the $E_{\mathrm{T}}^{\mathrm{miss}}$, the p_{T} of signal leptons and the p_{T} of all jets with $p_{\mathrm{T}} > 40\,\mathrm{GeV}$. The $p_{\mathrm{T}} > 40\,\mathrm{GeV}$ requirement for jets aims to suppress contributions from pile-up and the underlying event. A selection using the m_{eff} rather than the $E_{\mathrm{T}}^{\mathrm{miss}}$ is particularly effective for the RPV SUSY scenarios, which produce multiple high-energy leptons (and in some cases jets), but only low to moderate $E_{\mathrm{T}}^{\mathrm{miss}}$ from neutrinos in the final state. The chosen m_{eff} thresholds are found to be broadly optimal for the wide range of RPV scenarios with different NLSPs considered in this paper.

Three general signal regions are defined with a Z veto, no b-tagged jets, and $m_{\mathrm{eff}} > 600\,\mathrm{GeV}$: $\texttt{SR0}_{\mathrm{bveto}}^{\mathrm{loose}}$ with $4L0T$, $\texttt{SR1}_{\mathrm{bveto}}^{\mathrm{loose}}$ with $3L1T$, and $\texttt{SR2}_{\mathrm{bveto}}^{\mathrm{loose}}$ with $2L2T$. These signal regions are non-optimal for the SUSY scenarios considered here and select regions with low levels of SM background to target new phenomena decaying to four-lepton final states. Two further signal regions are defined with $4L0T$ and a Z veto: a high-m_{eff} signal region ($\texttt{SR0}_{\mathrm{bveto}}^{\mathrm{tight}}$) with no b-tagged jets and $m_{\mathrm{eff}} > 1250\,\mathrm{GeV}$, and a signal region ($\texttt{SR0}_{\mathrm{breq}}$) with one or more b-tagged jets and $m_{\mathrm{eff}} > 1300\,\mathrm{GeV}$, both optimised for RPV $LL\bar{E}12k$ scenarios. Similarly, two further signal regions are defined with $3L1T$ and a Z veto: a high-m_{eff} signal region ($\texttt{SR1}_{\mathrm{bveto}}^{\mathrm{tight}}$) with no b-tagged jets and $m_{\mathrm{eff}} > 1000\,\mathrm{GeV}$, and a signal region ($\texttt{SR1}_{\mathrm{breq}}$)

JHEP07(2021)167

Name	Signal Region	$N(e,\mu)$	$N(\tau_{\text{had}})$	$N(b\text{-tagged jets})$	Z boson	Selection	Target
$4L0T$	$\texttt{SR0-ZZ}^{\text{loose}}_{\text{bveto}}$	≥ 4	≥ 0	$= 0$	require 1st & 2nd	$E_{\text{T}}^{\text{miss}} > 100\,\text{GeV}$	higgsino GGM
	$\texttt{SR0-ZZ}^{\text{tight}}_{\text{bveto}}$	≥ 4	≥ 0	$= 0$	require 1st & 2nd	$E_{\text{T}}^{\text{miss}} > 200\,\text{GeV}$	higgsino GGM
	$\texttt{SR0-ZZ}^{\text{loose}}$	≥ 4	≥ 0	≥ 0	require 1st & 2nd	$E_{\text{T}}^{\text{miss}} > 50\,\text{GeV}$	Excess from ref. [18]
	$\texttt{SR0-ZZ}^{\text{tight}}$	≥ 4	≥ 0	≥ 0	require 1st & 2nd	$E_{\text{T}}^{\text{miss}} > 100\,\text{GeV}$	Excess from ref. [18]
	$\texttt{SR0}^{\text{loose}}_{\text{bveto}}$	≥ 4	≥ 0	$= 0$	veto	$m_{\text{eff}} > 600\,\text{GeV}$	General
	$\texttt{SR0}^{\text{tight}}_{\text{bveto}}$	≥ 4	≥ 0	$= 0$	veto	$m_{\text{eff}} > 1250\,\text{GeV}$	RPV $LL\bar{E}12k$
	$\texttt{SR0}_{\text{breq}}$	≥ 4	≥ 0	≥ 1	veto	$m_{\text{eff}} > 1300\,\text{GeV}$	RPV $LL\bar{E}12k$
$3L1T$	$\texttt{SR1}^{\text{loose}}_{\text{bveto}}$	$= 3$	≥ 1	$= 0$	veto	$m_{\text{eff}} > 600\,\text{GeV}$	General
	$\texttt{SR1}^{\text{tight}}_{\text{bveto}}$	$= 3$	≥ 1	$= 0$	veto	$m_{\text{eff}} > 1000\,\text{GeV}$	RPV $LL\bar{E}i33$
	$\texttt{SR1}_{\text{breq}}$	$= 3$	≥ 1	≥ 1	veto	$m_{\text{eff}} > 1300\,\text{GeV}$	RPV $LL\bar{E}i33$
$2L2T$	$\texttt{SR2}^{\text{loose}}_{\text{bveto}}$	$= 2$	≥ 2	$= 0$	veto	$m_{\text{eff}} > 600\,\text{GeV}$	General
	$\texttt{SR2}^{\text{tight}}_{\text{bveto}}$	$= 2$	≥ 2	$= 0$	veto	$m_{\text{eff}} > 1000\,\text{GeV}$	RPV $LL\bar{E}i33$
	$\texttt{SR2}_{\text{breq}}$	$= 2$	≥ 2	≥ 1	veto	$m_{\text{eff}} > 1100\,\text{GeV}$	RPV $LL\bar{E}i33$
$5L0T$	SR5L	≥ 5	≥ 0	≥ 0	—	–	General

Table 4. Signal region definitions. The Z boson column refers to the Z veto or selection of a first and second Z candidate as described in the text.

with one or more b-tagged jets and $m_{\text{eff}} > 1300\,\text{GeV}$, both optimised for RPV $LL\bar{E}i33$ scenarios. Finally, two signal regions are defined with $2L2T$ and a Z veto: a high-m_{eff} signal region ($\texttt{SR2}^{\text{tight}}_{\text{bveto}}$) with no b-tagged jets and $m_{\text{eff}} > 1000\,\text{GeV}$, and a signal region ($\texttt{SR2}_{\text{breq}}$) with one or more b-tagged jets and $m_{\text{eff}} > 1100\,\text{GeV}$, both optimised for RPV $LL\bar{E}i33$ scenarios.

A general signal region, SR5L, with at least five light leptons is also defined, with no further selection applied.

7 Background determination

The SM background is composed of processes that can give rise to four real or fake/non-prompt leptons and these are classified into two categories:

Irreducible background: hard-scattering processes giving rise to events with four or more real leptons, ZZ, $t\bar{t}Z$, $t\bar{t}WW$, $t\bar{t}ZZ$, $t\bar{t}WZ$, $t\bar{t}WH$, $t\bar{t}HH$, tWZ, VVZ (ZZZ, WZZ, WWZ), Higgs (H via ggF, WH, ZH, H via VBF, $t\bar{t}H$), $t\bar{t}t\bar{t}$, $t\bar{t}tW$.

Reducible background: processes leading to events with at least one fake/non-prompt lepton, $t\bar{t}$, Z+jets, WZ, WW, WWW, $t\bar{t}W$, $t\bar{t}t$. Processes listed under irreducible that do not undergo a decay to four real leptons (e.g. $ZZ \to q\bar{q}\ell\ell$) are also included in the reducible background.

Backgrounds with three or more fake/non-prompt leptons (e.g. W+jets) are found to be $< 1\%$ of the total SM background in four-lepton regions using the method outlined in section 7.2 and are neglected. The systematic uncertainty of the reducible background is increased to cover any effect from neglected backgrounds (discussed in section 8).

JHEP07(2021)167

In the four-lepton signal regions, the main irreducible backgrounds are ZZ, and $t\bar{t}Z$, while the reducible background is dominated by the two-fake/non-prompt-lepton backgrounds $t\bar{t}$ and Z+jets. The ZZ and $t\bar{t}Z$ backgrounds are estimated using MC simulation normalised to data in control regions (CR), while the other irreducible backgrounds are estimated from MC simulation. The reducible backgrounds are derived from data using a fake-factor method. Signal regions with $4L0T$ are dominated by irreducible background processes, whereas the reducible background processes dominate the $3L1T$ and $2L2T$ regions. The predictions for irreducible and reducible backgrounds are tested in validation regions (section 9).

For `SR5L`, the main irreducible background processes are VZZ and Higgs, followed by small contributions from $ZZ \to 6\ell$ and $t\bar{t}Z \to 5\ell$, where virtual photons convert into lepton pairs (internal conversions). However, reducible background processes are the leading source of events in the $5L0T$ signal region, and are dominated by $ZZ \to 4\ell$ and $t\bar{t}Z \to 4\ell$.

The HistFitter [120] software framework is used when constraining the ZZ and $t\bar{t}Z$ background normalisations and a 'background-only fit' of observations in the CRs is used to estimate the expected background in the SRs, without considering any CR signal contamination. A likelihood function is built as a product of Poisson probability functions, describing the observed and expected number of events in the CRs and SRs. The observed numbers of events in various CRs and SRs are used in a combined profile likelihood fit to determine the expected SM background yields in each of the SRs. The systematic uncertainties in the expected SM background yields described in section 8 are included as nuisance parameters, constrained to be Gaussian with a width determined by the size of the uncertainty. Common nuisance parameters take into account the correlations between CRs and SRs, and background processes. The fit parameters are determined by maximising the product of the Poisson probability functions and the Gaussian constraints on the nuisance parameters.

7.1 Irreducible background determination

The irreducible background processes ZZ and $t\bar{t}Z$ are estimated using MC simulation normalised to data yields in CRs which are orthogonal to the SRs and minimise potential signal contamination. By normalising the MC simulation to data, the estimation of ZZ and $t\bar{t}Z$ is improved in the SRs. A simultaneous fit to the CRs and SRs (see in section 10) provides the final estimate of the yields and their uncertainties.

The ZZ and $t\bar{t}Z$ control region definitions are shown in table 5. The ZZ CR, `CRZZ`, is defined with at least four light leptons, no b-tagged jets, a first- and second-Z requirement, and $E_{\mathrm{T}}^{\mathrm{miss}} < 50\,\mathrm{GeV}$, while the $t\bar{t}Z$ CR, `CRttZ`, is defined with $4L0T$, at least one b-tagged jet, only one Z boson candidate, and $E_{\mathrm{T}}^{\mathrm{miss}} > 100\,\mathrm{GeV}$. The background-only fit is used to obtain normalisation factors for the ZZ and $t\bar{t}Z$ MC simulation in their CRs of 1.15 ± 0.09 and 1.06 ± 0.24, respectively. The uncertainties quoted for the normalisation factors include the statistical uncertainty of the data and MC simulation in the CR, as well as the experimental and theory uncertainties from the subtraction of contaminating SM processes (see section 8). The m_{eff} distributions for `CRZZ` and `CRttZ` after the simultaneous fit is performed are shown in figure 3.

JHEP07(2021)167

Region	$N(e,\mu)$	$N(\tau_{\text{had}})$	$N(b\text{-tagged jets})$	Z boson	Selection
CRZZ	≥ 4	≥ 0	$= 0$	require 1st & 2nd	$E_{\text{T}}^{\text{miss}} < 50\,\text{GeV}$
CRttZ	≥ 4	≥ 0	≥ 1	require 1st & veto 2nd	$E_{\text{T}}^{\text{miss}} > 100\,\text{GeV}$

Table 5. Irreducible background control region definitions. Both CRZZ and CRttZ are restricted to $N(e,\mu) = 4$ when considering SR5L. The Z boson column refers to the Z veto or selection of a first/second Z candidate as described in the text.

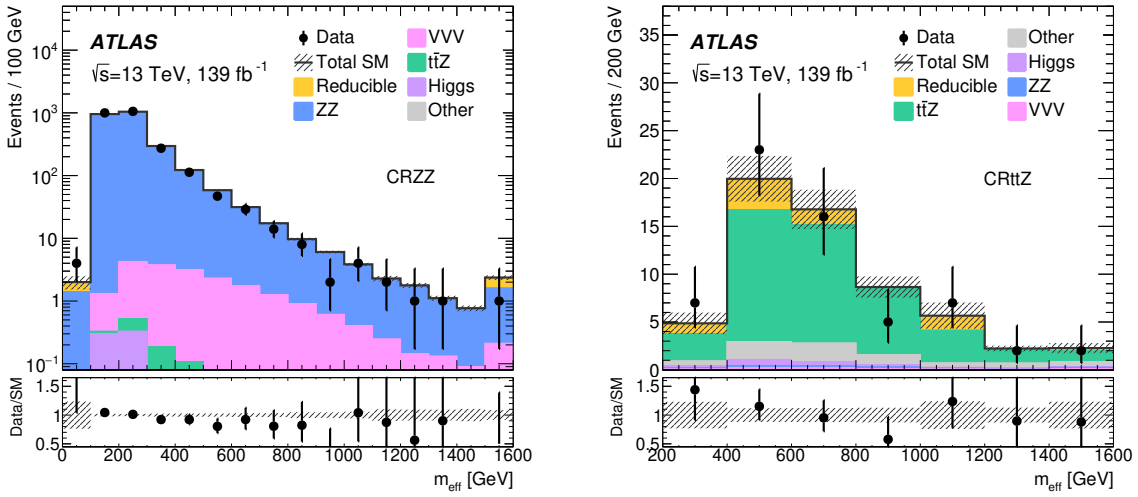

(a) m_{eff} in CRZZ. **(b)** m_{eff} in CRttZ.

Figure 3. The m_{eff} distributions for data and the SM backgrounds in CRZZ and CRttZ after the background-only fit. "Other" is the sum of the tWZ, $t\bar{t}WW$, $t\bar{t}ZZ$, $t\bar{t}WZ$, $t\bar{t}WH$, $t\bar{t}HH$, $t\bar{t}tW$, and $t\bar{t}t\bar{t}$ backgrounds. The last bin includes the overflow. The lower panel shows the ratio of the observed data to the expected SM background yield in each bin. Both the statistical and systematic uncertainties in the SM background are included in the shaded band.

Since the regions CRZZ and CRttZ include five-light-lepton events, they are both restricted to exactly four light leptons when estimating the backgrounds for SR5L. In these restricted CRs, normalisation factors of 1.14 ± 0.09 and 1.07 ± 0.25 are obtained for the ZZ and $t\bar{t}Z$ backgrounds, respectively.

7.2 Reducible background determination

The number of reducible background events in a given region is estimated from data with a hybrid fake-factor method that uses a combination of data and MC simulation. Preselected leptons surviving overlap removal are classified as 'signal' or 'loose' depending on whether they pass or fail the signal lepton requirements, respectively. A very loose selection on the identification RNN of > 0.05 is also applied to the preselected τ_{had}, as those with very low RNN scores are typically gluon-induced jets and jets arising from pile-up, which is not the case for the signal τ_{had} candidates. Probabilities for a fake/non-prompt lepton to be identified as a signal or loose lepton are calculated from simulation and corrected to data

JHEP07(2021)167

Reducible bkg. estimation for	Control Region	$N(e,\mu)$ signal	$N(e,\mu)$ loose	$N(\tau_{\text{had}})$ signal	$N(\tau_{\text{had}})$ loose
$4L0T$	CR1_LLLl	$= 3$	≥ 1	≥ 0	≥ 0
	CR2_LLll	$= 2$	≥ 2	≥ 0	≥ 0
$3L1T$	CR1_LLLt	$= 3$	$= 0$	$= 0$	≥ 1
	CR1_LLTl	$= 2$	$= 1$	≥ 1	≥ 0
	CR2_LLlt	$= 2$	$= 1$	$= 0$	≥ 1
$2L2T$	CR1_LLTt	$= 2$	$= 0$	$= 1$	≥ 1
	CR2_LLtt	$= 2$	$= 0$	$= 0$	≥ 2
$5L0T$	CR1_LLLLl	$= 4$	≥ 1	≥ 0	≥ 0

Table 6. Reducible background control region definitions where "L" and "T" denote signal light leptons and τ_{had}, while "l" and "t" denote loose light leptons and τ_{had}. Loose leptons are preselected leptons surviving overlap removal that do not pass signal lepton requirements. Additional selections for b-tagged jets, Z veto/requirement, $E_{\text{T}}^{\text{miss}}$, and m_{eff} are applied to match a given signal or validation region.

where possible. The ratio $F = f/\bar{f}$ for fake/non-prompt leptons is then defined as the "fake factor", where f ($\bar{f}$) is the probability that a fake/non-prompt lepton is identified as a signal (loose) lepton.

The reducible background prediction is extracted by applying fake factors to control regions in data. The CR definition only differs from that of the associated SR in the quality of the required leptons; here exactly one (CR1) or two (CR2) of the four leptons must be identified as a loose lepton, as shown in table 6. In $3L1T$ and $5L0T$ events, the contribution from events with two fake/non-prompt light leptons is negligible, as is the contribution from one and two fake/non-prompt light leptons in $2L2T$ events.

The fake factors depend on the lepton flavour, the source of the fake/non-prompt lepton, and the production process. Fake factors are calculated separately for each fake/non-prompt-lepton flavour (e, μ, τ_{had}) and source (light-flavour jets, heavy-flavour jets, gluon-initiated jets for τ_{had} only, and photon conversions for electrons and τ_{had} only), where these categories are referred to as fake/non-prompt-lepton 'types'. The fake factor per fake/non-prompt-lepton type for each production process ($t\bar{t}$ and Z+jets, or ZZ for $5L$) is binned in lepton p_{T}, η, proximity to other leptons (ΔR) for electrons and muons, and number of prongs for τ_{had}. The statistical uncertainties on the fake factors for the dominant types of fake/non-prompt-lepton are very small. To correctly account for the relative abundances of fake/non-prompt-lepton types and production processes, a weighted average F_w of fake factors is computed in each CR, as

$$F_w = \sum_{i,j} \left(F^{ij} \times R^{ij} \times s^i \right).$$

The term F^{ij} is the corresponding fake factor for fake/non-prompt leptons of type i from process j calculated using MC simulation. The fake factors are weighted by the 'process fractions', R^{ij}, that describe the fraction of fake/non-prompt leptons of type i from process

JHEP07(2021)167

j in that region. The process fractions are determined from MC simulation in the corresponding CR2, and are similar to the process fractions obtained in the signal regions from MC simulation, which suffer from having few events. For the five lepton regions, no corresponding CR2 is used for the reducible estimation and the process fractions are determined from MC simulation in the corresponding CR1. To account for possible differences between data and MC simulation, the fake factors obtained from simulation are corrected to data using 'scale factors', s^i. The scale factors are assumed to be independent of the physical process (e.g. $t\bar{t}$, Z+jets) and depend on the fake/non-prompt-lepton type only. They are determined from data in regions enriched in objects of a given fake/non-prompt-lepton type, where MC simulation is used to remove any small contamination from leptons not from the fake/non-prompt-lepton type under study.

For fake/non-prompt leptons from heavy-flavour jets, the scale factor is measured in a $t\bar{t}$-dominated control sample. The heavy-flavour scale factors are seen to have a modest p_{T}-dependence, decreasing for electrons from 1.18 ± 0.10 to 1.08 ± 0.08 as the electron p_{T} increases from 7 GeV to 20 GeV. For muons, the heavy-flavour scale factor is seen to be less dependent on p_{T}, changing from 1.00 ± 0.04 to 0.94 ± 0.10 as the muon p_{T} increases from 5 GeV to 20 GeV. For 1-prong (3-prong) τ_{had}, the heavy-flavour scale factor decreases from 1.26 ± 0.07 to 0.93 ± 0.11 (1.15 ± 0.06 to 0.97 ± 0.12) as the τ_{had} p_{T} increases from 20 GeV to 50 GeV. Uncertainties quoted for the scale factors include the statistical uncertainties of the data and MC simulation.

The scale factor for fake/non-prompt τ_{had} originating from light-flavour jets is measured separately for one- and three-prong τ_{had} in a control sample dominated by Z+jets events. The scale factors are seen to be p_{T}-dependent, decreasing from 1.115 ± 0.009 to 0.919 ± 0.017 (1.340 ± 0.023 to 1.04 ± 0.05) as the 1-prong (3-prong) τ_{had} p_{T} increases from 20 GeV to 50 GeV. The scale factor for τ_{had} originating from gluon-initiated jets is assumed to be the same as the one obtained from light-flavour jets. The scale factor for fake/non-prompt electrons originating from light-flavour jets is measured in a W+jets-dominated control sample, where the light-flavour scale factor increases from 1.05 ± 0.29 to 1.38 ± 0.09 as the electron p_{T} increases from 7 GeV to 20 GeV. The contribution to the signal regions from fake/non-prompt muons originating from light-flavour jets or leptons from photon conversions is very small and the scale factor cannot be measured reliably using data. Therefore, values of 1.00 ± 0.10 are used instead, motivated by similar uncertainties in the other scale factor measurements.

The final estimate of the number $N_{\mathrm{red}}^{\mathrm{SR}}$ of background events with one or two fake/non-prompt leptons in each SR is determined from the number of events in data in the corresponding CRs, $N_{\mathrm{data}}^{\mathrm{CR1}}$ and $N_{\mathrm{data}}^{\mathrm{CR2}}$, according to

$$N_{\mathrm{red}}^{\mathrm{SR}} = [N_{\mathrm{data}}^{\mathrm{CR1}} - N_{\mathrm{irr}}^{\mathrm{CR1}}] \times F_{w,1} - [N_{\mathrm{data}}^{\mathrm{CR2}} - N_{\mathrm{irr}}^{\mathrm{CR2}}] \times F_{w,1} \times F_{w,2}, \tag{7.1}$$

where $F_{w,1}$ and $F_{w,2}$ are the two weighted fake factors constructed using the highest- and second-highest-p_{T} loose leptons in the CRs, respectively. Only the first term is used to estimate the reducible background for five lepton events. The small contributions from irreducible background processes in the CRs, $N_{\mathrm{irr}}^{\mathrm{CR1,CR2}}$, are evaluated using MC simulation and subtracted from the corresponding number of events seen in data. The second term removes

JHEP07(2021)167

the double-counting of events with two fake/non-prompt leptons in the first term. Processes with one fake/non-prompt-lepton are included in the reducible background estimation, but have very low contributions to CR1 and CR2 because of their small cross-sections e.g. WZ and $t\bar{t}W$. Both CR1 and CR2 are dominated by the two-fake/non-prompt-lepton processes $t\bar{t}$ and Z+jets, so the first term is roughly twice the second term. Higher-order terms in F_w describing three- and four-fake/non-prompt-lepton backgrounds are neglected, as are some terms with a very small contribution; e.g. in $3L1T$ events, the contribution from events with two fake/non-prompt light leptons is negligible. A systematic uncertainty is applied to account for these neglected terms, as described in the following section.

8 Systematic uncertainties

The uncertainties affecting the SM and signal simulation-based estimates can be divided into three components: statistical uncertainty of the MC simulation, experimental uncertainty in event reconstruction (e, μ, τ_{had} and jets, $E_{\text{T}}^{\text{miss}}$), and theoretical uncertainty. The reducible background estimation is affected by different sources of uncertainty associated with data counts in control regions and uncertainties in the weighted fake factors. The leading SM background in the signal regions targeting the higgsino GGM models (SR0-ZZ) is generally ZZ production, and the jet experimental and theoretical uncertainties are seen to dominate the total uncertainty. The exception is $\texttt{SR0-ZZ}^{\text{tight}}_{\text{bveto}}$, where the reducible background and its associated uncertainties are the leading contribution to the total SM background and its uncertainty. The reducible background is also the leading component of the SM background in most of the high-m_{eff} signal regions targeting the RPV models, as well as the five-lepton signal region, and the uncertainty in the reducible background dominates the total uncertainty. The exceptions to this are $\texttt{SR0}^{\text{loose}}_{\text{bveto}}$ and $\texttt{SR0}_{\text{breq}}$, where the irreducible processes and theory uncertainties also contribute significantly to the total SM background and uncertainty. The primary sources of systematic uncertainty, described below, are summarised in figure 4.

The statistical uncertainty of the MC simulation-based background estimate is small and typically less than 5% of the total background estimate in the signal regions. However, this rises to 10–15% in $\texttt{SR0}_{\text{breq}}$, $\texttt{SR2}^{\text{tight}}_{\text{bveto}}$, and $\texttt{SR2}_{\text{breq}}$ where tight selections on m_{eff} are made. The experimental uncertainties include the uncertainties associated with electrons, muons, τ_{had}, jets, and $E_{\text{T}}^{\text{miss}}$, as well as the uncertainty associated with the simulation of pile-up, and uncertainty in the luminosity. The uncertainty in the combined 2015–2018 integrated luminosity is 1.7% [7], obtained using the LUCID-2 detector [121] for the primary luminosity measurements. The uncertainties associated with pile-up and luminosity are included in the total uncertainty in figure 4. The experimental uncertainties pertaining to electrons, muons and τ_{had} include the uncertainties due to the lepton identification efficiencies, lepton energy scale and energy resolution, and isolation and trigger efficiencies. Systematic uncertainties from electron, muon, and τ_{had} sources are generally small in all signal regions, at a few percent relative to the total expected background. The uncertainties associated with jets are due to the jet energy scale, jet energy resolution, jet vertex tagging, and b-tagging. The jet energy resolution is the dominant source of uncertainty for jets in the signal re-

JHEP07(2021)167

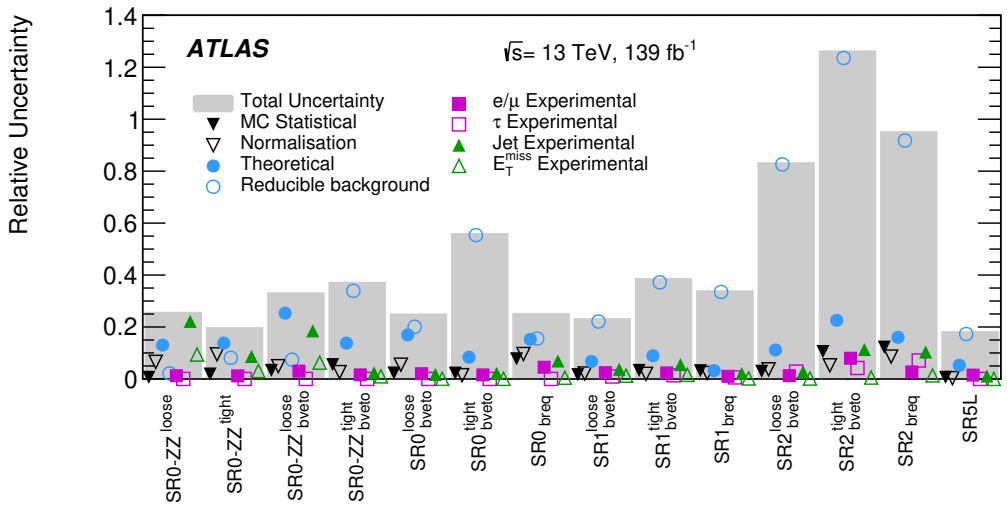

Figure 4. Breakdown of the dominant systematic uncertainties in the background estimates for the signal regions. Theoretical uncertainties in the simulation-based estimates, including those in the acceptance for events in ZZ and $t\bar{t}Z$ simulations, are grouped under the "Theoretical" category, while the "Normalisation" category includes the statistical uncertainties of the data counts in `CRZZ` and `CRttZ` and the uncertainty from the fitted normalisation factors. For simplicity, the individual uncertainties are added in quadrature for each category, without accounting for correlations. The total background uncertainty is taken from the background-only fit where correlations of individual uncertainties are accounted for.

gions. Uncertainties in the object momenta are propagated to the $E_{\mathrm{T}}^{\mathrm{miss}}$ measurement, and additional uncertainties in $E_{\mathrm{T}}^{\mathrm{miss}}$ arising from energy deposits not associated with any reconstructed objects are also considered. The jet and $E_{\mathrm{T}}^{\mathrm{miss}}$ uncertainties are generally of the order of a few percent in the signal regions, but approach 10–20% in $\texttt{SR0-ZZ}^{\mathrm{loose}}$, $\texttt{SR0-ZZ}^{\mathrm{tight}}$ and $\texttt{SR0-ZZ}^{\mathrm{loose}}_{\mathrm{bveto}}$, where selections on $E_{\mathrm{T}}^{\mathrm{miss}}$ are made.

Theoretical uncertainties in the simulation-based estimates include the theoretical cross-section uncertainties due to the choice of renormalisation and factorisation scales and PDFs, the acceptance uncertainty due to PDF and scale variations, and the choice of MC generator. The theoretical cross-section uncertainties for the irreducible backgrounds used in this analysis are 20% for VVV [83], 10% for $t\bar{t}H$ [122], 5% for H via ggF [122], and 20% for $t\bar{t}WZ/WW/WH/HH$, tWZ, and Higgs via VBF/VH, where the order of each cross-section calculation is shown in table 3.

Uncertainties in the acceptance are evaluated for the irreducible processes ZZ, $t\bar{t}Z$, VVV, $t\bar{t}H$ and Higgs, where for each background the uncertainties are correlated across all regions. The uncertainty in the acceptance from varying the strong coupling constant α_{S} within its uncertainty is included for the ZZ, VVV, Higgs, and $t\bar{t}H$ backgrounds. Uncertainties arising from varying the renormalisation and factorisation scales (μ_{r} and μ_{f}) by factors of 2 and 1/2 are considered — the μ_{r} and μ_{f} variations are taken as uncorrelated and the additional coherent up/down variation of μ_{r} and μ_{f} is also considered. Resummation and merging-scale variations are also considered for the ZZ sample. The uncertainty

JHEP07(2021)167

related to the choice of CKKW merging scale (20 GeV) was evaluated by considering alternative values of 15 GeV and 30 GeV. The uncertainty related to the resummation scale μ_q (2 GeV, the upper cut-off in perturbative calculations of parton shower evolution), was evaluated by varying the scale by factors of 1/4 and 4. Finally, for Sherpa ZZ samples the impact of using an alternative recoil scheme for single-particle emission in the Sherpa parton shower is studied by comparing the nominal samples with alternative ones in which the CSS scheme is used (CSSKIN) [123]. The theoretical uncertainties in the ZZ acceptance dominate the total uncertainties in signal regions where the irreducible backgrounds are a large fraction of the total SM background: $\texttt{SR0-ZZ}^{\text{tight}}$, $\texttt{SR0-ZZ}^{\text{loose}}_{\text{bveto}}$, $\texttt{SR0}^{\text{loose}}_{\text{bveto}}$, and $\texttt{SR0}_{\text{breq}}$.

The uncertainty in the reducible background is dominated by the statistical uncertainty of the data events in the corresponding CR1 and CR2, which is the leading source of uncertainty in many of the signal regions where the reducible background is a large fraction of the total SM background, as seen in figure 4. The uncertainty in the weighted fake factors includes the statistical uncertainty of the MC simulation in the process fractions, the uncertainty in the fake/non-prompt-lepton scale factors, and the statistical uncertainty from the fake factors determined from simulation. The uncertainties in the fake factors from each fake/non-prompt-lepton type are treated as correlated across processes. Thus, since both CR1 and CR2 are dominated by two-fake/non-prompt-lepton processes with the same source of fake/non-prompt lepton, correlations in the fake factors applied to CR1 and CR2 cause the uncertainties from the weighted fake factors to largely cancel out between the first and second terms in eq. (7.1). Finally, a conservative uncertainty is applied to account for the neglected terms in eq. (7.1). For example, for $4L0T$ events the three- and four-fake/non-prompt-lepton terms are neglected. Weighted fake factors are applied to data events with one signal light lepton and three loose light leptons to estimate an upper limit on this neglected contribution for each $4L0T$ region. The calculated upper limit plus its 1σ statistical uncertainty is then added to the reducible background uncertainty, adding an absolute uncertainty of 0.17 events in $\texttt{SR0}^{\text{loose}}_{\text{bveto}}$. This is repeated for the $3L1T$ and $2L2T$ regions, accounting for the neglected terms with one or two fake/non-prompt light leptons as necessary, adding an absolute uncertainty of 0.59 events in $\texttt{SR1}^{\text{loose}}_{\text{bveto}}$, and 2.5 events in $\texttt{SR2}^{\text{loose}}_{\text{bveto}}$. Finally, for SR5L, the neglected terms with two or three fake/non-prompt light leptons are evaluated in the same way, adding an absolute uncertainty of 0.5 events.

Systematic uncertainties in the SUSY signal yields from experimental sources are typically of the order of 10%, while typical uncertainties in the signal acceptance and distribution shapes due to scale and parton shower variations are found to range from $\sim 5\%$ in $4L0T$ regions to $\sim 20\%$ in $2L2T$ regions. The systematic uncertainty in the signal cross-section is described in section 4.

9 Background modelling validation

To validate the modelling of the SM backgrounds, the yields and shapes of key kinematic variable distributions are compared with data in validation regions (VR). The VRs are defined to be close to, yet disjoint from the SRs and CRs, and be dominated by the background process under consideration, as shown in table 7. The $ZZ^{(*)}$ modelling is validated

JHEP07(2021)167

Name	Validation Region	$N(e,\mu)$	$N(\tau_{\text{had}})$	$N(b\text{-jets})$	Z boson	Selection	Target
$4L0T$	VRZZ	≥ 4	$= 0$	$= 0$	require 1st & veto 2nd	—	$ZZ^{(*)}$
	VRttZ	≥ 4	$= 0$	≥ 1	veto	$400 < m_{\text{eff}} < 1300\,\text{GeV}$	$t\bar{t}Z^{(*)}$
	VR0-noZ	≥ 4	$= 0$	$= 0$	veto	$m_{\text{eff}} < 600\,\text{GeV}$	$t\bar{t}$, Z+jets, $Z^{(*)}Z^{(*)}$
$3L1T$	VR1-noZ	$= 3$	≥ 1	$= 0$	veto	$m_{\text{eff}} < 600\,\text{GeV}$	$t\bar{t}$, Z+jets
	VR1-Z	$= 3$	≥ 1	$= 0$	require 1st	—	Z+jets
$2L2T$	VR2-noZ	$= 2$	≥ 2	$= 0$	veto	$m_{\text{eff}} < 600\,\text{GeV}$	$t\bar{t}$, Z+jets
	VR2-Z	$= 2$	≥ 2	$= 0$	require 1st	—	Z+jets

Table 7. Validation region definitions. The Z boson column refers to the Z veto or selection of a first/second Z candidate as described in the text.

	VRZZ	VRttZ	VR0-noZ	VR1-noZ	VR1-Z	VR2-noZ	VR2-Z
Observed	874	42	216	192	620	156	505
Total SM	929^{+43}_{-34}	40 ± 5	230 ± 12	199 ± 19	624^{+46}_{-47}	164 ± 30	479 ± 20
ZZ	737 ± 20	$2.7^{+1.0}_{-1.1}$	160 ± 7	36.8 ± 2.3	200^{+9}_{-11}	$23.3^{+1.2}_{-1.3}$	119 ± 7
$t\bar{t}Z$	$5.2^{+1.3}_{-1.4}$	16 ± 4	2.0 ± 0.5	0.9 ± 0.4	$2.3^{+1.2}_{-1.1}$	0.36 ± 0.1	0.14 ± 0.04
Higgs	77^{+36}_{-26}	5.5 ± 0.8	$3.1^{+1.0}_{-0.7}$	2.4 ± 0.5	13.6 ± 3.0	1.87 ± 0.31	8.8 ± 1.8
VVV	26 ± 5	$0.43^{+0.10}_{-0.11}$	5.4 ± 1.1	2.8 ± 0.8	$8.7^{+2.1}_{-2.2}$	1.23 ± 0.26	1.52 ± 0.33
Other	$2.2^{+0.4}_{-0.5}$	3.1 ± 0.4	$0.45^{+0.10}_{-0.11}$	$0.24^{+0.19}_{-0.20}$	0.9 ± 0.5	0.15 ± 0.04	$0.082^{+0.025}_{-0.028}$
Reducible	81^{+10}_{-11}	$12.1^{+3.5}_{-3.6}$	59 ± 9	156 ± 19	397 ± 45	137 ± 30	350 ± 19

Table 8. Expected and observed yields for $139\,\text{fb}^{-1}$ in the validation regions after the background-only fit. "Other" is the sum of the tWZ, $t\bar{t}WW$, $t\bar{t}ZZ$, $t\bar{t}WZ$, $t\bar{t}WH$, $t\bar{t}HH$, $t\bar{t}tW$, and $t\bar{t}t\bar{t}$ backgrounds. Both the statistical and systematic uncertainties in the SM background are included in the uncertainties shown.

in a region (VRZZ) defined with $4L0T$, no b-tagged jets, and only one Z boson candidate, while the $t\bar{t}Z$ modelling is validated in a region (VRttZ) with $4L0T$, a Z veto, at least one b-tagged jet, and high m_{eff}. For signal regions that veto Z boson candidates, three general VRs are defined by reversing the m_{eff} requirement: VR0-noZ, VR1-noZ, and VR2-noZ. Two further VRs with $3L1T$ and $2L2T$ are defined with one Z boson requirement to check the reducible background modelling across the full range of m_{eff}: VR1-Z and VR2-Z. The background model adopted in the VRs is the same as in the SRs, with the ZZ and $t\bar{t}$ backgrounds obtained from MC simulation normalised to data, the other irreducible processes from MC simulation, and the reducible background estimated from data using the fake-factor method with process fractions and loose lepton control regions corresponding to the VRs. The systematic uncertainties of the SM backgrounds in the VRs are evaluated as in section 8.

Observed and expected event yields in the VRs are shown in table 8, where good agreement is seen in general within statistical and systematic uncertainties. No significant deviations from SM expectations are observed in any VR.

JHEP07(2021)167

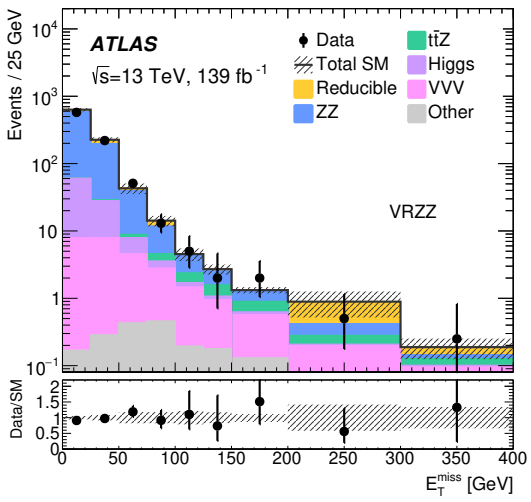

(a) $E_{\mathrm{T}}^{\mathrm{miss}}$ in `VRZZ`.

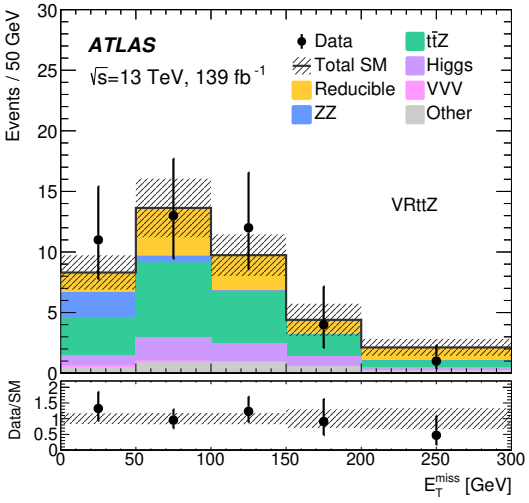

(b) $E_{\mathrm{T}}^{\mathrm{miss}}$ in `VRttZ`.

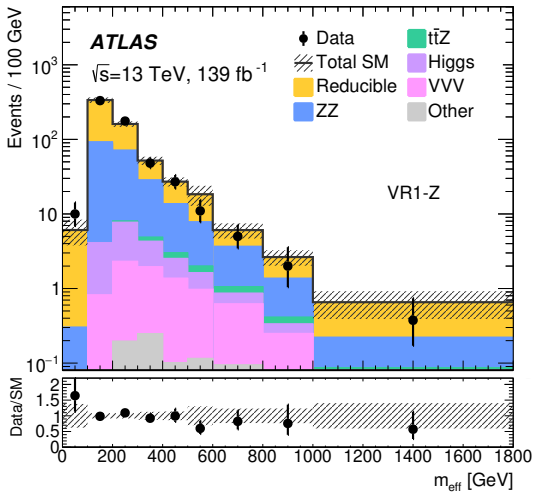

(c) m_{eff} in `VR1-Z`.

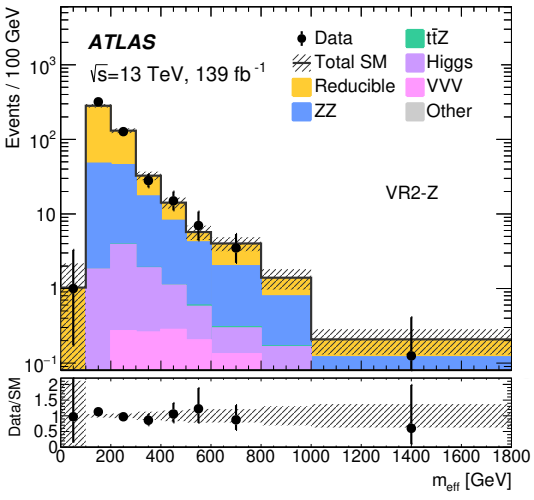

(d) m_{eff} in `VR2-Z`.

Figure 5. The distributions for data and the estimated SM backgrounds in the validation regions after the background-only fit, for the $E_{\mathrm{T}}^{\mathrm{miss}}$ in (a) `VRZZ` and (b) in `VRttZ`, and the m_{eff} in (c) `VR1-Z` and in (d) `VR2-Z`. "Other" is the sum of the tWZ, $t\bar{t}WW$, $t\bar{t}ZZ$, $t\bar{t}WZ$, $t\bar{t}WH$, $t\bar{t}HH$, $t\bar{t}tW$, and $t\bar{t}t\bar{t}$ backgrounds. The last bin includes the overflow. The lower panel shows the ratio of the observed data to the expected SM background yield in each bin. Both the statistical and systematic uncertainties in the SM background are included in the shaded band.

The $E_{\mathrm{T}}^{\mathrm{miss}}$, m_{eff}, and lepton p_{T} distributions in the VRs are shown in figure 5 and figure 6. The m_{eff} distributions in `VR0-noZ`, `VR1-noZ`, `VR2-noZ`, and `VRttZ` can be seen in the lower m_{eff} bins in figure 9a, figure 9b, figure 9c, and figure 10a, respectively.

JHEP07(2021)167

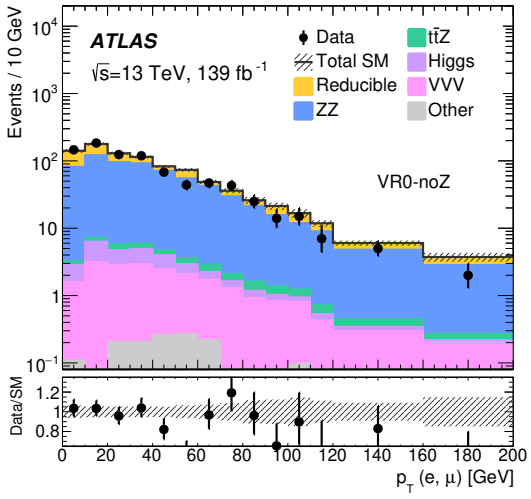

(a) $p_{\mathrm{T}}\,(e,\mu)$ in `VR0-noZ`.

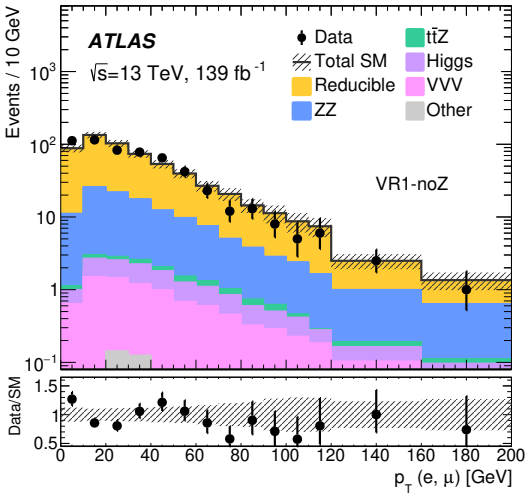

(b) $p_{\mathrm{T}}\,(e,\mu)$ in `VR1-noZ`.

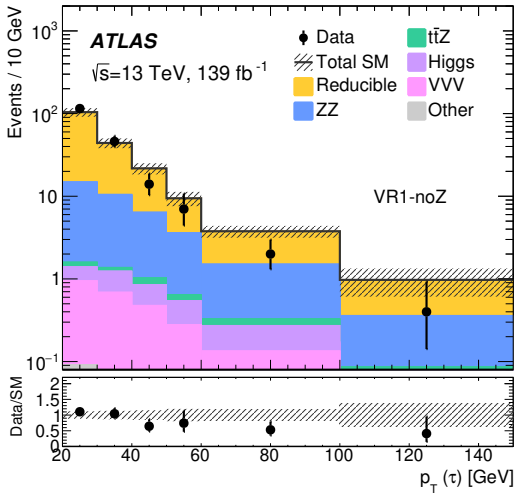

(c) $p_{\mathrm{T}}\,(\tau_{\mathrm{had}})$ in `VR1-noZ`.

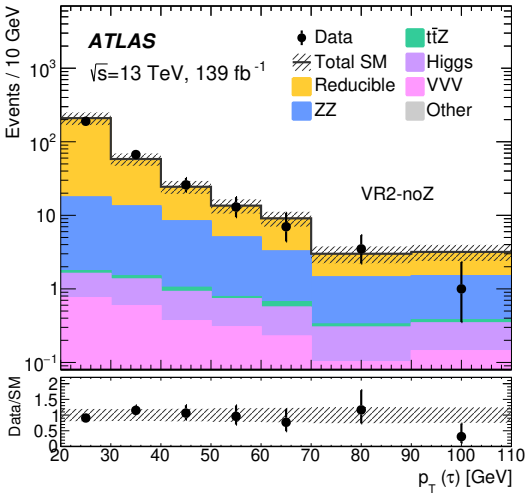

(d) $p_{\mathrm{T}}\,(\tau_{\mathrm{had}})$ in `VR2-noZ`.

Figure 6. The distributions for data and the estimated SM backgrounds in the validation regions after the background-only fit, for the light lepton p_{T} in (a) `VR0-noZ` and (b) `VR1-noZ`, and the τ_{had} p_{T} in (c) `VR1-noZ` and (d) `VR2-noZ`. "Other" is the sum of the tWZ, $t\bar{t}WW$, $t\bar{t}ZZ$, $t\bar{t}WZ$, $t\bar{t}WH$, $t\bar{t}HH$, $t\bar{t}tW$, and $t\bar{t}t\bar{t}$ backgrounds. The last bin includes the overflow. The lower panel shows the ratio of the observed data to the expected SM background yield in each bin. Both the statistical and systematic uncertainties in the SM background are included in the shaded band.

JHEP07(2021)167

	SR0-ZZ$^{\text{loose}}$	SR0-ZZ$^{\text{tight}}$	SR0-ZZ$^{\text{loose}}_{\text{bveto}}$	SR0-ZZ$^{\text{tight}}_{\text{bveto}}$	SR0$^{\text{loose}}_{\text{bveto}}$	SR0$^{\text{tight}}_{\text{bveto}}$	SR0$_{\text{breq}}$
Observed	157	17	5	1	11	1	3
Total SM	161^{+41}_{-43}	$18.4^{+3.6}_{-3.3}$	$7.3^{+2.4}_{-1.9}$	1.1 ± 0.4	$11.5^{+2.9}_{-2.2}$	$3.5^{+2.0}_{-2.2}$	$1.19^{+0.30}_{-0.28}$
ZZ	125^{+40}_{-42}	$4.5^{+2.6}_{-2.1}$	$3.7^{+2.2}_{-1.7}$	$0.05^{+0.11}_{-0.04}$	$7.6^{+1.6}_{-1.7}$	$0.64^{+0.28}_{-0.29}$	$0.19^{+0.15}_{-0.19}$
$t\bar{t}Z$	15 ± 4	7.4 ± 1.8	0.87 ± 0.24	$0.12^{+0.05}_{-0.04}$	$0.7^{+0.18}_{-0.19}$	$0.02^{+0.014}_{-0.015}$	0.49 ± 0.13
Higgs	0.79 ± 0.1	0.29 ± 0.05	$0.09^{+0.028}_{-0.027}$	$0.0046^{+0.0019}_{-0.0018}$	0.24 ± 0.04	$0.02^{+0.007}_{-0.006}$	$0.16^{+0.05}_{-0.06}$
VVV	$7.9^{+1.9}_{-2.0}$	2.4 ± 0.6	2.2 ± 0.5	0.44 ± 0.12	1.6 ± 0.4	0.21 ± 0.06	$0.083^{+0.027}_{-0.029}$
Other	3.3 ± 0.7	1.7 ± 0.4	0.32 ± 0.09	$0.04^{+0.013}_{-0.014}$	$0.142^{+0.029}_{-0.032}$	$0.032^{+0.019}_{-0.022}$	$0.27^{+0.06}_{-0.05}$
Reducible	$9.1^{+3.4}_{-4.4}$	$2.0^{+1.5}_{-1.7}$	$0.15^{+0.54}_{-0.15}$	0.4 ± 0.4	$1.2^{+2.3}_{-1.2}$	$2.6^{+1.9}_{-2.2}$	$0.00^{+0.19}_{-0.00}$
	SR1$^{\text{loose}}_{\text{bveto}}$	SR1$^{\text{tight}}_{\text{bveto}}$	SR1$_{\text{breq}}$	SR2$^{\text{loose}}_{\text{bveto}}$	SR2$^{\text{tight}}_{\text{bveto}}$	SR2$_{\text{breq}}$	SR5L
Observed	7	2	2	5	2	1	21
Total SM	$7.7^{+1.8}_{-1.9}$	$1.6^{+0.6}_{-0.7}$	2.2 ± 0.7	$3.4^{+2.8}_{-1.6}$	$0.35^{+0.44}_{-0.13}$	$0.52^{+0.50}_{-0.13}$	12.4 ± 2.3
ZZ	$2.0^{+0.4}_{-0.6}$	$0.39^{+0.13}_{-0.19}$	0.04 ± 0.04	$1.54^{+0.3}_{-0.4}$	$0.23^{+0.08}_{-0.13}$	0.06 ± 0.06	0.49 ± 0.04
$t\bar{t}Z$	0.19 ± 0.1	$0.029^{+0.047}_{-0.029}$	0.22 ± 0.06	$0.058^{+0.024}_{-0.025}$	0.0 ± 0.0	0.19 ± 0.07	0.034 ± 0.009
Higgs	0.24 ± 0.07	$0.033^{+0.019}_{-0.020}$	$0.14^{+0.05}_{-0.06}$	0.2 ± 0.04	$0.033^{+0.010}_{-0.011}$	0.2 ± 0.07	0.96 ± 0.14
VVV	$0.66^{+0.16}_{-0.17}$	$0.16^{+0.04}_{-0.05}$	0.021 ± 0.008	$0.38^{+0.09}_{-0.10}$	$0.084^{+0.025}_{-0.027}$	$0.024^{+0.009}_{-0.010}$	$3.0^{+0.6}_{-0.7}$
Other	0.009 ± 0.005	$0.02^{+0.013}_{-0.018}$	$0.183^{+0.039}_{-0.034}$	0.005 ± 0.005	0.0014 ± 0.0012	$0.054^{+0.019}_{-0.015}$	0.22 ± 0.19
Reducible	4.7 ± 1.7	1.0 ± 0.6	1.6 ± 0.7	$1.2^{+2.8}_{-1.2}$	$0.0^{+0.4}_{-0.0}$	$0.0^{+0.5}_{-0.0}$	7.7 ± 2.1

Table 9. Expected and observed yields for 139 fb^{-1} in the signal regions after the background-only fit. "Other" is the sum of the tWZ, $t\bar{t}WW$, $t\bar{t}ZZ$, $t\bar{t}WZ$, $t\bar{t}WH$, $t\bar{t}HH$, $t\bar{t}tW$, and $t\bar{t}t\bar{t}$ backgrounds. Both the statistical and systematic uncertainties in the SM background are included in the uncertainties shown.

10 Results

The observed number of events in each signal region is reported in table 9 and figure 7, along with the background expectations and uncertainties. The $E_{\text{T}}^{\text{miss}}$ and m_{eff} distributions for all events passing signal region requirements, except the $E_{\text{T}}^{\text{miss}}$ or m_{eff} requirement itself, are shown in figures 8–10.

The HistFitter software framework is used for the statistical interpretation of the results. In order to quantify the probability for the background-only hypothesis to fluctuate to the observed number of events or higher, a one-sided p_0-value is calculated using pseudo-experiments, where the profile likelihood ratio is used as a test statistic [125] to exclude the signal-plus-background hypothesis. Signal contamination in the CRs is assumed to be zero in this model-independent fit. The observations are consistent with the SM expectations, with SR5L giving rise to the highest local significance of 1.9σ.

A signal model can be excluded at 95% confidence level (CL) if the CL$_{\text{s}}$ [126] of the signal-plus-background hypothesis is below 0.05. For each signal region, the expected and observed upper limits at 95% CL on the number of beyond-the-SM events (S_{exp}^{95} and S_{obs}^{95})

JHEP07(2021)167

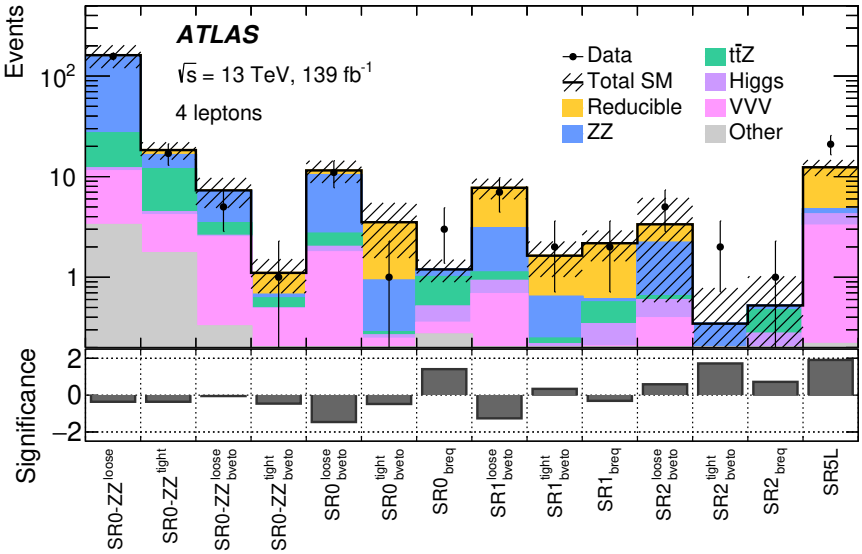

Figure 7. Expected and observed yields in the signal regions after the background-only fit. "Other" is the sum of the tWZ, $t\bar{t}WW$, $t\bar{t}ZZ$, $t\bar{t}WZ$, $t\bar{t}WH$, $t\bar{t}HH$, $t\bar{t}tW$, and $t\bar{t}t\bar{t}$ backgrounds. Both the statistical and systematic uncertainties in the SM background are included in the uncertainties shown. The significance of any difference between observed and expected yields is shown in the bottom panel, calculated with the profile likelihood method from ref. [124].

are calculated using the model-independent signal fit. The 95% CL upper limits on the signal cross-section times efficiency ($\langle\epsilon\sigma\rangle^{95}_{\text{obs}}$) also calculated for each signal region and shown in table 10.

Exclusion limits at 95% CL are calculated for the SUSY models and shown in figure 11. A statistical combination is performed using the results from a number of disjoint signal regions targeting the SUSY model, and signal contamination in the CRs used to constrain ZZ and $t\bar{t}Z$ background is accounted for. Where two (or more) signal regions overlap, the signal region with the better (best) expected exclusion is used in the combination: specifically either $\texttt{SR0-ZZ}^{\text{loose}}$ or $\texttt{SR0-ZZ}^{\text{tight}}$ or $\texttt{SR0-ZZ}^{\text{loose}}_{\text{bveto}}$ or $\texttt{SR0-ZZ}^{\text{tight}}_{\text{bveto}}$, and either $\texttt{SR0}^{\text{loose}}_{\text{bveto}}$ or $\texttt{SR0}^{\text{tight}}_{\text{bveto}}$, and either $\texttt{SR1}^{\text{loose}}_{\text{bveto}}$ or $\texttt{SR1}^{\text{tight}}_{\text{bveto}}$, and either $\texttt{SR2}^{\text{loose}}_{\text{bveto}}$ or $\texttt{SR2}^{\text{tight}}_{\text{bveto}}$. The four-lepton signal regions are more sensitive than SR5L in all signal models considered and so SR5L is not used to calculate model-dependent exclusion limits.

For the exclusion limits, the observed and expected 95% CL limits take into account the theoretical and experimental uncertainties in the SM background and the experimental uncertainties in the signal. For all expected and observed exclusion limit contours, the $\pm1\sigma_{\text{exp}}$ uncertainty band shows the impact on the expected limit of the systematic and statistical uncertainties included in the fit. The $\pm1\sigma^{\text{SUSY}}_{\text{theory}}$ uncertainty lines around the observed limit illustrate the change in the observed limit as the nominal signal cross-section is scaled up and down by the theoretical cross-section uncertainty. Experimental uncertainties affecting irreducible backgrounds and signal are treated as correlated between regions and processes, while uncertainties associated with the estimate of the reducible background are correlated

JHEP07(2021)167

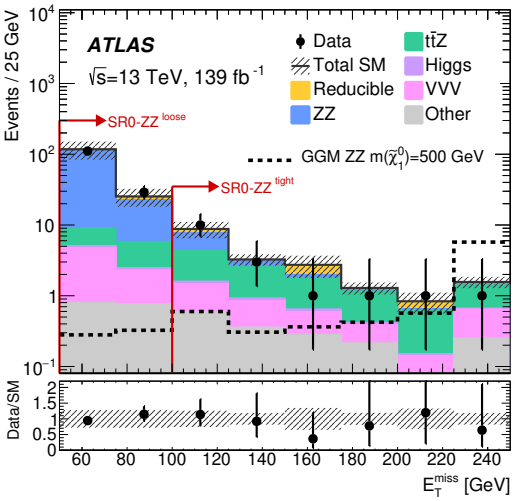

(a) $E_{\mathrm{T}}^{\mathrm{miss}}$ in SR0-ZZ$^{\mathrm{loose}}$ and SR0-ZZ$^{\mathrm{tight}}$.

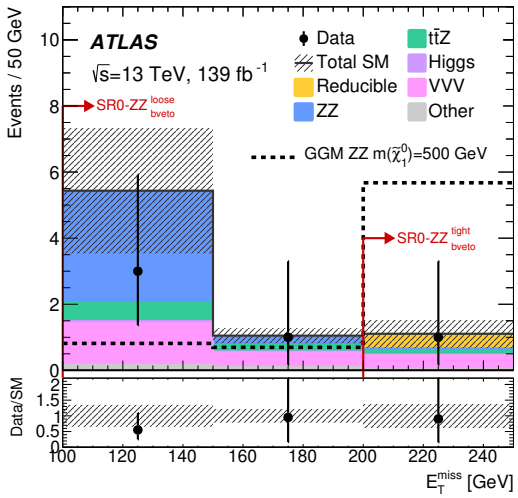

(b) $E_{\mathrm{T}}^{\mathrm{miss}}$ in SR0-ZZ$^{\mathrm{loose}}_{\mathrm{bveto}}$ and SR0-ZZ$^{\mathrm{tight}}_{\mathrm{bveto}}$.

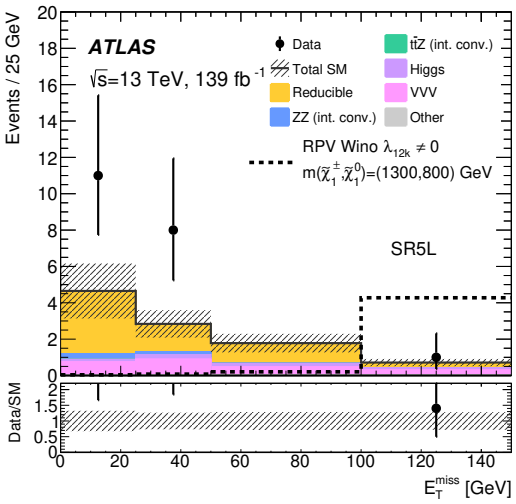

(c) $E_{\mathrm{T}}^{\mathrm{miss}}$ in SR5L.

Figure 8. The $E_{\mathrm{T}}^{\mathrm{miss}}$ distribution in (a) SR0-ZZ$^{\mathrm{loose}}$ and SR0-ZZ$^{\mathrm{tight}}$, (b) SR0-ZZ$^{\mathrm{loose}}_{\mathrm{bveto}}$ and SR0-ZZ$^{\mathrm{tight}}_{\mathrm{bveto}}$, and (c) SR5L for events passing the signal region requirements except the $E_{\mathrm{T}}^{\mathrm{miss}}$ requirement. Distributions for data, the estimated SM backgrounds after the background-only fit, and an example SUSY scenario are shown. "Other" is the sum of the tWZ, $t\bar{t}WW$, $t\bar{t}ZZ$, $t\bar{t}WZ$, $t\bar{t}WH$, $t\bar{t}HH$, $t\bar{t}tW$, and $t\bar{t}t\bar{t}$ backgrounds. The last bin captures the overflow events. The lower panel shows the ratio of the observed data to the expected SM background yield in each bin. Both the statistical and systematic uncertainties in the SM background are included in the shaded band. The red arrows indicate the $E_{\mathrm{T}}^{\mathrm{miss}}$ selections in the signal regions.

JHEP07(2021)167

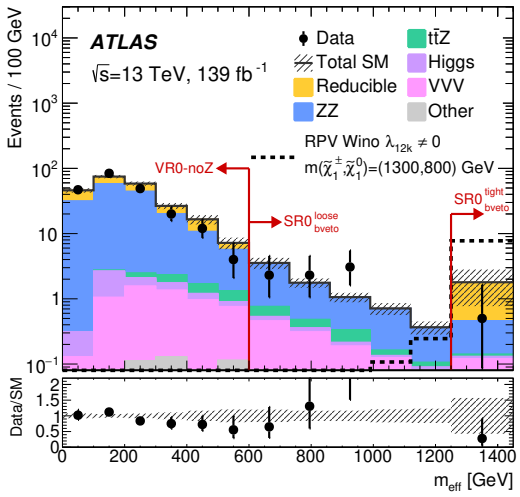

(a) m_{eff} in $\texttt{SR0}^{\text{loose}}_{\text{bveto}}$ and $\texttt{SR0}^{\text{tight}}_{\text{bveto}}$.

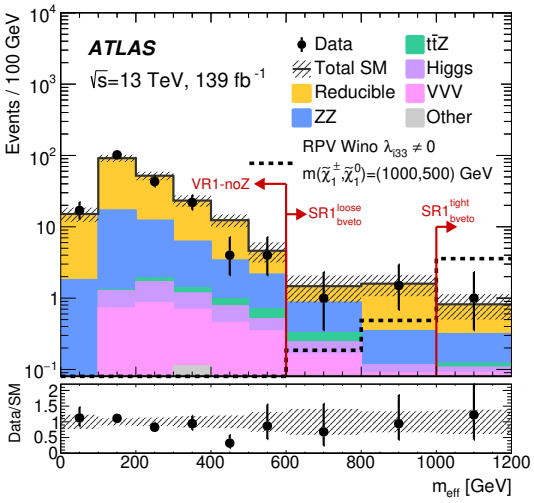

(b) m_{eff} in $\texttt{SR1}^{\text{loose}}_{\text{bveto}}$ and $\texttt{SR1}^{\text{tight}}_{\text{bveto}}$.

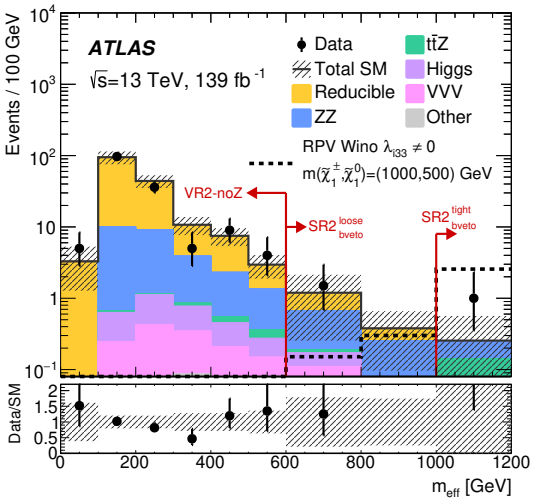

(c) m_{eff} in $\texttt{SR2}^{\text{loose}}_{\text{bveto}}$ and $\texttt{SR2}^{\text{tight}}_{\text{bveto}}$.

Figure 9. The m_{eff} distribution in (a) $\texttt{SR0}^{\text{loose}}_{\text{bveto}}$ and $\texttt{SR0}^{\text{tight}}_{\text{bveto}}$, (b) $\texttt{SR1}^{\text{loose}}_{\text{bveto}}$ and $\texttt{SR1}^{\text{tight}}_{\text{bveto}}$, and (c) $\texttt{SR2}^{\text{loose}}_{\text{bveto}}$ and $\texttt{SR2}^{\text{tight}}_{\text{bveto}}$ for events passing the signal region requirements except the m_{eff} requirement. Distributions for data, the estimated SM backgrounds after the background-only fit, and an example SUSY scenario are shown. "Other" is the sum of the tWZ, $t\bar{t}WW$, $t\bar{t}ZZ$, $t\bar{t}WZ$, $t\bar{t}WH$, $t\bar{t}HH$, $t\bar{t}tW$, and $t\bar{t}t\bar{t}$ backgrounds. The last bin captures the overflow events. The lower panel shows the ratio of the observed data to the expected SM background yield in each bin. Both the statistical and systematic uncertainties in the SM background are included in the shaded band. The red arrows indicate the m_{eff} selections in the signal and validation regions.

JHEP07(2021)167

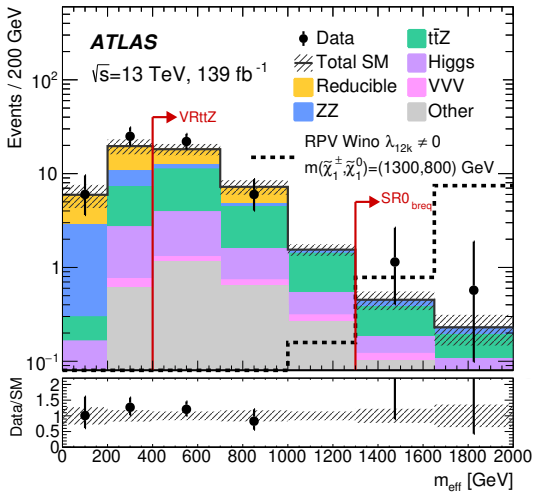

(a) m_{eff} in $\texttt{SR0}_{\text{breq}}$.

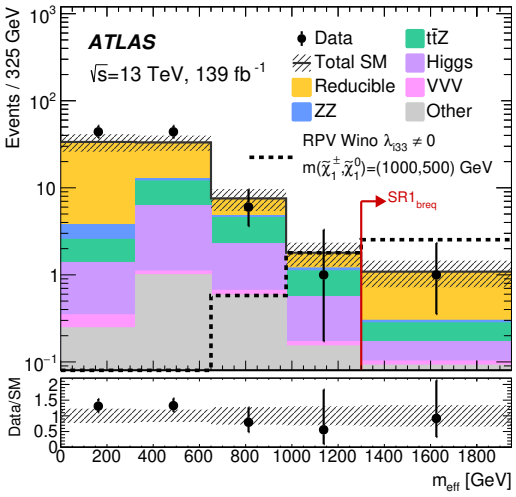

(b) m_{eff} in $\texttt{SR1}_{\text{breq}}$.

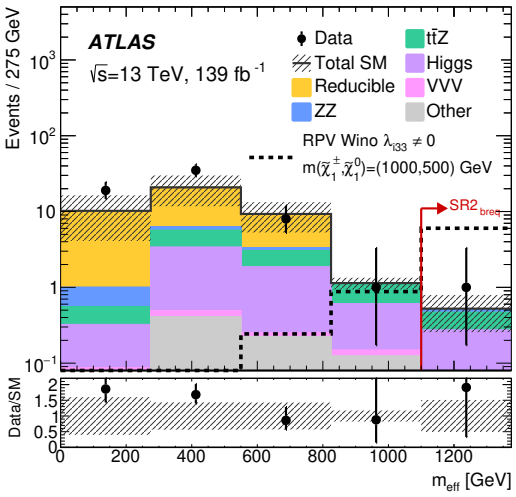

(c) m_{eff} in $\texttt{SR2}_{\text{breq}}$.

Figure 10. The m_{eff} distribution in (a) $\texttt{SR0}_{\text{breq}}$, (b) $\texttt{SR1}_{\text{breq}}$, and (c) $\texttt{SR2}_{\text{breq}}$ for events passing the signal region requirements except the m_{eff} requirement. Distributions for data, the estimated SM backgrounds after the background-only fit, and an example SUSY scenario are shown. "Other" is the sum of the tWZ, $t\bar{t}WW$, $t\bar{t}ZZ$, $t\bar{t}WZ$, $t\bar{t}WH$, $t\bar{t}HH$, $t\bar{t}tW$, and $t\bar{t}t\bar{t}$ backgrounds. The last bin captures the overflow events. The lower panel shows the ratio of the observed data to the expected SM background yield in each bin. Both the statistical and systematic uncertainties in the SM background are included in the shaded band. The red arrows indicate the m_{eff} selections in the signal and validation regions.

JHEP07(2021)167

	$\langle\epsilon\sigma\rangle^{95}_{\text{obs}}$ [fb]	S^{95}_{obs}	S^{95}_{exp}
SR0-ZZ$^{\text{loose}}$	0.481	66.86	$67.43^{+20.43}_{-15.71}$
SR0-ZZ$^{\text{tight}}$	0.081	11.28	$11.52^{+4.81}_{-3.34}$
SR0-ZZ$^{\text{loose}}_{\text{bveto}}$	0.043	6.01	$7.10^{+2.82}_{-1.90}$
SR0-ZZ$^{\text{tight}}_{\text{bveto}}$	0.028	3.87	$3.63^{+1.44}_{-0.63}$
SR0$^{\text{loose}}_{\text{bveto}}$	0.070	9.79	$8.28^{+3.58}_{-2.30}$
SR0$^{\text{tight}}_{\text{bveto}}$	0.028	3.87	$4.29^{+1.56}_{-0.86}$
SR0$_{\text{breq}}$	0.046	6.33	$3.78^{+1.59}_{-0.66}$
SR1$^{\text{loose}}_{\text{bveto}}$	0.046	6.37	$7.46^{+2.92}_{-2.04}$
SR1$^{\text{tight}}_{\text{bveto}}$	0.032	4.47	$4.22^{+1.63}_{-1.04}$
SR1$_{\text{breq}}$	0.033	4.56	$4.59^{+1.77}_{-1.22}$
SR2$^{\text{loose}}_{\text{bveto}}$	0.061	8.45	$7.45^{+2.36}_{-1.24}$
SR2$^{\text{tight}}_{\text{bveto}}$	0.041	5.63	$3.53^{+1.06}_{-0.15}$
SR2$_{\text{breq}}$	0.030	4.17	$3.16^{+1.20}_{-0.16}$
SR5L	0.129	17.88	$9.88^{+4.08}_{-2.44}$

Table 10. The model-independent limits calculated from the signal region observations; the 95% CL upper limit on the visible cross-section times efficiency ($\langle\epsilon\sigma\rangle^{95}_{\text{obs}}$), the observed number of signal events(S^{95}_{obs}), and the signal events given the expected number of background events (S^{95}_{exp}, $\pm1\sigma$ variations of the expected number) calculated by performing pseudo-experiments for each signal region.

between regions only. Theoretical uncertainties in the irreducible background and signal are treated as correlated between regions, while statistical uncertainties from MC simulation and data in the CR are treated as uncorrelated between regions and processes.

The exclusion contours for the higgsino GGM models are shown in figure 11a, where SR0-ZZ$^{\text{loose}}_{\text{bveto}}$ and SR0-ZZ$^{\text{tight}}_{\text{bveto}}$ dominate the exclusion for low and high higgsino masses, respectively. The analysis is more sensitive to scenarios with higher $\mathcal{B}(\tilde{\chi}^0_1 \to Z + \tilde{G})$ as they produce more four-lepton events. For scenarios with $\mathcal{B}(\tilde{\chi}^0_1 \to h + \tilde{G}) = 100\%$, final states with lower lepton multiplicity are more sensitive [127]. Higgsino masses up to 540 GeV are excluded for $\mathcal{B}(\tilde{\chi}^0_1 \to Z + \tilde{G}) = 100\%$, while the exclusion is weaker for scenarios with $\mathcal{B}(\tilde{\chi}^0_1 \to Z + \tilde{G}) < 100\%$. These results significantly improve upon limits in ref. [18] by around 200–260 GeV, and in particular, set stronger limits for scenarios with $\mathcal{B}(\tilde{\chi}^0_1 \to Z + \tilde{G}) < 100\%$.

Figure 11 also shows the exclusion contours for the RPV models considered here, where the limits extend to high NLSP masses due to the high lepton multiplicity in these scenarios ($\tilde{\chi}^0_1 \to \ell\ell\nu$ with 100% branching ratio) and the high efficiency of the m_{eff} selections. The exclusion in the $LL\bar{E}12k$ models is dominated by the combination of SR0$^{\text{tight}}_{\text{bveto}}$ and SR0$_{\text{breq}}$ while the combination of SR1$^{\text{tight}}_{\text{bveto}}$ and SR2$^{\text{tight}}_{\text{bveto}}$ is important for the $LL\bar{E}i33$ models. The sensitivity is reduced for large mass splittings between the NLSP and the $\tilde{\chi}^0_1$, where the decay products are strongly boosted. These results improve on the limits set in similar models in ref. [18] by around 100–350 GeV.

JHEP07(2021)167

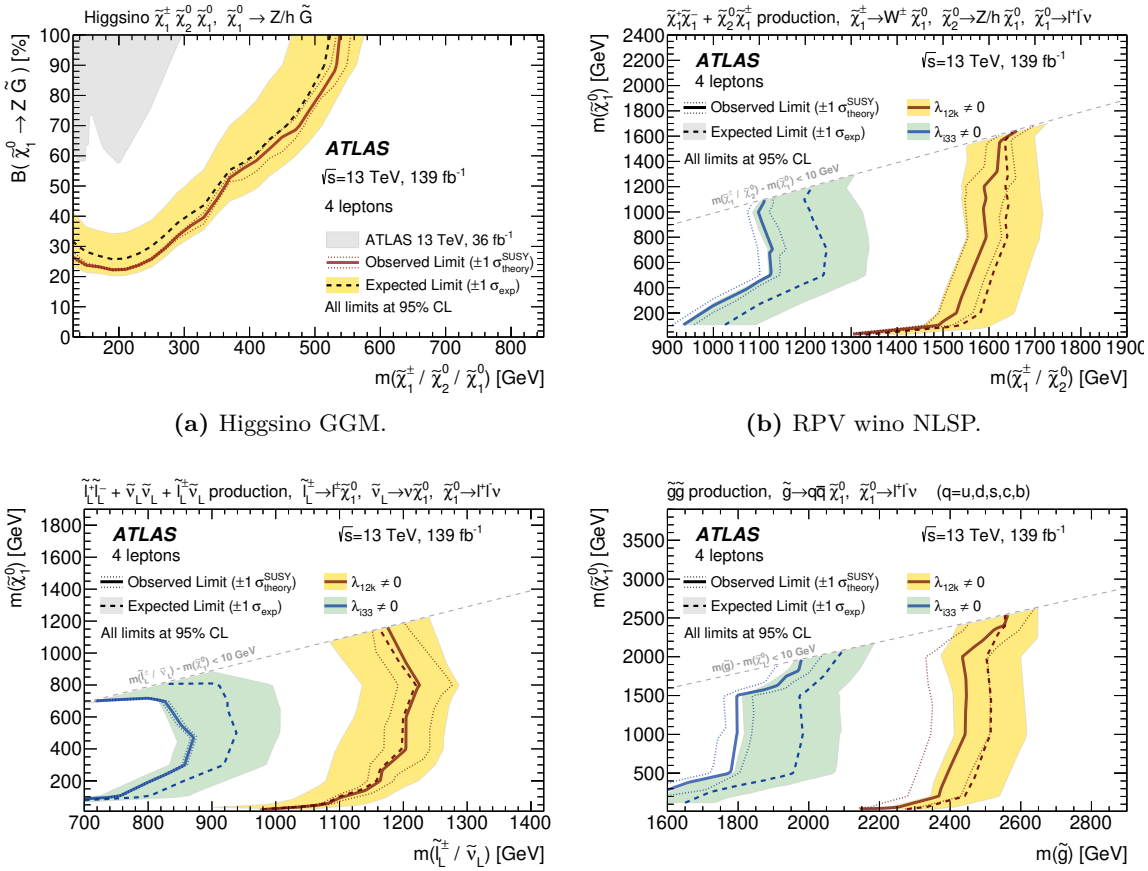

(a) Higgsino GGM. **(b)** RPV wino NLSP.

(c) RPV $\tilde{\ell}_L/\tilde{\nu}$ NLSP. **(d)** RPV $\tilde{g}$ NLSP.

Figure 11. Expected (dashed) and observed (solid) 95% CL exclusion limits on (a) the higgsino GGM models, and (b) wino NLSP, (c) $\tilde{\ell}_L/\tilde{\nu}$ NLSP, and (d) gluino NLSP pair production with RPV $\tilde{\chi}_1^0$ decays via λ_{12k}, or λ_{i33} where $i,k \in 1,2$. The limits are set using a statistical combination of disjoint signal regions. Where two (or more) signal regions overlap, the signal region contributing its observed CL_s value to the combination is the one with the better (best) expected CL_s value.

The exclusion contours for the RPV wino NLSP $LL\bar{E}12k$ models are shown in figure 11b, where $\tilde{\chi}_1^\pm/\tilde{\chi}_2^0$ masses up to $\sim 1.6\,\text{TeV}$ are excluded for $m(\tilde{\chi}_1^0) > 800\,\text{GeV}$. Figure 11b also shows exclusion contours for the RPV wino NLSP $LL\bar{E}i33$ models, where $\tilde{\chi}_1^\pm/\tilde{\chi}_2^0$ masses up to $\sim 1.13\,\text{TeV}$ are excluded for $500\,\text{GeV} < m(\tilde{\chi}_1^0) < 700\,\text{GeV}$. Figure 11c shows exclusion contours for the RPV $\tilde{\ell}_L/\tilde{\nu}$ NLSP model, where left-handed slepton/sneutrino masses are excluded up to $\sim 1.2\,\text{TeV}$ for $m(\tilde{\chi}_1^0) \simeq 800\,\text{GeV}$ for $LL\bar{E}12k$ models, and up to 0.87 TeV for $m(\tilde{\chi}_1^0) \simeq 500\,\text{GeV}$ for $LL\bar{E}i33$ models. Finally, the exclusion contours for the RPV $\tilde{g}$ NLSP model are shown in figure 11d, where gluino masses are excluded up to $\sim 2.45\,\text{TeV}$ for $m(\tilde{\chi}_1^0) > 1\,\text{TeV}$ for $LL\bar{E}12k$ models, increasing to $\sim 2.55\,\text{TeV}$ for $m(\tilde{\chi}_1^0) > 2.4\,\text{TeV}$. For $LL\bar{E}i33$ models, gluino masses are excluded up to $\sim 1.78\,\text{TeV}$ for $m(\tilde{\chi}_1^0) > 500\,\text{GeV}$, increasing to $\sim 1.97\,\text{TeV}$ for $m(\tilde{\chi}_1^0) > 1.8\,\text{TeV}$.

JHEP07(2021)167

11 Conclusion

A search for new physics in final states with four or more leptons (electrons, muons or hadronically decaying τ-leptons) is presented, using 139 fb^{-1} of $\sqrt{s} = 13$ TeV pp collision data collected by the ATLAS detector at the LHC from 2015 to 2018. No significant excess over the expected background is observed. Observed 95% CL limits on the visible cross-section are placed in each signal region, and the null result is interpreted in simplified higgsino GGM models, where higgsino $\tilde{\chi}_1^{\pm}/\tilde{\chi}_2^0/\tilde{\chi}_1^0$ masses up to 540 GeV are excluded in scenarios with a 100% branching ratio for $\tilde{\chi}_1^0$ decay into a Z boson and a gravitino. This significantly improves upon previous GGM higgsino mass limits by around 200–260 GeV. The results are also interpreted in simplified models of NLSP pair production with RPV LSP decays, where wino $\tilde{\chi}_1^{\pm}/\tilde{\chi}_2^0$, $\tilde{\ell}_{\mathrm{L}}/\tilde{\nu}$, and $\tilde{g}$ masses up to 1.6 TeV, 1.2 TeV, and 2.5 TeV are excluded, respectively, improving upon previous limits set in similar models by around 100–350 GeV.

Acknowledgments

We thank CERN for the very successful operation of the LHC, as well as the support staff from our institutions without whom ATLAS could not be operated efficiently.

We acknowledge the support of ANPCyT, Argentina; YerPhI, Armenia; ARC, Australia; BMWFW and FWF, Austria; ANAS, Azerbaijan; SSTC, Belarus; CNPq and FAPESP, Brazil; NSERC, NRC and CFI, Canada; CERN; ANID, Chile; CAS, MOST and NSFC, China; Minciencias, Colombia; MSMT CR, MPO CR and VSC CR, Czech Republic; DNRF and DNSRC, Denmark; IN2P3-CNRS and CEA-DRF/IRFU, France; SRNSFG, Georgia; BMBF, HGF and MPG, Germany; GSRT, Greece; RGC and Hong Kong SAR, China; ISF and Benoziyo Center, Israel; INFN, Italy; MEXT and JSPS, Japan; CNRST, Morocco; NWO, Netherlands; RCN, Norway; MNiSW and NCN, Poland; FCT, Portugal; MNE/IFA, Romania; JINR; MES of Russia and NRC KI, Russian Federation; MESTD, Serbia; MSSR, Slovakia; ARRS and MIZŠ, Slovenia; DST/NRF, South Africa; MICINN, Spain; SRC and Wallenberg Foundation, Sweden; SERI, SNSF and Cantons of Bern and Geneva, Switzerland; MOST, Taiwan; TAEK, Turkey; STFC, United Kingdom; DOE and NSF, United States of America. In addition, individual groups and members have received support from BCKDF, CANARIE, Compute Canada, CRC and IVADO, Canada; Beijing Municipal Science & Technology Commission, China; COST, ERC, ERDF, Horizon 2020 and Marie Skłodowska-Curie Actions, European Union; Investissements d'Avenir Labex, Investissements d'Avenir Idex and ANR, France; DFG and AvH Foundation, Germany; Herakleitos, Thales and Aristeia programmes co-financed by EU-ESF and the Greek NSRF, Greece; BSF-NSF and GIF, Israel; La Caixa Banking Foundation, CERCA Programme Generalitat de Catalunya and PROMETEO and GenT Programmes Generalitat Valenciana, Spain; Göran Gustafssons Stiftelse, Sweden; The Royal Society and Leverhulme Trust, United Kingdom.

The crucial computing support from all WLCG partners is acknowledged gratefully, in particular from CERN, the ATLAS Tier-1 facilities at TRIUMF (Canada), NDGF

JHEP07(2021)167

(Denmark, Norway, Sweden), CC-IN2P3 (France), KIT/GridKA (Germany), INFN-CNAF (Italy), NL-T1 (Netherlands), PIC (Spain), ASGC (Taiwan), RAL (U.K.) and BNL (U.S.A.), the Tier-2 facilities worldwide and large non-WLCG resource providers. Major contributors of computing resources are listed in ref. [128].

References

[1] Y.A. Golfand and E.P. Likhtman, *Extension of the algebra of Poincaré group generators and violation of p invariance*, *JETP Lett.* **13** (1971) 323 [*Pisma Zh. Eksp. Teor. Fiz.* **13** (1971) 452] [INSPIRE].

[2] D.V. Volkov and V.P. Akulov, *Is the neutrino a Goldstone particle?*, *Phys. Lett. B* **46** (1973) 109 [INSPIRE].

[3] J. Wess and B. Zumino, *Supergauge transformations in four-dimensions*, *Nucl. Phys. B* **70** (1974) 39 [INSPIRE].

[4] J. Wess and B. Zumino, *Supergauge invariant extension of quantum electrodynamics*, *Nucl. Phys. B* **78** (1974) 1 [INSPIRE].

[5] S. Ferrara and B. Zumino, *Supergauge invariant Yang-Mills theories*, *Nucl. Phys. B* **79** (1974) 413.

[6] A. Salam and J.A. Strathdee, *Supersymmetry and non-Abelian gauges*, *Phys. Lett. B* **51** (1974) 353 [INSPIRE].

[7] ATLAS collaboration, *Luminosity determination in pp collisions at* $\sqrt{s} = 13$ *TeV using the ATLAS detector at the LHC*, Tech. Rep. ATLAS-CONF-2019-021, CERN, Geneva, Switzerland (2019).

[8] D0 collaboration, *Search for supersymmetry via associated production of charginos and neutralinos in final states with three leptons*, *Phys. Rev. Lett.* **95** (2005) 151805 [hep-ex/0504032] [INSPIRE].

[9] D0 collaboration, *Search for associated production of charginos and neutralinos in the trilepton final state using* $2.3\,fb^{-1}$ *of data*, *Phys. Lett. B* **680** (2009) 34 [arXiv:0901.0646] [INSPIRE].

[10] D0 collaboration, *Search for R-parity violating supersymmetry via the* $LL\bar{E}$ *couplings* λ_{121}, λ_{122} *or* λ_{133} *in* $p\bar{p}$ *collisions at* $\sqrt{s} = 1.96$ *TeV*, *Phys. Lett. B* **638** (2006) 441 [hep-ex/0605005] [INSPIRE].

[11] CDF collaboration, *Search for chargino-neutralino production in* $p\bar{p}$ *collisions at* $\sqrt{s} = 1.96$ *TeV*, *Phys. Rev. Lett.* **99** (2007) 191806 [arXiv:0707.2362] [INSPIRE].

[12] CDF collaboration, *Search for supersymmetry in* $p\bar{p}$ *collisions at* $\sqrt{s} = 1.96$ *TeV using the trilepton signature of chargino-neutralino production*, *Phys. Rev. Lett.* **101** (2008) 251801 [arXiv:0808.2446] [INSPIRE].

[13] CDF collaboration, *Search for anomalous production of multi-lepton events in* $p\bar{p}$ *collisions at* $\sqrt{s} = 1.96$ *TeV*, *Phys. Rev. Lett.* **98** (2007) 131804 [arXiv:0706.4448] [INSPIRE].

JHEP07(2021)167

[14] ATLAS collaboration, *Search for R-parity-violating supersymmetry in events with four or more leptons in $\sqrt{s} = 7$ TeV pp collisions with the ATLAS detector*, *JHEP* **12** (2012) 124 [arXiv:1210.4457] [INSPIRE].

[15] ATLAS collaboration, *Search for supersymmetry in events with three leptons and missing transverse momentum in $\sqrt{s} = 7$ TeV pp collisions with the ATLAS detector*, *Phys. Rev. Lett.* **108** (2012) 261804 [arXiv:1204.5638] [INSPIRE].

[16] ATLAS collaboration, *Search for direct production of charginos and neutralinos in events with three leptons and missing transverse momentum in $\sqrt{s} = 8$ TeV pp collisions with the ATLAS detector*, *JHEP* **04** (2014) 169 [arXiv:1402.7029] [INSPIRE].

[17] ATLAS collaboration, *Search for supersymmetry in events with four or more leptons in $\sqrt{s} = 8$ TeV pp collisions with the ATLAS detector*, *Phys. Rev. D* **90** (2014) 052001 [arXiv:1405.5086] [INSPIRE].

[18] ATLAS collaboration, *Search for supersymmetry in events with four or more leptons in $\sqrt{s} = 13$ TeV pp collisions with ATLAS*, *Phys. Rev. D* **98** (2018) 032009 [arXiv:1804.03602] [INSPIRE].

[19] ATLAS collaboration, *Search for chargino-neutralino production using recursive jigsaw reconstruction in final states with two or three charged leptons in proton-proton collisions at $\sqrt{s} = 13$ TeV with the ATLAS detector*, *Phys. Rev. D* **98** (2018) 092012 [arXiv:1806.02293] [INSPIRE].

[20] CMS collaboration, *Search for physics beyond the standard model using multilepton signatures in pp collisions at $\sqrt{s} = 7$ TeV*, *Phys. Lett. B* **704** (2011) 411 [arXiv:1106.0933] [INSPIRE].

[21] CMS collaboration, *Search for anomalous production of multilepton events in pp collisions at $\sqrt{s} = 7$ TeV*, *JHEP* **06** (2012) 169 [arXiv:1204.5341] [INSPIRE].

[22] CMS collaboration, *Search for top squarks in R-parity-violating supersymmetry using three or more leptons and B-tagged jets*, *Phys. Rev. Lett.* **111** (2013) 221801 [arXiv:1306.6643] [INSPIRE].

[23] CMS collaboration, *Search for anomalous production of events with three or more leptons in pp collisions at $\sqrt{s} = 8$ TeV*, *Phys. Rev. D* **90** (2014) 032006 [arXiv:1404.5801] [INSPIRE].

[24] CMS collaboration, *Search for electroweak production of charginos and neutralinos in multilepton final states in proton-proton collisions at $\sqrt{s} = 13$ TeV*, *JHEP* **03** (2018) 166 [arXiv:1709.05406] [INSPIRE].

[25] CMS collaboration, *Search for physics beyond the standard model in multilepton final states in proton-proton collisions at $\sqrt{s} = 13$ TeV*, *JHEP* **03** (2020) 051 [arXiv:1911.04968] [INSPIRE].

[26] N. Sakai, *Naturalness in supersymmetric GUTs*, *Z. Phys. C* **11** (1981) 153 [INSPIRE].

[27] S. Dimopoulos, S. Raby and F. Wilczek, *Supersymmetry and the scale of unification*, *Phys. Rev. D* **24** (1981) 1681 [INSPIRE].

[28] L.E. Ibáñez and G.G. Ross, *Low-energy predictions in supersymmetric grand unified theories*, *Phys. Lett. B* **105** (1981) 439 [INSPIRE].

[29] S. Dimopoulos and H. Georgi, *Softly broken supersymmetry and* SU(5), *Nucl. Phys. B* **193** (1981) 150.

JHEP07(2021)167

[30] SNO+ collaboration, *Search for invisible modes of nucleon decay in water with the SNO+ detector*, *Phys. Rev. D* **99** (2019) 032008 [arXiv:1812.05552] [INSPIRE].

[31] G.R. Farrar and P. Fayet, *Phenomenology of the production, decay, and detection of new hadronic states associated with supersymmetry*, *Phys. Lett. B* **76** (1978) 575 [INSPIRE].

[32] S. Weinberg, *Supersymmetry at ordinary energies. 1. Masses and conservation laws*, *Phys. Rev. D* **26** (1982) 287 [INSPIRE].

[33] N. Sakai and T. Yanagida, *Proton decay in a class of supersymmetric grand unified models*, *Nucl. Phys. B* **197** (1982) 533 [INSPIRE].

[34] H. Goldberg, *Constraint on the photino mass from cosmology*, *Phys. Rev. Lett.* **50** (1983) 1419 [*Erratum ibid.* **103** (2009) 099905] [INSPIRE].

[35] J.R. Ellis, J.S. Hagelin, D.V. Nanopoulos, K.A. Olive and M. Srednicki, *Supersymmetric relics from the big bang*, *Nucl. Phys. B* **238** (1984) 453 [INSPIRE].

[36] P. Fayet, *Supersymmetry and weak, electromagnetic and strong interactions*, *Phys. Lett. B* **64** (1976) 159 [INSPIRE].

[37] P. Fayet, *Spontaneously broken supersymmetric theories of weak, electromagnetic and strong interactions*, *Phys. Lett. B* **69** (1977) 489 [INSPIRE].

[38] M. Carena, S. Heinemeyer, O. Stål, C.E.M. Wagner and G. Weiglein, *MSSM Higgs boson searches at the LHC: benchmark scenarios after the discovery of a Higgs-like particle*, *Eur. Phys. J. C* **73** (2013) 2552 [arXiv:1302.7033] [INSPIRE].

[39] ATLAS collaboration, *Measurement of the Higgs boson mass in the $H \to ZZ^* \to 4\ell$ and $H \to \gamma\gamma$ channels with $\sqrt{s} = 13$ TeV pp collisions using the ATLAS detector*, *Phys. Lett. B* **784** (2018) 345 [arXiv:1806.00242] [INSPIRE].

[40] CMS collaboration, *A measurement of the Higgs boson mass in the diphoton decay channel*, *Phys. Lett. B* **805** (2020) 135425 [arXiv:2002.06398] [INSPIRE].

[41] ATLAS collaboration, *Combined measurements of Higgs boson production and decay using up to 80 fb^{-1} of proton-proton collision data at $\sqrt{s} = 13$ TeV collected with the ATLAS experiment*, *Phys. Rev. D* **101** (2020) 012002 [arXiv:1909.02845] [INSPIRE].

[42] CMS collaboration, *Combined measurements of Higgs boson couplings in proton-proton collisions at $\sqrt{s} = 13$ TeV*, *Eur. Phys. J. C* **79** (2019) 421 [arXiv:1809.10733] [INSPIRE].

[43] R. Barbieri and G.F. Giudice, *Upper bounds on supersymmetric particle masses*, *Nucl. Phys. B* **306** (1988) 63 [INSPIRE].

[44] B. de Carlos and J.A. Casas, *One loop analysis of the electroweak breaking in supersymmetric models and the fine tuning problem*, *Phys. Lett. B* **309** (1993) 320 [hep-ph/9303291] [INSPIRE].

[45] LEP SUSY Working Group, ALEPH, DELPHI, L3 and OPAL collaborations, *Combined LEP chargino results, up to* 208 *GeV for large* m_0, notes LEPSUSYWG/01-03.1, http://lepsusy.web.cern.ch/lepsusy/Welcome.html.

[46] LEP SUSY Working Group, ALEPH, DELPHI, L3 and OPAL collaborations, *Combined LEP selectron/smuon/stau results,* 183–208 *GeV*, notes LEPSUSYWG/04-01.1, http://lepsusy.web.cern.ch/lepsusy/Welcome.html.

[47] ATLAS collaboration, *Searches for electroweak production of supersymmetric particles with compressed mass spectra in $\sqrt{s} = 13$ TeV pp collisions with the ATLAS detector*, *Phys. Rev. D* **101** (2020) 052005 [arXiv:1911.12606] [INSPIRE].

JHEP07(2021)167

[48] CMS collaboration, *Search for new physics in events with two soft oppositely charged leptons and missing transverse momentum in proton-proton collisions at $\sqrt{s} = 13$ TeV*, *Phys. Lett. B* **782** (2018) 440 [arXiv:1801.01846] [INSPIRE].

[49] P. Meade, N. Seiberg and D. Shih, *General gauge mediation*, *Prog. Theor. Phys. Suppl.* **177** (2009) 143 [arXiv:0801.3278] [INSPIRE].

[50] A.B. Lahanas and D.V. Nanopoulos, *The road to no scale supergravity*, *Phys. Rept.* **145** (1987) 1 [INSPIRE].

[51] H.P. Nilles, *Supersymmetry, supergravity and particle physics*, *Phys. Rept.* **110** (1984) 1 [INSPIRE].

[52] J. Alwall, M.-P. Le, M. Lisanti and J.G. Wacker, *Searching for directly decaying gluinos at the Tevatron*, *Phys. Lett. B* **666** (2008) 34 [arXiv:0803.0019] [INSPIRE].

[53] J. Alwall, P. Schuster and N. Toro, *Simplified models for a first characterization of new physics at the LHC*, *Phys. Rev. D* **79** (2009) 075020 [arXiv:0810.3921] [INSPIRE].

[54] LHC New Physics Working Group collaboration, *Simplified models for LHC new physics searches*, *J. Phys. G* **39** (2012) 105005 [arXiv:1105.2838] [INSPIRE].

[55] R. Barbier et al., *R-parity violating supersymmetry*, *Phys. Rept.* **420** (2005) 1 [hep-ph/0406039] [INSPIRE].

[56] ATLAS collaboration, *Search for massive, long-lived particles using multitrack displaced vertices or displaced lepton pairs in pp collisions at $\sqrt{s} = 8$ TeV with the ATLAS detector*, *Phys. Rev. D* **92** (2015) 072004 [arXiv:1504.05162] [INSPIRE].

[57] ATLAS collaboration, *Search for displaced vertices of oppositely charged leptons from decays of long-lived particles in pp collisions at $\sqrt{s} = 13$ TeV with the ATLAS detector*, *Phys. Lett. B* **801** (2020) 135114 [arXiv:1907.10037] [INSPIRE].

[58] ATLAS collaboration, *The ATLAS experiment at the CERN Large Hadron Collider*, 2008 *JINST* **3** S08003 [INSPIRE].

[59] ATLAS collaboration, *ATLAS insertable B-layer technical design report*, Tech. Rep. ATLAS-TDR-19, CERN, Geneva, Switzerland (2010) [CERN-LHCC-2010-013].

[60] ATLAS IBL collaboration, *Production and integration of the ATLAS insertable B-layer*, 2018 *JINST* **13** T05008 [arXiv:1803.00844] [INSPIRE].

[61] ATLAS collaboration, *ATLAS data quality operations and performance for* 2015–2018 *data-taking*, 2020 *JINST* **15** P04003 [arXiv:1911.04632] [INSPIRE].

[62] ATLAS collaboration, *Performance of electron and photon triggers in ATLAS during LHC run* 2, *Eur. Phys. J. C* **80** (2020) 47 [arXiv:1909.00761] [INSPIRE].

[63] ATLAS collaboration, *Performance of the ATLAS muon triggers in run* 2, 2020 *JINST* **15** P09015 [arXiv:2004.13447] [INSPIRE].

[64] L. Lönnblad and S. Prestel, *Merging multi-leg NLO matrix elements with parton showers*, *JHEP* **03** (2013) 166 [arXiv:1211.7278] [INSPIRE].

[65] W. Beenakker, R. Höpker, M. Spira and P.M. Zerwas, *Squark and gluino production at hadron colliders*, *Nucl. Phys. B* **492** (1997) 51 [hep-ph/9610490] [INSPIRE].

[66] A. Kulesza and L. Motyka, *Threshold resummation for squark-antisquark and gluino-pair production at the LHC*, *Phys. Rev. Lett.* **102** (2009) 111802 [arXiv:0807.2405] [INSPIRE].

JHEP07(2021)167

[67] A. Kulesza and L. Motyka, *Soft gluon resummation for the production of gluino-gluino and squark-antisquark pairs at the LHC*, *Phys. Rev. D* **80** (2009) 095004 [arXiv:0905.4749] [INSPIRE].

[68] W. Beenakker, S. Brensing, M. Krämer, A. Kulesza, E. Laenen and I. Niessen, *Soft-gluon resummation for squark and gluino hadroproduction*, *JHEP* **12** (2009) 041 [arXiv:0909.4418] [INSPIRE].

[69] W. Beenakker et al., *Squark and gluino hadroproduction*, *Int. J. Mod. Phys. A* **26** (2011) 2637 [arXiv:1105.1110] [INSPIRE].

[70] B. Fuks, M. Klasen, D.R. Lamprea and M. Rothering, *Gaugino production in proton-proton collisions at a center-of-mass energy of* 8 *TeV*, *JHEP* **10** (2012) 081 [arXiv:1207.2159] [INSPIRE].

[71] B. Fuks, M. Klasen, D.R. Lamprea and M. Rothering, *Precision predictions for electroweak superpartner production at hadron colliders with Resummino*, *Eur. Phys. J. C* **73** (2013) 2480 [arXiv:1304.0790] [INSPIRE].

[72] B. Fuks, M. Klasen, D.R. Lamprea and M. Rothering, *Revisiting slepton pair production at the Large Hadron Collider*, *JHEP* **01** (2014) 168 [arXiv:1310.2621] [INSPIRE].

[73] C. Borschensky et al., *Squark and gluino production cross sections in pp collisions at* $\sqrt{s} = 13$, 14, 33 *and* 100 *TeV*, *Eur. Phys. J. C* **74** (2014) 3174 [arXiv:1407.5066] [INSPIRE].

[74] ATLAS collaboration, *Improvements in* $t\bar{t}$ *modelling using NLO+PS Monte Carlo generators for run*2, Tech. Rep. ATL-PHYS-PUB-2018-009, CERN, Geneva, Switzerland (2018).

[75] ATLAS collaboration, *ATLAS simulation of boson plus jets processes in run* 2, Tech. Rep. ATL-PHYS-PUB-2017-006, CERN, Geneva, Switzerland (2017).

[76] GEANT4 collaboration, *GEANT4 — a simulation toolkit*, *Nucl. Instrum. Meth. A* **506** (2003) 250 [INSPIRE].

[77] ATLAS collaboration, *The ATLAS simulation infrastructure*, *Eur. Phys. J. C* **70** (2010) 823 [arXiv:1005.4568] [INSPIRE].

[78] ATLAS collaboration, *The simulation principle and performance of the ATLAS fast calorimeter simulation FastCaloSim*, Tech. Rep. ATL-PHYS-PUB-2010-013, CERN, Geneva, Switzerland (2010).

[79] T. Sjöstrand et al., *An introduction to PYTHIA* 8.2, *Comput. Phys. Commun.* **191** (2015) 159 [arXiv:1410.3012] [INSPIRE].

[80] ATLAS collaboration, *The PYTHIA* 8 *A*3 *tune description of ATLAS minimum bias and inelastic measurements incorporating the Donnachie-Landshoff diffractive model*, Tech. Rep. ATL-PHYS-PUB-2016-017, CERN, Geneva, Switzerland (2016).

[81] A.D. Martin, W.J. Stirling, R.S. Thorne and G. Watt, *Parton distributions for the LHC*, *Eur. Phys. J. C* **63** (2009) 189 [arXiv:0901.0002] [INSPIRE].

[82] SHERPA collaboration, *Event generation with Sherpa* 2.2, *SciPost Phys.* **7** (2019) 034 [arXiv:1905.09127] [INSPIRE].

[83] ATLAS collaboration, *Multi-boson simulation for* 13 *TeV ATLAS analyses*, Tech. Rep. ATL-PHYS-PUB-2016-002, CERN, Geneva, Switzerland (2016).

JHEP07(2021)167

[84] NNPDF collaboration, *Parton distributions for the LHC run 2*, *JHEP* **04** (2015) 040 [arXiv:1410.8849] [INSPIRE].

[85] P. Nason, *A new method for combining NLO QCD with shower Monte Carlo algorithms*, *JHEP* **11** (2004) 040 [hep-ph/0409146] [INSPIRE].

[86] S. Frixione, P. Nason and C. Oleari, *Matching NLO QCD computations with parton shower simulations: the POWHEG method*, *JHEP* **11** (2007) 070 [arXiv:0709.2092] [INSPIRE].

[87] S. Alioli, P. Nason, C. Oleari and E. Re, *A general framework for implementing NLO calculations in shower Monte Carlo programs: the POWHEG BOX*, *JHEP* **06** (2010) 043 [arXiv:1002.2581] [INSPIRE].

[88] LHC Higgs Cross Section Working Group collaboration, *Handbook of LHC Higgs cross sections: 4. Deciphering the nature of the Higgs sector*, arXiv:1610.07922 [INSPIRE].

[89] C. Anastasiou et al., *High precision determination of the gluon fusion Higgs boson cross-section at the LHC*, *JHEP* **05** (2016) 058 [arXiv:1602.00695] [INSPIRE].

[90] C. Anastasiou, C. Duhr, F. Dulat, F. Herzog and B. Mistlberger, *Higgs boson gluon-fusion production in QCD at three loops*, *Phys. Rev. Lett.* **114** (2015) 212001 [arXiv:1503.06056] [INSPIRE].

[91] F. Dulat, A. Lazopoulos and B. Mistlberger, *iHixs 2 — inclusive Higgs cross sections*, *Comput. Phys. Commun.* **233** (2018) 243 [arXiv:1802.00827] [INSPIRE].

[92] U. Aglietti, R. Bonciani, G. Degrassi and A. Vicini, *Two loop light fermion contribution to Higgs production and decays*, *Phys. Lett. B* **595** (2004) 432 [hep-ph/0404071] [INSPIRE].

[93] S. Actis, G. Passarino, C. Sturm and S. Uccirati, *NLO electroweak corrections to Higgs boson production at hadron colliders*, *Phys. Lett. B* **670** (2008) 12 [arXiv:0809.1301] [INSPIRE].

[94] M. Bonetti, K. Melnikov and L. Tancredi, *Higher order corrections to mixed QCD-EW contributions to Higgs boson production in gluon fusion*, *Phys. Rev. D* **97** (2018) 056017 [*Erratum ibid.* **97** (2018) 099906] [arXiv:1801.10403] [INSPIRE].

[95] ATLAS collaboration, *Measurement of the Z/γ^* boson transverse momentum distribution in pp collisions at $\sqrt{s} = 7$ TeV with the ATLAS detector*, *JHEP* **09** (2014) 145 [arXiv:1406.3660] [INSPIRE].

[96] J. Pumplin, D.R. Stump, J. Huston, H.L. Lai, P.M. Nadolsky and W.K. Tung, *New generation of parton distributions with uncertainties from global QCD analysis*, *JHEP* **07** (2002) 012 [hep-ph/0201195] [INSPIRE].

[97] ATLAS collaboration, *ATLAS PYTHIA 8 tunes to 7 TeV data*, Tech. Rep. ATL-PHYS-PUB-2014-021, CERN, Geneva, Switzerland (2014).

[98] R.D. Ball et al., *Parton distributions with LHC data*, *Nucl. Phys. B* **867** (2013) 244 [arXiv:1207.1303] [INSPIRE].

[99] J. Alwall et al., *The automated computation of tree-level and next-to-leading order differential cross sections, and their matching to parton shower simulations*, *JHEP* **07** (2014) 079 [arXiv:1405.0301] [INSPIRE].

[100] ATLAS collaboration, *Modelling of the $t\bar{t}H$ and $t\bar{t}V$ ($V = W, Z$) processes for $\sqrt{s} = 13$ TeV ATLAS analyses*, Tech. Rep. ATL-PHYS-PUB-2016-005, CERN, Geneva, Switzerland (2016).

JHEP07(2021)167

[101] M. Beneke, P. Falgari, S. Klein and C. Schwinn, *Hadronic top-quark pair production with NNLL threshold resummation*, *Nucl. Phys. B* **855** (2012) 695 [arXiv:1109.1536] [INSPIRE].

[102] M. Cacciari, M. Czakon, M. Mangano, A. Mitov and P. Nason, *Top-pair production at hadron colliders with next-to-next-to-leading logarithmic soft-gluon resummation*, *Phys. Lett. B* **710** (2012) 612 [arXiv:1111.5869] [INSPIRE].

[103] P. Bärnreuther, M. Czakon and A. Mitov, *Percent level precision physics at the Tevatron: first genuine NNLO QCD corrections to $q\bar{q} \to t\bar{t} + X$*, *Phys. Rev. Lett.* **109** (2012) 132001 [arXiv:1204.5201] [INSPIRE].

[104] M. Czakon and A. Mitov, *NNLO corrections to top-pair production at hadron colliders: the all-fermionic scattering channels*, *JHEP* **12** (2012) 054 [arXiv:1207.0236] [INSPIRE].

[105] M. Czakon and A. Mitov, *NNLO corrections to top pair production at hadron colliders: the quark-gluon reaction*, *JHEP* **01** (2013) 080 [arXiv:1210.6832] [INSPIRE].

[106] M. Czakon, P. Fiedler and A. Mitov, *Total top-quark pair-production cross section at hadron colliders through $O(\alpha_S^4)$*, *Phys. Rev. Lett.* **110** (2013) 252004 [arXiv:1303.6254] [INSPIRE].

[107] M. Czakon and A. Mitov, *Top++: a program for the calculation of the top-pair cross-section at hadron colliders*, *Comput. Phys. Commun.* **185** (2014) 2930 [arXiv:1112.5675] [INSPIRE].

[108] C. Anastasiou, L.J. Dixon, K. Melnikov and F. Petriello, *High precision QCD at hadron colliders: electroweak gauge boson rapidity distributions at NNLO*, *Phys. Rev. D* **69** (2004) 094008 [hep-ph/0312266] [INSPIRE].

[109] ATLAS collaboration, *E_T^{miss} performance in the ATLAS detector using* 2015–2016 *LHC pp collisions*, Tech. Rep. ATLAS-CONF-2018-023, CERN, Geneva, Switzerland (2018).

[110] ATLAS collaboration, *Performance of missing transverse momentum reconstruction with the ATLAS detector using proton-proton collisions at $\sqrt{s} = 13$ TeV*, *Eur. Phys. J. C* **78** (2018) 903 [arXiv:1802.08168] [INSPIRE].

[111] ATLAS collaboration, *Electron and photon performance measurements with the ATLAS detector using the* 2015–2017 *LHC proton-proton collision data*, 2019 *JINST* **14** P12006 [arXiv:1908.00005] [INSPIRE].

[112] ATLAS collaboration, *Muon reconstruction and identification efficiency in ATLAS using the full run* 2 *pp collision data set at $\sqrt{s} = 13$ TeV*, *Eur. Phys. J. C* **81** (2021) 578 [arXiv:2012.00578] [INSPIRE].

[113] M. Cacciari, G.P. Salam and G. Soyez, *The anti-k_t jet clustering algorithm*, *JHEP* **04** (2008) 063 [arXiv:0802.1189] [INSPIRE].

[114] ATLAS collaboration, *Jet energy scale measurements and their systematic uncertainties in proton-proton collisions at $\sqrt{s} = 13$ TeV with the ATLAS detector*, *Phys. Rev. D* **96** (2017) 072002 [arXiv:1703.09665] [INSPIRE].

[115] ATLAS collaboration, *Selection of jets produced in* 13 *TeV proton-proton collisions with the ATLAS detector*, Tech. Rep. ATLAS-CONF-2015-029, CERN, Geneva, Switzerland (2015).

[116] ATLAS collaboration, *ATLAS b-jet identification performance and efficiency measurement with $t\bar{t}$ events in pp collisions at $\sqrt{s} = 13$ TeV*, *Eur. Phys. J. C* **79** (2019) 970 [arXiv:1907.05120] [INSPIRE].

JHEP07(2021)167

[117] ATLAS collaboration, *Measurement of the tau lepton reconstruction and identification performance in the ATLAS experiment using pp collisions at* $\sqrt{s} = 13$ *TeV*, Tech. Rep. ATLAS-CONF-2017-029, CERN, Geneva, Switzerland (2017).

[118] ATLAS collaboration, *Identification of hadronic tau lepton decays using neural networks in the ATLAS experiment*, Tech. Rep. ATL-PHYS-PUB-2019-033, CERN, Geneva, Switzerland (2019).

[119] ATLAS collaboration, *Performance of pile-up mitigation techniques for jets in pp collisions at* $\sqrt{s} = 8$ *TeV using the ATLAS detector*, *Eur. Phys. J. C* **76** (2016) 581 [arXiv:1510.03823] [INSPIRE].

[120] M. Baak, G.J. Besjes, D. Côté, A. Koutsman, J. Lorenz and D. Short, *HistFitter software framework for statistical data analysis*, *Eur. Phys. J. C* **75** (2015) 153 [arXiv:1410.1280] [INSPIRE].

[121] G. Avoni et al., *The new LUCID-2 detector for luminosity measurement and monitoring in ATLAS*, 2018 *JINST* **13** P07017 [INSPIRE].

[122] S. Dittmaier et al., *Handbook of LHC Higgs cross sections: 2. Differential distributions*, arXiv:1201.3084 [INSPIRE].

[123] S. Schumann and F. Krauss, *A parton shower algorithm based on Catani-Seymour dipole factorisation*, *JHEP* **03** (2008) 038 [arXiv:0709.1027] [INSPIRE].

[124] R.D. Cousins, J.T. Linnemann and J. Tucker, *Evaluation of three methods for calculating statistical significance when incorporating a systematic uncertainty into a test of the background-only hypothesis for a Poisson process*, *Nucl. Instrum. Meth. A* **595** (2008) 480 [physics/0702156] [INSPIRE].

[125] G. Cowan, K. Cranmer, E. Gross and O. Vitells, *Asymptotic formulae for likelihood-based tests of new physics*, *Eur. Phys. J. C* **71** (2011) 1554 [*Erratum ibid.* **73** (2013) 2501] [arXiv:1007.1727] [INSPIRE].

[126] A.L. Read, *Presentation of search results: the* CL_s *technique*, *J. Phys. G* **28** (2002) 2693 [INSPIRE].

[127] ATLAS collaboration, *Search for pair production of higgsinos in final states with at least three b-tagged jets in* $\sqrt{s} = 13$ *TeV pp collisions using the ATLAS detector*, *Phys. Rev. D* **98** (2018) 092002 [arXiv:1806.04030] [INSPIRE].

[128] ATLAS collaboration, *ATLAS computing acknowledgements*, Tech. Rep. ATL-SOFT-PUB-2020-001, CERN, Geneva, Switzerland (2020).

JHEP07(2021)167

The ATLAS collaboration

G. Aad[102], B. Abbott[128], D.C. Abbott[103], A. Abed Abud[36], K. Abeling[53], D.K. Abhayasinghe[94], S.H. Abidi[167], O.S. AbouZeid[40], N.L. Abraham[156], H. Abramowicz[161], H. Abreu[160], Y. Abulaiti[6], B.S. Acharya[67a,67b,o], B. Achkar[53], L. Adam[100], C. Adam Bourdarios[5], L. Adamczyk[84a], L. Adamek[167], J. Adelman[121], A. Adiguzel[12c,ad], S. Adorni[54], T. Adye[143], A.A. Affolder[145], Y. Afik[160], C. Agapopoulou[65], M.N. Agaras[38], A. Aggarwal[119], C. Agheorghiesei[27c], J.A. Aguilar-Saavedra[139f,139a,ac], A. Ahmad[36], F. Ahmadov[80], W.S. Ahmed[104], X. Ai[18], G. Aielli[74a,74b], S. Akatsuka[86], M. Akbiyik[100], T.P.A. Åkesson[97], E. Akilli[54], A.V. Akimov[111], K. Al Khoury[65], G.L. Alberghi[23b,23a], J. Albert[176], M.J. Alconada Verzini[161], S. Alderweireldt[36], M. Aleksa[36], I.N. Aleksandrov[80], C. Alexa[27b], T. Alexopoulos[10], A. Alfonsi[120], F. Alfonsi[23b,23a], M. Alhroob[128], B. Ali[141], S. Ali[158], M. Aliev[166], G. Alimonti[69a], C. Allaire[36], B.M.M. Allbrooke[156], B.W. Allen[131], P.P. Allport[21], A. Aloisio[70a,70b], F. Alonso[89], C. Alpigiani[148], E. Alunno Camelia[74a,74b], M. Alvarez Estevez[99], M.G. Alviggi[70a,70b], Y. Amaral Coutinho[81b], A. Ambler[104], L. Ambroz[134], C. Amelung[36], D. Amidei[106], S.P. Amor Dos Santos[139a], S. Amoroso[46], C.S. Amrouche[54], F. An[79], C. Anastopoulos[149], N. Andari[144], T. Andeen[11], J.K. Anders[20], S.Y. Andrean[45a,45b], A. Andreazza[69a,69b], V. Andrei[61a], C.R. Anelli[176], S. Angelidakis[9], A. Angerami[39], A.V. Anisenkov[122b,122a], A. Annovi[72a], C. Antel[54], M.T. Anthony[149], E. Antipov[129], M. Antonelli[51], D.J.A. Antrim[18], F. Anulli[73a], M. Aoki[82], J.A. Aparisi Pozo[174], M.A. Aparo[156], L. Aperio Bella[46], N. Aranzabal[36], V. Araujo Ferraz[81a], R. Araujo Pereira[81b], C. Arcangeletti[51], A.T.H. Arce[49], J-F. Arguin[110], S. Argyropoulos[52], J.-H. Arling[46], A.J. Armbruster[36], A. Armstrong[171], O. Arnaez[167], H. Arnold[120], Z.P. Arrubarrena Tame[114], G. Artoni[134], H. Asada[117], K. Asai[126], S. Asai[163], T. Asawatavonvanich[165], N.A. Asbah[59], E.M. Asimakopoulou[172], L. Asquith[156], J. Assahsah[35d], K. Assamagan[29], R. Astalos[28a], R.J. Atkin[33a], M. Atkinson[173], N.B. Atlay[19], H. Atmani[65], P.A. Atmasiddha[106], K. Augsten[141], V.A. Austrup[182], G. Avolio[36], M.K. Ayoub[15a], G. Azuelos[110,ak], D. Babal[28a], H. Bachacou[144], K. Bachas[162], F. Backman[45a,45b], P. Bagnaia[73a,73b], H. Bahrasemani[152], A.J. Bailey[174], V.R. Bailey[173], J.T. Baines[143], C. Bakalis[10], O.K. Baker[183], P.J. Bakker[120], E. Bakos[16], D. Bakshi Gupta[8], S. Balaji[157], R. Balasubramanian[120], E.M. Baldin[122b,122a], P. Balek[180], F. Balli[144], W.K. Balunas[134], J. Balz[100], E. Banas[85], M. Bandieramonte[138], A. Bandyopadhyay[19], Sw. Banerjee[181,j], L. Barak[161], W.M. Barbe[38], E.L. Barberio[105], D. Barberis[55b,55a], M. Barbero[102], G. Barbour[95], T. Barillari[115], M-S. Barisits[36], J. Barkeloo[131], T. Barklow[153], R. Barnea[160], B.M. Barnett[143], R.M. Barnett[18], Z. Barnovska-Blenessy[60a], A. Baroncelli[60a], G. Barone[29], A.J. Barr[134], L. Barranco Navarro[45a,45b], F. Barreiro[99], J. Barreiro Guimarães da Costa[15a], U. Barron[161], S. Barsov[137], F. Bartels[61a], R. Bartoldus[153], G. Bartolini[102], A.E. Barton[90], P. Bartos[28a], A. Basalaev[46], A. Basan[100], A. Bassalat[65,ah], M.J. Basso[167], R.L. Bates[57], S. Batlamous[35e], J.R. Batley[32], B. Batool[151], M. Battaglia[145], M. Bauce[73a,73b], F. Bauer[144,*], P. Bauer[24], H.S. Bawa[31], A. Bayirli[12c], J.B. Beacham[49], T. Beau[135], P.H. Beauchemin[170], F. Becherer[52], P. Bechtle[24], H.C. Beck[53], H.P. Beck[20,q], K. Becker[178], C. Becot[46], A. Beddall[12d], A.J. Beddall[12a], V.A. Bednyakov[80], M. Bedognetti[120], C.P. Bee[155], T.A. Beermann[182], M. Begalli[81b], M. Begel[29], A. Behera[155], J.K. Behr[46], F. Beisiegel[24], M. Belfkir[5], A.S. Bell[95], G. Bella[161], L. Bellagamba[23b], A. Bellerive[34], P. Bellos[9], K. Beloborodov[122b,122a], K. Belotskiy[112], N.L. Belyaev[112], D. Benchekroun[35a], N. Benekos[10], Y. Benhammou[161], D.P. Benjamin[6], M. Benoit[29], J.R. Bensinger[26], S. Bentvelsen[120], L. Beresford[134], M. Beretta[51], D. Berge[19], E. Bergeaas Kuutmann[172], N. Berger[5], B. Bergmann[141], L.J. Bergsten[26], J. Beringer[18], S. Berlendis[7], G. Bernardi[135], C. Bernius[153], F.U. Bernlochner[24], T. Berry[94], P. Berta[100], A. Berthold[48], I.A. Bertram[90], O. Bessidskaia Bylund[182], N. Besson[144], S. Bethke[115], A. Betti[42],

JHEP07(2021)167

A.J. Bevan[93], J. Beyer[115], S. Bhatta[155], D.S. Bhattacharya[177], P. Bhattarai[26], V.S. Bhopatkar[6], R. Bi[138], R.M. Bianchi[138], O. Biebel[114], D. Biedermann[19], R. Bielski[36], K. Bierwagen[100], N.V. Biesuz[72a,72b], M. Biglietti[75a], T.R.V. Billoud[141], M. Bindi[53], A. Bingul[12d], C. Bini[73a,73b], S. Biondi[23b,23a], C.J. Birch-sykes[101], M. Birman[180], T. Bisanz[36], J.P. Biswal[3], D. Biswas[181,j], A. Bitadze[101], C. Bittrich[48], K. Bjørke[133], T. Blazek[28a], I. Bloch[46], C. Blocker[26], A. Blue[57], U. Blumenschein[93], G.J. Bobbink[120], V.S. Bobrovnikov[122b,122a], S.S. Bocchetta[97], D. Bogavac[14], A.G. Bogdanchikov[122b,122a], C. Bohm[45a], V. Boisvert[94], P. Bokan[172,53], T. Bold[84a], A.E. Bolz[61b], M. Bomben[135], M. Bona[93], J.S. Bonilla[131], M. Boonekamp[144], C.D. Booth[94], A.G. Borbély[57], H.M. Borecka-Bielska[91], L.S. Borgna[95], A. Borisov[123], G. Borissov[90], D. Bortoletto[134], D. Boscherini[23b], M. Bosman[14], J.D. Bossio Sola[104], K. Bouaouda[35a], J. Boudreau[138], E.V. Bouhova-Thacker[90], D. Boumediene[38], A. Boveia[127], J. Boyd[36], D. Boye[33c], I.R. Boyko[80], A.J. Bozson[94], J. Bracinik[21], N. Brahimi[60d,60c], G. Brandt[182], O. Brandt[32], F. Braren[46], B. Brau[103], J.E. Brau[131], W.D. Breaden Madden[57], K. Brendlinger[46], R. Brener[160], L. Brenner[36], R. Brenner[172], S. Bressler[180], B. Brickwedde[100], D.L. Briglin[21], D. Britton[57], D. Britzger[115], I. Brock[24], R. Brock[107], G. Brooijmans[39], W.K. Brooks[146d], E. Brost[29], P.A. Bruckman de Renstrom[85], B. Brüers[46], D. Bruncko[28b], A. Bruni[23b], G. Bruni[23b], M. Bruschi[23b], N. Bruscino[73a,73b], L. Bryngemark[153], T. Buanes[17], Q. Buat[155], P. Buchholz[151], A.G. Buckley[57], I.A. Budagov[80], M.K. Bugge[133], O. Bulekov[112], B.A. Bullard[59], T.J. Burch[121], S. Burdin[91], C.D. Burgard[120], A.M. Burger[129], B. Burghgrave[8], J.T.P. Burr[46], C.D. Burton[11], J.C. Burzynski[103], V. Büscher[100], E. Buschmann[53], P.J. Bussey[57], J.M. Butler[25], C.M. Buttar[57], J.M. Butterworth[95], P. Butti[36], W. Buttinger[143], C.J. Buxo Vazquez[107], A. Buzatu[158], A.R. Buzykaev[122b,122a], G. Cabras[23b,23a], S. Cabrera Urbán[174], D. Caforio[56], H. Cai[138], V.M.M. Cairo[153], O. Cakir[4a], N. Calace[36], P. Calafiura[18], G. Calderini[135], P. Calfayan[66], G. Callea[57], L.P. Caloba[81b], A. Caltabiano[74a,74b], S. Calvente Lopez[99], D. Calvet[38], S. Calvet[38], T.P. Calvet[102], M. Calvetti[72a,72b], R. Camacho Toro[135], S. Camarda[36], D. Camarero Munoz[99], P. Camarri[74a,74b], M.T. Camerlingo[75a,75b], D. Cameron[133], C. Camincher[36], S. Campana[36], M. Campanelli[95], A. Camplani[40], V. Canale[70a,70b], A. Canesse[104], M. Cano Bret[78], J. Cantero[129], T. Cao[161], Y. Cao[173], M. Capua[41b,41a], R. Cardarelli[74a], F. Cardillo[174], G. Carducci[41b,41a], I. Carli[142], T. Carli[36], G. Carlino[70a], B.T. Carlson[138], E.M. Carlson[176,168a], L. Carminati[69a,69b], R.M.D. Carney[153], S. Caron[119], E. Carquin[146d], S. Carrá[46], G. Carratta[23b,23a], J.W.S. Carter[167], T.M. Carter[50], M.P. Casado[14,g], A.F. Casha[167], E.G. Castiglia[183], F.L. Castillo[174], L. Castillo Garcia[14], V. Castillo Gimenez[174], N.F. Castro[139a,139e], A. Catinaccio[36], J.R. Catmore[133], A. Cattai[36], V. Cavaliere[29], V. Cavasinni[72a,72b], E. Celebi[12b], F. Celli[134], K. Cerny[130], A.S. Cerqueira[81a], A. Cerri[156], L. Cerrito[74a,74b], F. Cerutti[18], A. Cervelli[23b,23a], S.A. Cetin[12b], Z. Chadi[35a], D. Chakraborty[121], J. Chan[181], W.S. Chan[120], W.Y. Chan[91], J.D. Chapman[32], B. Chargeishvili[159b], D.G. Charlton[21], T.P. Charman[93], M. Chatterjee[20], C.C. Chau[34], S. Che[127], S. Chekanov[6], S.V. Chekulaev[168a], G.A. Chelkov[80,af], B. Chen[79], C. Chen[60a], C.H. Chen[79], H. Chen[15c], H. Chen[29], J. Chen[60a], J. Chen[39], J. Chen[26], S. Chen[136], S.J. Chen[15c], X. Chen[15b], Y. Chen[60a], Y-H. Chen[46], H.C. Cheng[63a], H.J. Cheng[15a], A. Cheplakov[80], E. Cheremushkina[123], R. Cherkaoui El Moursli[35e], E. Cheu[7], K. Cheung[64], T.J.A. Chevalérias[144], L. Chevalier[144], V. Chiarella[51], G. Chiarelli[72a], G. Chiodini[68a], A.S. Chisholm[21], A. Chitan[27b], I. Chiu[163], Y.H. Chiu[176], M.V. Chizhov[80], K. Choi[11], A.R. Chomont[73a,73b], Y. Chou[103], Y.S. Chow[120], L.D. Christopher[33f], M.C. Chu[63a], X. Chu[15a,15d], J. Chudoba[140], J.J. Chwastowski[85], L. Chytka[130], D. Cieri[115], K.M. Ciesla[85], V. Cindro[92], I.A. Cioară[27b], A. Ciocio[18], F. Cirotto[70a,70b], Z.H. Citron[180,k], M. Citterio[69a], D.A. Ciubotaru[27b], B.M. Ciungu[167], A. Clark[54], P.J. Clark[50], S.E. Clawson[101], C. Clement[45a,45b], L. Clissa[23b,23a], Y. Coadou[102], M. Cobal[67a,67c], A. Coccaro[55b], J. Cochran[79], R. Coelho Lopes De Sa[103], H. Cohen[161], A.E.C. Coimbra[36], B. Cole[39], A.P. Colijn[120], J. Collot[58],

JHEP07(2021)167

P. Conde Muiño[139a,139h], S.H. Connell[33c], I.A. Connelly[57], S. Constantinescu[27b], F. Conventi[70a,al], A.M. Cooper-Sarkar[134], F. Cormier[175], K.J.R. Cormier[167], L.D. Corpe[95], M. Corradi[73a,73b], E.E. Corrigan[97], F. Corriveau[104,aa], M.J. Costa[174], F. Costanza[5], D. Costanzo[149], G. Cowan[94], J.W. Cowley[32], J. Crane[101], K. Cranmer[125], R.A. Creager[136], S. Crépé-Renaudin[58], F. Crescioli[135], M. Cristinziani[24], V. Croft[170], G. Crosetti[41b,41a], A. Cueto[5], T. Cuhadar Donszelmann[171], H. Cui[15a,15d], A.R. Cukierman[153], W.R. Cunningham[57], S. Czekierda[85], P. Czodrowski[36], M.M. Czurylo[61b], M.J. Da Cunha Sargedas De Sousa[60b], J.V. Da Fonseca Pinto[81b], C. Da Via[101], W. Dabrowski[84a], F. Dachs[36], T. Dado[47], S. Dahbi[33f], T. Dai[106], C. Dallapiccola[103], M. Dam[40], G. D'amen[29], V. D'Amico[75a,75b], J. Damp[100], J.R. Dandoy[136], M.F. Daneri[30], M. Danninger[152], V. Dao[36], G. Darbo[55b], O. Dartsi[5], A. Dattagupta[131], T. Daubney[46], S. D'Auria[69a,69b], C. David[168b], T. Davidek[142], D.R. Davis[49], I. Dawson[149], K. De[8], R. De Asmundis[70a], M. De Beurs[120], S. De Castro[23b,23a], N. De Groot[119], P. de Jong[120], H. De la Torre[107], A. De Maria[15c], D. De Pedis[73a], A. De Salvo[73a], U. De Sanctis[74a,74b], M. De Santis[74a,74b], A. De Santo[156], J.B. De Vivie De Regie[65], D.V. Dedovich[80], A.M. Deiana[42], J. Del Peso[99], Y. Delabat Diaz[46], D. Delgove[65], F. Deliot[144], C.M. Delitzsch[7], M. Della Pietra[70a,70b], D. Della Volpe[54], A. Dell'Acqua[36], L. Dell'Asta[74a,74b], M. Delmastro[5], C. Delporte[65], P.A. Delsart[58], S. Demers[183], M. Demichev[80], G. Demontigny[110], S.P. Denisov[123], L. D'Eramo[121], D. Derendarz[85], J.E. Derkaoui[35d], F. Derue[135], P. Dervan[91], K. Desch[24], K. Dette[167], C. Deutsch[24], M.R. Devesa[30], P.O. Deviveiros[36], F.A. Di Bello[73a,73b], A. Di Ciaccio[74a,74b], L. Di Ciaccio[5], C. Di Donato[70a,70b], A. Di Girolamo[36], G. Di Gregorio[72a,72b], A. Di Luca[76a,76b], B. Di Micco[75a,75b], R. Di Nardo[75a,75b], K.F. Di Petrillo[59], R. Di Sipio[167], C. Diaconu[102], F.A. Dias[120], T. Dias Do Vale[139a], M.A. Diaz[146a], F.G. Diaz Capriles[24], J. Dickinson[18], M. Didenko[166], E.B. Diehl[106], J. Dietrich[19], S. Díez Cornell[46], C. Diez Pardos[151], A. Dimitrievska[18], W. Ding[15b], J. Dingfelder[24], S.J. Dittmeier[61b], F. Dittus[36], F. Djama[102], T. Djobava[159b], J.I. Djuvsland[17], M.A.B. Do Vale[147], M. Dobre[27b], D. Dodsworth[26], C. Doglioni[97], J. Dolejsi[142], Z. Dolezal[142], M. Donadelli[81c], B. Dong[60c], J. Donini[38], A. D'onofrio[15c], M. D'Onofrio[91], J. Dopke[143], A. Doria[70a], M.T. Dova[89], A.T. Doyle[57], E. Drechsler[152], E. Dreyer[152], T. Dreyer[53], A.S. Drobac[170], D. Du[60b], T.A. du Pree[120], Y. Duan[60d], F. Dubinin[111], M. Dubovsky[28a], A. Dubreuil[54], E. Duchovni[180], G. Duckeck[114], O.A. Ducu[36,27b], D. Duda[115], A. Dudarev[36], A.C. Dudder[100], E.M. Duffield[18], M. D'uffizi[101], L. Duflot[65], M. Dührssen[36], C. Dülsen[182], M. Dumancic[180], A.E. Dumitriu[27b], M. Dunford[61a], S. Dungs[47], A. Duperrin[102], H. Duran Yildiz[4a], M. Düren[56], A. Durglishvili[159b], D. Duschinger[48], B. Dutta[46], D. Duvnjak[1], G.I. Dyckes[136], M. Dyndal[36], S. Dysch[101], B.S. Dziedzic[85], M.G. Eggleston[49], T. Eifert[8], G. Eigen[17], K. Einsweiler[18], T. Ekelof[172], H. El Jarrari[35e], V. Ellajosyula[172], M. Ellert[172], F. Ellinghaus[182], A.A. Elliot[93], N. Ellis[36], J. Elmsheuser[29], M. Elsing[36], D. Emeliyanov[143], A. Emerman[39], Y. Enari[163], M.B. Epland[49], J. Erdmann[47], A. Ereditato[20], P.A. Erland[85], M. Errenst[182], M. Escalier[65], C. Escobar[174], O. Estrada Pastor[174], E. Etzion[161], G. Evans[139a], H. Evans[66], M.O. Evans[156], A. Ezhilov[137], F. Fabbri[57], L. Fabbri[23b,23a], V. Fabiani[119], G. Facini[178], R.M. Fakhrutdinov[123], S. Falciano[73a], P.J. Falke[24], S. Falke[36], J. Faltova[142], Y. Fang[15a], Y. Fang[15a], G. Fanourakis[44], M. Fanti[69a,69b], M. Faraj[67a,67c], A. Farbin[8], A. Farilla[75a], E.M. Farina[71a,71b], T. Farooque[107], S.M. Farrington[50], P. Farthouat[36], F. Fassi[35e], P. Fassnacht[36], D. Fassouliotis[9], M. Faucci Giannelli[50], W.J. Fawcett[32], L. Fayard[65], O.L. Fedin[137,p], W. Fedorko[175], A. Fehr[20], M. Feickert[173], L. Feligioni[102], A. Fell[149], C. Feng[60b], M. Feng[49], M.J. Fenton[171], A.B. Fenyuk[123], S.W. Ferguson[43], J. Ferrando[46], A. Ferrari[172], P. Ferrari[120], R. Ferrari[71a], D.E. Ferreira de Lima[61b], A. Ferrer[174], D. Ferrere[54], C. Ferretti[106], F. Fiedler[100], A. Filipčič[92], F. Filthaut[119], K.D. Finelli[25], M.C.N. Fiolhais[139a,139c,a], L. Fiorini[174], F. Fischer[114], J. Fischer[100], W.C. Fisher[107], T. Fitschen[21], I. Fleck[151], P. Fleischmann[106], T. Flick[182], B.M. Flierl[114], L. Flores[136], L.R. Flores Castillo[63a], F.M. Follega[76a,76b], N. Fomin[17],

JHEP07(2021)167

J.H. Foo[167], G.T. Forcolin[76a,76b], B.C. Forland[66], A. Formica[144], F.A. Förster[14], A.C. Forti[101], E. Fortin[102], M.G. Foti[134], D. Fournier[65], H. Fox[90], P. Francavilla[72a,72b], S. Francescato[73a,73b], M. Franchini[23b,23a], S. Franchino[61a], D. Francis[36], L. Franco[5], L. Franconi[20], M. Franklin[59], G. Frattari[73a,73b], A.N. Fray[93], P.M. Freeman[21], B. Freund[110], W.S. Freund[81b], E.M. Freundlich[47], D.C. Frizzell[128], D. Froidevaux[36], J.A. Frost[134], M. Fujimoto[126], C. Fukunaga[164], E. Fullana Torregrosa[174], T. Fusayasu[116], J. Fuster[174], A. Gabrielli[23b,23a], A. Gabrielli[36], S. Gadatsch[54], P. Gadow[115], G. Gagliardi[55b,55a], L.G. Gagnon[110], G.E. Gallardo[134], E.J. Gallas[134], B.J. Gallop[143], R. Gamboa Goni[93], K.K. Gan[127], S. Ganguly[180], J. Gao[60a], Y. Gao[50], Y.S. Gao[31,m], F.M. Garay Walls[146a], C. García[174], J.E. García Navarro[174], J.A. García Pascual[15a], C. Garcia-Argos[52], M. Garcia-Sciveres[18], R.W. Gardner[37], N. Garelli[153], S. Gargiulo[52], C.A. Garner[167], V. Garonne[133], S.J. Gasiorowski[148], P. Gaspar[81b], A. Gaudiello[55b,55a], G. Gaudio[71a], P. Gauzzi[73a,73b], I.L. Gavrilenko[111], A. Gavrilyuk[124], C. Gay[175], G. Gaycken[46], E.N. Gazis[10], A.A. Geanta[27b], C.M. Gee[145], C.N.P. Gee[143], J. Geisen[97], M. Geisen[100], C. Gemme[55b], M.H. Genest[58], C. Geng[106], S. Gentile[73a,73b], S. George[94], T. Geralis[44], L.O. Gerlach[53], P. Gessinger-Befurt[100], G. Gessner[47], M. Ghasemi Bostanabad[176], M. Ghneimat[151], A. Ghosh[65], A. Ghosh[78], B. Giacobbe[23b], S. Giagu[73a,73b], N. Giangiacomi[167], P. Giannetti[72a], A. Giannini[70a,70b], G. Giannini[14], S.M. Gibson[94], M. Gignac[145], D.T. Gil[84b], B.J. Gilbert[39], D. Gillberg[34], G. Gilles[182], N.E.K. Gillwald[46], D.M. Gingrich[3,ak], M.P. Giordani[67a,67c], P.F. Giraud[144], G. Giugliarelli[67a,67c], D. Giugni[69a], F. Giuli[74a,74b], S. Gkaitatzis[162], I. Gkialas[9,h], E.L. Gkougkousis[14], P. Gkountoumis[10], L.K. Gladilin[113], C. Glasman[99], J. Glatzer[14], P.C.F. Glaysher[46], A. Glazov[46], G.R. Gledhill[131], I. Gnesi[41b,c], M. Goblirsch-Kolb[26], D. Godin[110], S. Goldfarb[105], T. Golling[54], D. Golubkov[123], A. Gomes[139a,139b], R. Goncalves Gama[53], R. Gonçalo[139a,139c], G. Gonella[131], L. Gonella[21], A. Gongadze[80], F. Gonnella[21], J.L. Gonski[39], S. González de la Hoz[174], S. Gonzalez Fernandez[14], R. Gonzalez Lopez[91], C. Gonzalez Renteria[18], R. Gonzalez Suarez[172], S. Gonzalez-Sevilla[54], G.R. Gonzalvo Rodriguez[174], L. Goossens[36], N.A. Gorasia[21], P.A. Gorbounov[124], H.A. Gordon[29], B. Gorini[36], E. Gorini[68a,68b], A. Gorišek[92], A.T. Goshaw[49], M.I. Gostkin[80], C.A. Gottardo[119], M. Gouighri[35b], A.G. Goussiou[148], N. Govender[33c], C. Goy[5], I. Grabowska-Bold[84a], E.C. Graham[91], J. Gramling[171], E. Gramstad[133], S. Grancagnolo[19], M. Grandi[156], V. Gratchev[137], P.M. Gravila[27f], F.G. Gravili[68a,68b], C. Gray[57], H.M. Gray[18], C. Grefe[24], K. Gregersen[97], I.M. Gregor[46], P. Grenier[153], K. Grevtsov[46], C. Grieco[14], N.A. Grieser[128], A.A. Grillo[145], K. Grimm[31,l], S. Grinstein[14,w], J.-F. Grivaz[65], S. Groh[100], E. Gross[180], J. Grosse-Knetter[53], Z.J. Grout[95], C. Grud[106], A. Grummer[118], J.C. Grundy[134], L. Guan[106], W. Guan[181], C. Gubbels[175], J. Guenther[77], A. Guerguichon[65], J.G.R. Guerrero Rojas[174], F. Guescini[115], D. Guest[77], R. Gugel[100], A. Guida[46], T. Guillemin[5], S. Guindon[36], J. Guo[60c], W. Guo[106], Y. Guo[60a], Z. Guo[102], R. Gupta[46], S. Gurbuz[12c], G. Gustavino[128], M. Guth[52], P. Gutierrez[128], C. Gutschow[95], C. Guyot[144], C. Gwenlan[134], C.B. Gwilliam[91], E.S. Haaland[133], A. Haas[125], C. Haber[18], H.K. Hadavand[8], A. Hadef[100], M. Haleem[177], J. Haley[129], J.J. Hall[149], G. Halladjian[107], G.D. Hallewell[102], K. Hamano[176], H. Hamdaoui[35e], M. Hamer[24], G.N. Hamity[50], K. Han[60a], L. Han[15c], L. Han[60a], S. Han[18], Y.F. Han[167], K. Hanagaki[82,u], M. Hance[145], D.M. Handl[114], M.D. Hank[37], R. Hankache[135], E. Hansen[97], J.B. Hansen[40], J.D. Hansen[40], M.C. Hansen[24], P.H. Hansen[40], E.C. Hanson[101], K. Hara[169], T. Harenberg[182], S. Harkusha[108], P.F. Harrison[178], N.M. Hartman[153], N.M. Hartmann[114], Y. Hasegawa[150], A. Hasib[50], S. Hassani[144], S. Haug[20], R. Hauser[107], M. Havranek[141], C.M. Hawkes[21], R.J. Hawkings[36], S. Hayashida[117], D. Hayden[107], C. Hayes[106], R.L. Hayes[175], C.P. Hays[134], J.M. Hays[93], H.S. Hayward[91], S.J. Haywood[143], F. He[60a], Y. He[165], M.P. Heath[50], V. Hedberg[97], A.L. Heggelund[133], N.D. Hehir[93], C. Heidegger[52], K.K. Heidegger[52], W.D. Heidorn[79], J. Heilman[34], S. Heim[46], T. Heim[18], B. Heinemann[46,ai], J.G. Heinlein[136], J.J. Heinrich[131],

JHEP07(2021)167

L. Heinrich[36], J. Hejbal[140], L. Helary[46], A. Held[125], S. Hellesund[133], C.M. Helling[145], S. Hellman[45a,45b], C. Helsens[36], R.C.W. Henderson[90], L. Henkelmann[32], A.M. Henriques Correia[36], H. Herde[26], Y. Hernández Jiménez[33f], H. Herr[100], M.G. Herrmann[114], T. Herrmann[48], G. Herten[52], R. Hertenberger[114], L. Hervas[36], G.G. Hesketh[95], N.P. Hessey[168a], H. Hibi[83], S. Higashino[82], E. Higón-Rodriguez[174], K. Hildebrand[37], J.C. Hill[32], K.K. Hill[29], K.H. Hiller[46], S.J. Hillier[21], M. Hils[48], I. Hinchliffe[18], F. Hinterkeuser[24], M. Hirose[132], S. Hirose[169], D. Hirschbuehl[182], B. Hiti[92], O. Hladik[140], J. Hobbs[155], R. Hobincu[27e], N. Hod[180], M.C. Hodgkinson[149], A. Hoecker[36], D. Hohn[52], D. Hohov[65], T. Holm[24], T.R. Holmes[37], M. Holzbock[115], L.B.A.H. Hommels[32], T.M. Hong[138], J.C. Honig[52], A. Hönle[115], B.H. Hooberman[173], W.H. Hopkins[6], Y. Horii[117], P. Horn[48], L.A. Horyn[37], S. Hou[158], A. Hoummada[35a], J. Howarth[57], J. Hoya[89], M. Hrabovsky[130], J. Hrivnac[65], A. Hrynevich[109], T. Hryn'ova[5], P.J. Hsu[64], S.-C. Hsu[148], Q. Hu[39], S. Hu[60c], Y.F. Hu[15a,15d,am], D.P. Huang[95], X. Huang[15c], Y. Huang[60a], Y. Huang[15a], Z. Hubacek[141], F. Hubaut[102], M. Huebner[24], F. Huegging[24], T.B. Huffman[134], M. Huhtinen[36], R. Hulsken[58], R.F.H. Hunter[34], N. Huseynov[80,ab], J. Huston[107], J. Huth[59], R. Hyneman[153], S. Hyrych[28a], G. Iacobucci[54], G. Iakovidis[29], I. Ibragimov[151], L. Iconomidou-Fayard[65], P. Iengo[36], R. Ignazzi[40], R. Iguchi[163], T. Iizawa[54], Y. Ikegami[82], M. Ikeno[82], N. Ilic[119,167,aa], F. Iltzsche[48], H. Imam[35a], G. Introzzi[71a,71b], M. Iodice[75a], K. Iordanidou[168a], V. Ippolito[73a,73b], M.F. Isacson[172], M. Ishino[163], W. Islam[129], C. Issever[19,46], S. Istin[160], J.M. Iturbe Ponce[63a], R. Iuppa[76a,76b], A. Ivina[180], J.M. Izen[43], V. Izzo[70a], P. Jacka[140], P. Jackson[1], R.M. Jacobs[46], B.P. Jaeger[152], V. Jain[2], G. Jäkel[182], K.B. Jakobi[100], K. Jakobs[52], T. Jakoubek[180], J. Jamieson[57], K.W. Janas[84a], R. Jansky[54], M. Janus[53], P.A. Janus[84a], G. Jarlskog[97], A.E. Jaspan[91], N. Javadov[80,ab], T. Javůrek[36], M. Javurkova[103], F. Jeanneau[144], L. Jeanty[131], J. Jejelava[159a], P. Jenni[52,d], N. Jeong[46], S. Jézéquel[5], J. Jia[155], Z. Jia[15c], H. Jiang[79], Y. Jiang[60a], Z. Jiang[153], S. Jiggins[52], F.A. Jimenez Morales[38], J. Jimenez Pena[115], S. Jin[15c], A. Jinaru[27b], O. Jinnouchi[165], H. Jivan[33f], P. Johansson[149], K.A. Johns[7], C.A. Johnson[66], E. Jones[178], R.W.L. Jones[90], S.D. Jones[156], T.J. Jones[91], J. Jovicevic[36], X. Ju[18], J.J. Junggeburth[115], A. Juste Rozas[14,w], A. Kaczmarska[85], M. Kado[73a,73b], H. Kagan[127], M. Kagan[153], A. Kahn[39], C. Kahra[100], T. Kaji[179], E. Kajomovitz[160], C.W. Kalderon[29], A. Kaluza[100], A. Kamenshchikov[123], M. Kaneda[163], N.J. Kang[145], S. Kang[79], Y. Kano[117], J. Kanzaki[82], L.S. Kaplan[181], D. Kar[33f], K. Karava[134], M.J. Kareem[168b], I. Karkanias[162], S.N. Karpov[80], Z.M. Karpova[80], V. Kartvelishvili[90], A.N. Karyukhin[123], E. Kasimi[162], A. Kastanas[45a,45b], C. Kato[60d], J. Katzy[46], K. Kawade[150], K. Kawagoe[88], T. Kawaguchi[117], T. Kawamoto[144], G. Kawamura[53], E.F. Kay[176], F.I. Kaya[170], S. Kazakos[14], V.F. Kazanin[122b,122a], J.M. Keaveney[33a], R. Keeler[176], J.S. Keller[34], E. Kellermann[97], D. Kelsey[156], J.J. Kempster[21], J. Kendrick[21], K.E. Kennedy[39], O. Kepka[140], S. Kersten[182], B.P. Kerševan[92], S. Ketabchi Haghighat[167], F. Khalil-Zada[13], M. Khandoga[144], A. Khanov[129], A.G. Kharlamov[122b,122a], T. Kharlamova[122b,122a], E.E. Khoda[175], T.J. Khoo[77], G. Khoriauli[177], E. Khramov[80], J. Khubua[159b], S. Kido[83], M. Kiehn[36], E. Kim[165], Y.K. Kim[37], N. Kimura[95], A. Kirchhoff[53], D. Kirchmeier[48], J. Kirk[143], A.E. Kiryunin[115], T. Kishimoto[163], D.P. Kisliuk[167], V. Kitali[46], C. Kitsaki[10], O. Kivernyk[24], T. Klapdor-Kleingrothaus[52], M. Klassen[61a], C. Klein[34], M.H. Klein[106], M. Klein[91], U. Klein[91], K. Kleinknecht[100], P. Klimek[36], A. Klimentov[29], F. Klimpel[36], T. Klingl[24], T. Klioutchnikova[36], F.F. Klitzner[114], P. Kluit[120], S. Kluth[115], E. Kneringer[77], E.B.F.G. Knoops[102], A. Knue[52], D. Kobayashi[88], M. Kobel[48], M. Kocian[153], T. Kodama[163], P. Kodys[142], D.M. Koeck[156], P.T. Koenig[24], T. Koffas[34], N.M. Köhler[36], M. Kolb[144], I. Koletsou[5], T. Komarek[130], T. Kondo[82], K. Köneke[52], A.X.Y. Kong[1], A.C. König[119], T. Kono[126], V. Konstantinides[95], N. Konstantinidis[95], B. Konya[97], R. Kopeliansky[66], S. Koperny[84a], K. Korcyl[85], K. Kordas[162], G. Koren[161], A. Korn[95], I. Korolkov[14], E.V. Korolkova[149], N. Korotkova[113], O. Kortner[115], S. Kortner[115],

JHEP07(2021)167

V.V. Kostyukhin[149,166], A. Kotsokechagia[65], A. Kotwal[49], A. Koulouris[10], A. Kourkoumeli-Charalampidi[71a,71b], C. Kourkoumelis[9], E. Kourlitis[6], V. Kouskoura[29], R. Kowalewski[176], W. Kozanecki[101], A.S. Kozhin[123], V.A. Kramarenko[113], G. Kramberger[92], D. Krasnopevtsev[60a], M.W. Krasny[135], A. Krasznahorkay[36], D. Krauss[115], J.A. Kremer[100], J. Kretzschmar[91], K. Kreul[19], P. Krieger[167], F. Krieter[114], S. Krishnamurthy[103], A. Krishnan[61b], M. Krivos[142], K. Krizka[18], K. Kroeninger[47], H. Kroha[115], J. Kroll[140], J. Kroll[136], K.S. Krowpman[107], U. Kruchonak[80], H. Krüger[24], N. Krumnack[79], M.C. Kruse[49], J.A. Krzysiak[85], A. Kubota[165], O. Kuchinskaia[166], S. Kuday[4b], D. Kuechler[46], J.T. Kuechler[46], S. Kuehn[36], T. Kuhl[46], V. Kukhtin[80], Y. Kulchitsky[108,ae], S. Kuleshov[146b], Y.P. Kulinich[173], M. Kuna[58], A. Kupco[140], T. Kupfer[47], O. Kuprash[52], H. Kurashige[83], L.L. Kurchaninov[168a], Y.A. Kurochkin[108], A. Kurova[112], M.G. Kurth[15a,15d], E.S. Kuwertz[36], M. Kuze[165], A.K. Kvam[148], J. Kvita[130], T. Kwan[104], C. Lacasta[174], F. Lacava[73a,73b], D.P.J. Lack[101], H. Lacker[19], D. Lacour[135], E. Ladygin[80], R. Lafaye[5], B. Laforge[135], T. Lagouri[146c], S. Lai[53], I.K. Lakomiec[84a], J.E. Lambert[128], S. Lammers[66], W. Lampl[7], C. Lampoudis[162], E. Lançon[29], U. Landgraf[52], M.P.J. Landon[93], V.S. Lang[52], J.C. Lange[53], R.J. Langenberg[103], A.J. Lankford[171], F. Lanni[29], K. Lantzsch[24], A. Lanza[71a], A. Lapertosa[55b,55a], J.F. Laporte[144], T. Lari[69a], F. Lasagni Manghi[23b,23a], M. Lassnig[36], V. Latonova[140], T.S. Lau[63a], A. Laudrain[100], A. Laurier[34], M. Lavorgna[70a,70b], S.D. Lawlor[94], M. Lazzaroni[69a,69b], B. Le[101], E. Le Guirriec[102], A. Lebedev[79], M. LeBlanc[7], T. LeCompte[6], F. Ledroit-Guillon[58], A.C.A. Lee[95], C.A. Lee[29], G.R. Lee[17], L. Lee[59], S.C. Lee[158], S. Lee[79], B. Lefebvre[168a], H.P. Lefebvre[94], M. Lefebvre[176], C. Leggett[18], K. Lehmann[152], N. Lehmann[20], G. Lehmann Miotto[36], W.A. Leight[46], A. Leisos[162,v], M.A.L. Leite[81c], C.E. Leitgeb[114], R. Leitner[142], K.J.C. Leney[42], T. Lenz[24], S. Leone[72a], C. Leonidopoulos[50], A. Leopold[135], C. Leroy[110], R. Les[107], C.G. Lester[32], M. Levchenko[137], J. Levêque[5], D. Levin[106], L.J. Levinson[180], D.J. Lewis[21], B. Li[15b], B. Li[106], C-Q. Li[60c,60d], F. Li[60c], H. Li[60a], H. Li[60b], J. Li[60c], K. Li[148], L. Li[60c], M. Li[15a,15d], Q.Y. Li[60a], S. Li[60d,60c,b], X. Li[46], Y. Li[46], Z. Li[60b], Z. Li[134], Z. Li[104], Z. Li[91], Z. Liang[15a], M. Liberatore[46], B. Liberti[74a], K. Lie[63c], S. Lim[29], C.Y. Lin[32], K. Lin[107], R.A. Linck[66], R.E. Lindley[7], J.H. Lindon[21], A. Linss[46], A.L. Lionti[54], E. Lipeles[136], A. Lipniacka[17], T.M. Liss[173,aj], A. Lister[175], J.D. Little[8], B. Liu[79], B.X. Liu[152], H.B. Liu[29], J.B. Liu[60a], J.K.K. Liu[37], K. Liu[60d,60c], M. Liu[60a], M.Y. Liu[60a], P. Liu[15a], X. Liu[60a], Y. Liu[46], Y. Liu[15a,15d], Y.L. Liu[106], Y.W. Liu[60a], M. Livan[71a,71b], A. Lleres[58], J. Llorente Merino[152], S.L. Lloyd[93], C.Y. Lo[63b], E.M. Lobodzinska[46], P. Loch[7], S. Loffredo[74a,74b], T. Lohse[19], K. Lohwasser[149], M. Lokajicek[140], J.D. Long[173], R.E. Long[90], I. Longarini[73a,73b], L. Longo[36], I. Lopez Paz[101], A. Lopez Solis[149], J. Lorenz[114], N. Lorenzo Martinez[5], A.M. Lory[114], A. Lösle[52], X. Lou[45a,45b], X. Lou[15a], A. Lounis[65], J. Love[6], P.A. Love[90], J.J. Lozano Bahilo[174], M. Lu[60a], Y.J. Lu[64], H.J. Lubatti[148], C. Luci[73a,73b], F.L. Lucio Alves[15c], A. Lucotte[58], F. Luehring[66], I. Luise[155], L. Luminari[73a], B. Lund-Jensen[154], N.A. Luongo[131], M.S. Lutz[161], D. Lynn[29], H. Lyons[91], R. Lysak[140], E. Lytken[97], F. Lyu[15a], V. Lyubushkin[80], T. Lyubushkina[80], H. Ma[29], L.L. Ma[60b], Y. Ma[95], D.M. Mac Donell[176], G. Maccarrone[51], C.M. Macdonald[149], J.C. MacDonald[149], J. Machado Miguens[136], R. Madar[38], W.F. Mader[48], M. Madugoda Ralalage Don[129], N. Madysa[48], J. Maeda[83], T. Maeno[29], M. Maerker[48], V. Magerl[52], N. Magini[79], J. Magro[67a,67c,r], D.J. Mahon[39], C. Maidantchik[81b], A. Maio[139a,139b,139d], K. Maj[84a], O. Majersky[28a], S. Majewski[131], Y. Makida[82], N. Makovec[65], B. Malaescu[135], Pa. Malecki[85], V.P. Maleev[137], F. Malek[58], D. Malito[41b,41a], U. Mallik[78], C. Malone[32], S. Maltezos[10], S. Malyukov[80], J. Mamuzic[174], G. Mancini[51], J.P. Mandalia[93], I. Mandić[92], L. Manhaes de Andrade Filho[81a], I.M. Maniatis[162], J. Manjarres Ramos[48], K.H. Mankinen[97], A. Mann[114], A. Manousos[77], B. Mansoulie[144], I. Manthos[162], S. Manzoni[120], A. Marantis[162,v], G. Marceca[30], L. Marchese[134], G. Marchiori[135], M. Marcisovsky[140], L. Marcoccia[74a,74b], C. Marcon[97], M. Marjanovic[128],

JHEP07(2021)167

Z. Marshall[18], M.U.F. Martensson[172], S. Marti-Garcia[174], C.B. Martin[127], T.A. Martin[178], V.J. Martin[50], B. Martin dit Latour[17], L. Martinelli[75a,75b], M. Martinez[14,w], P. Martinez Agullo[174], V.I. Martinez Outschoorn[103], S. Martin-Haugh[143], V.S. Martoiu[27b], A.C. Martyniuk[95], A. Marzin[36], S.R. Maschek[115], L. Masetti[100], T. Mashimo[163], R. Mashinistov[111], J. Masik[101], A.L. Maslennikov[122b,122a], L. Massa[23b,23a], P. Massarotti[70a,70b], P. Mastrandrea[72a,72b], A. Mastroberardino[41b,41a], T. Masubuchi[163], D. Matakias[29], A. Matic[114], N. Matsuzawa[163], P. Mättig[24], J. Maurer[27b], B. Maček[92], D.A. Maximov[122b,122a], R. Mazini[158], I. Maznas[162], S.M. Mazza[145], J.P. Mc Gowan[104], S.P. Mc Kee[106], T.G. McCarthy[115], W.P. McCormack[18], E.F. McDonald[105], A.E. McDougall[120], J.A. Mcfayden[18], G. Mchedlidze[159b], M.A. McKay[42], K.D. McLean[176], S.J. McMahon[143], P.C. McNamara[105], C.J. McNicol[178], R.A. McPherson[176,aa], J.E. Mdhluli[33f], Z.A. Meadows[103], S. Meehan[36], T. Megy[38], S. Mehlhase[114], A. Mehta[91], B. Meirose[43], D. Melini[160], B.R. Mellado Garcia[33f], J.D. Mellenthin[53], M. Melo[28a], F. Meloni[46], A. Melzer[24], E.D. Mendes Gouveia[139a,139e], A.M. Mendes Jacques Da Costa[21], H.Y. Meng[167], L. Meng[36], X.T. Meng[106], S. Menke[115], E. Meoni[41b,41a], S. Mergelmeyer[19], S.A.M. Merkt[138], C. Merlassino[134], P. Mermod[54,*], L. Merola[70a,70b], C. Meroni[69a], G. Merz[106], O. Meshkov[113,111], J.K.R. Meshreki[151], J. Metcalfe[6], A.S. Mete[6], C. Meyer[66], J-P. Meyer[144], M. Michetti[19], R.P. Middleton[143], L. Mijović[50], G. Mikenberg[180], M. Mikestikova[140], M. Mikuž[92], H. Mildner[149], A. Milic[167], C.D. Milke[42], D.W. Miller[37], L.S. Miller[34], A. Milov[180], D.A. Milstead[45a,45b], A.A. Minaenko[123], I.A. Minashvili[159b], L. Mince[57], A.I. Mincer[125], B. Mindur[84a], M. Mineev[80], Y. Minegishi[163], Y. Mino[86], L.M. Mir[14], M. Mironova[134], T. Mitani[179], J. Mitrevski[114], V.A. Mitsou[174], M. Mittal[60c], O. Miu[167], A. Miucci[20], P.S. Miyagawa[93], A. Mizukami[82], J.U. Mjörnmark[97], T. Mkrtchyan[61a], M. Mlynarikova[121], T. Moa[45a,45b], S. Mobius[53], K. Mochizuki[110], P. Moder[46], P. Mogg[114], S. Mohapatra[39], R. Moles-Valls[24], K. Mönig[46], E. Monnier[102], A. Montalbano[152], J. Montejo Berlingen[36], M. Montella[95], F. Monticelli[89], S. Monzani[69a], N. Morange[65], A.L. Moreira De Carvalho[139a], D. Moreno[22a], M. Moreno Llácer[174], C. Moreno Martinez[14], P. Morettini[55b], M. Morgenstern[160], S. Morgenstern[48], D. Mori[152], M. Morii[59], M. Morinaga[179], V. Morisbak[133], A.K. Morley[36], G. Mornacchi[36], A.P. Morris[95], L. Morvaj[36], P. Moschovakos[36], B. Moser[120], M. Mosidze[159b], T. Moskalets[144], P. Moskvitina[119], J. Moss[31,n], E.J.W. Moyse[103], S. Muanza[102], J. Mueller[138], R.S.P. Mueller[114], D. Muenstermann[90], G.A. Mullier[97], D.P. Mungo[69a,69b], J.L. Munoz Martinez[14], F.J. Munoz Sanchez[101], P. Murin[28b], W.J. Murray[178,143], A. Murrone[69a,69b], J.M. Muse[128], M. Muškinja[18], C. Mwewa[33a], A.G. Myagkov[123,af], A.A. Myers[138], G. Myers[66], J. Myers[131], M. Myska[141], B.P. Nachman[18], O. Nackenhorst[47], A.Nag Nag[48], K. Nagai[134], K. Nagano[82], Y. Nagasaka[62], J.L. Nagle[29], E. Nagy[102], A.M. Nairz[36], Y. Nakahama[117], K. Nakamura[82], T. Nakamura[163], H. Nanjo[132], F. Napolitano[61a], R.F. Naranjo Garcia[46], R. Narayan[42], I. Naryshkin[137], M. Naseri[34], T. Naumann[46], G. Navarro[22a], P.Y. Nechaeva[111], F. Nechansky[46], T.J. Neep[21], A. Negri[71a,71b], M. Negrini[23b], C. Nellist[119], C. Nelson[104], M.E. Nelson[45a,45b], S. Nemecek[140], M. Nessi[36,f], M.S. Neubauer[173], F. Neuhaus[100], M. Neumann[182], R. Newhouse[175], P.R. Newman[21], C.W. Ng[138], Y.S. Ng[19], Y.W.Y. Ng[171], B. Ngair[35e], H.D.N. Nguyen[102], T. Nguyen Manh[110], E. Nibigira[38], R.B. Nickerson[134], R. Nicolaidou[144], D.S. Nielsen[40], J. Nielsen[145], M. Niemeyer[53], N. Nikiforou[11], V. Nikolaenko[123,af], I. Nikolic-Audit[135], K. Nikolopoulos[21], P. Nilsson[29], H.R. Nindhito[54], A. Nisati[73a], N. Nishu[60c], R. Nisius[115], I. Nitsche[47], T. Nitta[179], T. Nobe[163], D.L. Noel[32], Y. Noguchi[86], I. Nomidis[135], M.A. Nomura[29], M. Nordberg[36], J. Novak[92], T. Novak[92], O. Novgorodova[48], R. Novotny[118], L. Nozka[130], K. Ntekas[171], E. Nurse[95], F.G. Oakham[34,ak], J. Ocariz[135], A. Ochi[83], I. Ochoa[139a], J.P. Ochoa-Ricoux[146a], K. O'Connor[26], S. Oda[88], S. Odaka[82], S. Oerdek[53], A. Ogrodnik[84a], A. Oh[101], C.C. Ohm[154], H. Oide[165], R. Oishi[163], M.L. Ojeda[167], H. Okawa[169], Y. Okazaki[86], M.W. O'Keefe[91], Y. Okumura[163],

JHEP07(2021)167

A. Olariu[27b], L.F. Oleiro Seabra[139a], S.A. Olivares Pino[146a], D. Oliveira Damazio[29], J.L. Oliver[1], M.J.R. Olsson[171], A. Olszewski[85], J. Olszowska[85], Ö.O. Öncel[24], D.C. O'Neil[152], A.P. O'neill[134], A. Onofre[139a,139e], P.U.E. Onyisi[11], H. Oppen[133], R.G. Oreamuno Madriz[121], M.J. Oreglia[37], G.E. Orellana[89], D. Orestano[75a,75b], N. Orlando[14], R.S. Orr[167], V. O'Shea[57], R. Ospanov[60a], G. Otero y Garzon[30], H. Otono[88], P.S. Ott[61a], G.J. Ottino[18], M. Ouchrif[35d], J. Ouellette[29], F. Ould-Saada[133], A. Ouraou[144,*], Q. Ouyang[15a], M. Owen[57], R.E. Owen[143], V.E. Ozcan[12c], N. Ozturk[8], J. Pacalt[130], H.A. Pacey[32], K. Pachal[49], A. Pacheco Pages[14], C. Padilla Aranda[14], S. Pagan Griso[18], G. Palacino[66], S. Palazzo[50], S. Palestini[36], M. Palka[84b], P. Palni[84a], C.E. Pandini[54], J.G. Panduro Vazquez[94], P. Pani[46], G. Panizzo[67a,67c], L. Paolozzi[54], C. Papadatos[110], K. Papageorgiou[9,h], S. Parajuli[42], A. Paramonov[6], C. Paraskevopoulos[10], D. Paredes Hernandez[63b], S.R. Paredes Saenz[134], B. Parida[180], T.H. Park[167], A.J. Parker[31], M.A. Parker[32], F. Parodi[55b,55a], E.W. Parrish[121], J.A. Parsons[39], U. Parzefall[52], L. Pascual Dominguez[135], V.R. Pascuzzi[18], J.M.P. Pasner[145], F. Pasquali[120], E. Pasqualucci[73a], S. Passaggio[55b], F. Pastore[94], P. Pasuwan[45a,45b], S. Pataraia[100], J.R. Pater[101], A. Pathak[181,j], J. Patton[91], T. Pauly[36], J. Pearkes[153], M. Pedersen[133], L. Pedraza Diaz[119], R. Pedro[139a], T. Peiffer[53], S.V. Peleganchuk[122b,122a], O. Penc[140], C. Peng[63b], H. Peng[60a], B.S. Peralva[81a], M.M. Perego[65], A.P. Pereira Peixoto[139a], L. Pereira Sanchez[45a,45b], D.V. Perepelitsa[29], E. Perez Codina[168a], L. Perini[69a,69b], H. Pernegger[36], S. Perrella[36], A. Perrevoort[120], K. Peters[46], R.F.Y. Peters[101], B.A. Petersen[36], T.C. Petersen[40], E. Petit[102], V. Petousis[141], C. Petridou[162], F. Petrucci[75a,75b], M. Pettee[183], N.E. Pettersson[103], K. Petukhova[142], A. Peyaud[144], R. Pezoa[146d], L. Pezzotti[71a,71b], T. Pham[105], P.W. Phillips[143], M.W. Phipps[173], G. Piacquadio[155], E. Pianori[18], A. Picazio[103], R.H. Pickles[101], R. Piegaia[30], D. Pietreanu[27b], J.E. Pilcher[37], A.D. Pilkington[101], M. Pinamonti[67a,67c], J.L. Pinfold[3], C. Pitman Donaldson[95], M. Pitt[161], L. Pizzimento[74a,74b], A. Pizzini[120], M.-A. Pleier[29], V. Plesanovs[52], V. Pleskot[142], E. Plotnikova[80], P. Podberezko[122b,122a], R. Poettgen[97], R. Poggi[54], L. Poggioli[135], I. Pogrebnyak[107], D. Pohl[24], I. Pokharel[53], G. Polesello[71a], A. Poley[152,168a], A. Policicchio[73a,73b], R. Polifka[142], A. Polini[23b], C.S. Pollard[46], V. Polychronakos[29], D. Ponomarenko[112], L. Pontecorvo[36], S. Popa[27a], G.A. Popeneciu[27d], L. Portales[5], D.M. Portillo Quintero[58], S. Pospisil[141], K. Potamianos[46], I.N. Potrap[80], C.J. Potter[32], H. Potti[11], T. Poulsen[97], J. Poveda[174], T.D. Powell[149], G. Pownall[46], M.E. Pozo Astigarraga[36], A. Prades Ibanez[174], P. Pralavorio[102], M.M. Prapa[44], S. Prell[79], D. Price[101], M. Primavera[68a], M.L. Proffitt[148], N. Proklova[112], K. Prokofiev[63c], F. Prokoshin[80], S. Protopopescu[29], J. Proudfoot[6], M. Przybycien[84a], D. Pudzha[137], A. Puri[173], P. Puzo[65], D. Pyatiizbyantseva[112], J. Qian[106], Y. Qin[101], A. Quadt[53], M. Queitsch-Maitland[36], G. Rabanal Bolanos[59], M. Racko[28a], F. Ragusa[69a,69b], G. Rahal[98], J.A. Raine[54], S. Rajagopalan[29], A. Ramirez Morales[93], K. Ran[15a,15d], D.F. Rassloff[61a], D.M. Rauch[46], F. Rauscher[114], S. Rave[100], B. Ravina[57], I. Ravinovich[180], J.H. Rawling[101], M. Raymond[36], A.L. Read[133], N.P. Readioff[149], M. Reale[68a,68b], D.M. Rebuzzi[71a,71b], G. Redlinger[29], K. Reeves[43], D. Reikher[161], A. Reiss[100], A. Rej[151], C. Rembser[36], A. Renardi[46], M. Renda[27b], M.B. Rendel[115], A.G. Rennie[57], S. Resconi[69a], E.D. Resseguie[18], S. Rettie[95], B. Reynolds[127], E. Reynolds[21], O.L. Rezanova[122b,122a], P. Reznicek[142], E. Ricci[76a,76b], R. Richter[115], S. Richter[46], E. Richter-Was[84b], M. Ridel[135], P. Rieck[115], O. Rifki[46], M. Rijssenbeek[155], A. Rimoldi[71a,71b], M. Rimoldi[46], L. Rinaldi[23b], T.T. Rinn[173], G. Ripellino[154], I. Riu[14], P. Rivadeneira[46], J.C. Rivera Vergara[176], F. Rizatdinova[129], E. Rizvi[93], C. Rizzi[36], S.H. Robertson[104,aa], M. Robin[46], D. Robinson[32], C.M. Robles Gajardo[146d], M. Robles Manzano[100], A. Robson[57], A. Rocchi[74a,74b], C. Roda[72a,72b], S. Rodriguez Bosca[174], A. Rodriguez Rodriguez[52], A.M. Rodríguez Vera[168b], S. Roe[36], J. Roggel[182], O. Røhne[133], R. Röhrig[115], R.A. Rojas[146d], B. Roland[52], C.P.A. Roland[66], J. Roloff[29], A. Romaniouk[112], M. Romano[23b,23a], N. Rompotis[91], M. Ronzani[125], L. Roos[135], S. Rosati[73a], G. Rosin[103], B.J. Rosser[136], E. Rossi[46], E. Rossi[75a,75b],

JHEP07(2021)167

E. Rossi[70a,70b], L.P. Rossi[55b], L. Rossini[46], R. Rosten[14], M. Rotaru[27b], B. Rottler[52], D. Rousseau[65], G. Rovelli[71a,71b], A. Roy[11], D. Roy[33f], A. Rozanov[102], Y. Rozen[160], X. Ruan[33f], T.A. Ruggeri[1], F. Rühr[52], A. Ruiz-Martinez[174], A. Rummler[36], Z. Rurikova[52], N.A. Rusakovich[80], H.L. Russell[104], L. Rustige[38,47], J.P. Rutherfoord[7], E.M. Rüttinger[149], M. Rybar[142], G. Rybkin[65], E.B. Rye[133], A. Ryzhov[123], J.A. Sabater Iglesias[46], P. Sabatini[174], L. Sabetta[73a,73b], S. Sacerdoti[65], H.F-W. Sadrozinski[145], R. Sadykov[80], F. Safai Tehrani[73a], B. Safarzadeh Samani[156], M. Safdari[153], P. Saha[121], S. Saha[104], M. Sahinsoy[115], A. Sahu[182], M. Saimpert[36], M. Saito[163], T. Saito[163], H. Sakamoto[163], D. Salamani[54], G. Salamanna[75a,75b], A. Salnikov[153], J. Salt[174], A. Salvador Salas[14], D. Salvatore[41b,41a], F. Salvatore[156], A. Salvucci[63a], A. Salzburger[36], J. Samarati[36], D. Sammel[52], D. Sampsonidis[162], D. Sampsonidou[60d,60c], J. Sánchez[174], A. Sanchez Pineda[67a,36,67c], H. Sandaker[133], C.O. Sander[46], I.G. Sanderswood[90], M. Sandhoff[182], C. Sandoval[22b], D.P.C. Sankey[143], M. Sannino[55b,55a], Y. Sano[117], A. Sansoni[51], C. Santoni[38], H. Santos[139a,139b], S.N. Santpur[18], A. Santra[174], K.A. Saoucha[149], A. Sapronov[80], J.G. Saraiva[139a,139d], O. Sasaki[82], K. Sato[169], F. Sauerburger[52], E. Sauvan[5], P. Savard[167,ak], R. Sawada[163], C. Sawyer[143], L. Sawyer[96], I. Sayago Galvan[174], C. Sbarra[23b], A. Sbrizzi[67a,67c], T. Scanlon[95], J. Schaarschmidt[148], P. Schacht[115], D. Schaefer[37], L. Schaefer[136], U. Schäfer[100], A.C. Schaffer[65], D. Schaile[114], R.D. Schamberger[155], E. Schanet[114], C. Scharf[19], N. Scharmberg[101], V.A. Schegelsky[137], D. Scheirich[142], F. Schenck[19], M. Schernau[171], C. Schiavi[55b,55a], L.K. Schildgen[24], Z.M. Schillaci[26], E.J. Schioppa[68a,68b], M. Schioppa[41b,41a], K.E. Schleicher[52], S. Schlenker[36], K.R. Schmidt-Sommerfeld[115], K. Schmieden[100], C. Schmitt[100], S. Schmitt[46], L. Schoeffel[144], A. Schoening[61b], P.G. Scholer[52], E. Schopf[134], M. Schott[100], J.F.P. Schouwenberg[119], J. Schovancova[36], S. Schramm[54], F. Schroeder[182], A. Schulte[100], H-C. Schultz-Coulon[61a], M. Schumacher[52], B.A. Schumm[145], Ph. Schune[144], A. Schwartzman[153], T.A. Schwarz[106], Ph. Schwemling[144], R. Schwienhorst[107], A. Sciandra[145], G. Sciolla[26], F. Scuri[72a], F. Scutti[105], L.M. Scyboz[115], C.D. Sebastiani[91], K. Sedlaczek[47], P. Seema[19], S.C. Seidel[118], A. Seiden[145], B.D. Seidlitz[29], T. Seiss[37], C. Seitz[46], J.M. Seixas[81b], G. Sekhniaidze[70a], S.J. Sekula[42], N. Semprini-Cesari[23b,23a], S. Sen[49], C. Serfon[29], L. Serin[65], L. Serkin[67a,67b], M. Sessa[60a], H. Severini[128], S. Sevova[153], F. Sforza[55b,55a], A. Sfyrla[54], E. Shabalina[53], J.D. Shahinian[136], N.W. Shaikh[45a,45b], D. Shaked Renous[180], L.Y. Shan[15a], M. Shapiro[18], A. Sharma[36], A.S. Sharma[1], P.B. Shatalov[124], K. Shaw[156], S.M. Shaw[101], M. Shehade[180], Y. Shen[128], A.D. Sherman[25], P. Sherwood[95], L. Shi[95], C.O. Shimmin[183], Y. Shimogama[179], M. Shimojima[116], J.D. Shinner[94], I.P.J. Shipsey[134], S. Shirabe[165], M. Shiyakova[80,y], J. Shlomi[180], A. Shmeleva[111], M.J. Shochet[37], J. Shojaii[105], D.R. Shope[154], S. Shrestha[127], E.M. Shrif[33f], M.J. Shroff[176], E. Shulga[180], P. Sicho[140], A.M. Sickles[173], E. Sideras Haddad[33f], O. Sidiropoulou[36], A. Sidoti[23b,23a], F. Siegert[48], Dj. Sijacki[16], M.Jr. Silva[181], M.V. Silva Oliveira[36], S.B. Silverstein[45a], S. Simion[65], R. Simoniello[100], C.J. Simpson-allsop[21], S. Simsek[12b], P. Sinervo[167], V. Sinetckii[113], S. Singh[152], S. Sinha[33f], M. Sioli[23b,23a], I. Siral[131], S.Yu. Sivoklokov[113], J. Sjölin[45a,45b], A. Skaf[53], E. Skorda[97], P. Skubic[128], M. Slawinska[85], K. Sliwa[170], V. Smakhtin[180], B.H. Smart[143], J. Smiesko[28b], N. Smirnov[112], S.Yu. Smirnov[112], Y. Smirnov[112], L.N. Smirnova[113,s], O. Smirnova[97], E.A. Smith[37], H.A. Smith[134], M. Smizanska[90], K. Smolek[141], A. Smykiewicz[85], A.A. Snesarev[111], H.L. Snoek[120], I.M. Snyder[131], S. Snyder[29], R. Sobie[176,aa], A. Soffer[161], A. Søgaard[50], F. Sohns[53], C.A. Solans Sanchez[36], E.Yu. Soldatov[112], U. Soldevila[174], A.A. Solodkov[123], A. Soloshenko[80], O.V. Solovyanov[123], V. Solovyev[137], P. Sommer[149], H. Son[170], A. Sonay[14], W. Song[143], W.Y. Song[168b], A. Sopczak[141], A.L. Sopio[95], F. Sopkova[28b], S. Sottocornola[71a,71b], R. Soualah[67a,67c], A.M. Soukharev[122b,122a], D. South[46], S. Spagnolo[68a,68b], M. Spalla[115], M. Spangenberg[178], F. Spanò[94], D. Sperlich[52], T.M. Spieker[61a], G. Spigo[36], M. Spina[156], D.P. Spiteri[57], M. Spousta[142], A. Stabile[69a,69b], B.L. Stamas[121], R. Stamen[61a], M. Stamenkovic[120], A. Stampekis[21], E. Stanecka[85], B. Stanislaus[134],

JHEP07(2021)167

M.M. Stanitzki[46], M. Stankaityte[134], B. Stapf[120], E.A. Starchenko[123], G.H. Stark[145], J. Stark[58], P. Staroba[140], P. Starovoitov[61a], S. Stärz[104], R. Staszewski[85], G. Stavropoulos[44], M. Stegler[46], P. Steinberg[29], A.L. Steinhebel[131], B. Stelzer[152,168a], H.J. Stelzer[138], O. Stelzer-Chilton[168a], H. Stenzel[56], T.J. Stevenson[156], G.A. Stewart[36], M.C. Stockton[36], G. Stoicea[27b], M. Stolarski[139a], S. Stonjek[115], A. Straessner[48], J. Strandberg[154], S. Strandberg[45a,45b], M. Strauss[128], T. Strebler[102], P. Strizenec[28b], R. Ströhmer[177], D.M. Strom[131], R. Stroynowski[42], A. Strubig[45a,45b], S.A. Stucci[29], B. Stugu[17], J. Stupak[128], N.A. Styles[46], D. Su[153], W. Su[60d,148,60c], X. Su[60a], N.B. Suarez[138], V.V. Sulin[111], M.J. Sullivan[91], D.M.S. Sultan[54], S. Sultansoy[4c], T. Sumida[86], S. Sun[106], X. Sun[101], C.J.E. Suster[157], M.R. Sutton[156], S. Suzuki[82], M. Svatos[140], M. Swiatlowski[168a], S.P. Swift[2], T. Swirski[177], A. Sydorenko[100], I. Sykora[28a], M. Sykora[142], T. Sykora[142], D. Ta[100], K. Tackmann[46,x], J. Taenzer[161], A. Taffard[171], R. Tafirout[168a], E. Tagiev[123], R.H.M. Taibah[135], R. Takashima[87], K. Takeda[83], T. Takeshita[150], E.P. Takeva[50], Y. Takubo[82], M. Talby[102], A.A. Talyshev[122b,122a], K.C. Tam[63b], N.M. Tamir[161], J. Tanaka[163], R. Tanaka[65], S. Tapia Araya[173], S. Tapprogge[100], A. Tarek Abouelfadl Mohamed[107], S. Tarem[160], K. Tariq[60b], G. Tarna[27b,e], G.F. Tartarelli[69a], P. Tas[142], M. Tasevsky[140], E. Tassi[41b,41a], G. Tateno[163], A. Tavares Delgado[139a], Y. Tayalati[35e], A.J. Taylor[50], G.N. Taylor[105], W. Taylor[168b], H. Teagle[91], A.S. Tee[90], R. Teixeira De Lima[153], P. Teixeira-Dias[94], H. Ten Kate[36], J.J. Teoh[120], K. Terashi[163], J. Terron[99], S. Terzo[14], M. Testa[51], R.J. Teuscher[167,aa], N. Themistokleous[50], T. Theveneaux-Pelzer[19], D.W. Thomas[94], J.P. Thomas[21], E.A. Thompson[46], P.D. Thompson[21], E. Thomson[136], E.J. Thorpe[93], V.O. Tikhomirov[111,ag], Yu.A. Tikhonov[122b,122a], S. Timoshenko[112], P. Tipton[183], S. Tisserant[102], K. Todome[23b,23a], S. Todorova-Nova[142], S. Todt[48], J. Tojo[88], S. Tokár[28a], K. Tokushuku[82], E. Tolley[127], R. Tombs[32], K.G. Tomiwa[33f], M. Tomoto[82,117], L. Tompkins[153], P. Tornambe[103], E. Torrence[131], H. Torres[48], E. Torró Pastor[174], M. Toscani[30], C. Tosciri[134], J. Toth[102,z], D.R. Tovey[149], A. Traeet[17], C.J. Treado[125], T. Trefzger[177], F. Tresoldi[156], A. Tricoli[29], I.M. Trigger[168a], S. Trincaz-Duvoid[135], D.A. Trischuk[175], W. Trischuk[167], B. Trocmé[58], A. Trofymov[65], C. Troncon[69a], F. Trovato[156], L. Truong[33c], M. Trzebinski[85], A. Trzupek[85], F. Tsai[46], P.V. Tsiareshka[108,ae], A. Tsirigotis[162,v], V. Tsiskaridze[155], E.G. Tskhadadze[159a], M. Tsopoulou[162], I.I. Tsukerman[124], V. Tsulaia[18], S. Tsuno[82], D. Tsybychev[155], Y. Tu[63b], A. Tudorache[27b], V. Tudorache[27b], A.N. Tuna[36], S. Turchikhin[80], D. Turgeman[180], I. Turk Cakir[4b,t], R.J. Turner[21], R. Turra[69a], P.M. Tuts[39], S. Tzamarias[162], E. Tzovara[100], K. Uchida[163], F. Ukegawa[169], G. Unal[36], M. Unal[11], A. Undrus[29], G. Unel[171], F.C. Ungaro[105], Y. Unno[82], K. Uno[163], J. Urban[28b], P. Urquijo[105], G. Usai[8], Z. Uysal[12d], V. Vacek[141], B. Vachon[104], K.O.H. Vadla[133], T. Vafeiadis[36], A. Vaidya[95], C. Valderanis[114], E. Valdes Santurio[45a,45b], M. Valente[168a], S. Valentinetti[23b,23a], A. Valero[174], L. Valéry[46], R.A. Vallance[21], A. Vallier[36], J.A. Valls Ferrer[174], T.R. Van Daalen[14], P. Van Gemmeren[6], S. Van Stroud[95], I. Van Vulpen[120], M. Vanadia[74a,74b], W. Vandelli[36], M. Vandenbroucke[144], E.R. Vandewall[129], D. Vannicola[73a,73b], R. Vari[73a], E.W. Varnes[7], C. Varni[55b,55a], T. Varol[158], D. Varouchas[65], K.E. Varvell[157], M.E. Vasile[27b], G.A. Vasquez[176], F. Vazeille[38], D. Vazquez Furelos[14], T. Vazquez Schroeder[36], J. Veatch[53], V. Vecchio[101], M.J. Veen[120], L.M. Veloce[167], F. Veloso[139a,139c], S. Veneziano[73a], A. Ventura[68a,68b], A. Verbytskyi[115], V. Vercesi[71a], M. Verducci[72a,72b], C.M. Vergel Infante[79], C. Vergis[24], W. Verkerke[120], A.T. Vermeulen[120], J.C. Vermeulen[120], C. Vernieri[153], P.J. Verschuuren[94], M.C. Vetterli[152,ak], N. Viaux Maira[146d], T. Vickey[149], O.E. Vickey Boeriu[149], G.H.A. Viehhauser[134], L. Vigani[61b], M. Villa[23b,23a], M. Villaplana Perez[174], E.M. Villhauer[50], E. Vilucchi[51], M.G. Vincter[34], G.S. Virdee[21], A. Vishwakarma[50], C. Vittori[23b,23a], I. Vivarelli[156], M. Vogel[182], P. Vokac[141], J. Von Ahnen[46], S.E. von Buddenbrock[33f], E. Von Toerne[24], V. Vorobel[142], K. Vorobev[112], M. Vos[174], J.H. Vossebeld[91], M. Vozak[101], N. Vranjes[16], M. Vranjes Milosavljevic[16], V. Vrba[141,*],

JHEP07(2021)167

M. Vreeswijk[120], N.K. Vu[102], R. Vuillermet[36], I. Vukotic[37], S. Wada[169], P. Wagner[24], W. Wagner[182], J. Wagner-Kuhr[114], S. Wahdan[182], H. Wahlberg[89], R. Wakasa[169], V.M. Walbrecht[115], J. Walder[143], R. Walker[114], S.D. Walker[94], W. Walkowiak[151], V. Wallangen[45a,45b], A.M. Wang[59], A.Z. Wang[181], C. Wang[60a], C. Wang[60c], H. Wang[18], H. Wang[3], J. Wang[63a], P. Wang[42], Q. Wang[128], R.-J. Wang[100], R. Wang[60a], R. Wang[6], S.M. Wang[158], W.T. Wang[60a], W. Wang[15c], W.X. Wang[60a], Y. Wang[60a], Z. Wang[106], C. Wanotayaroj[46], A. Warburton[104], C.P. Ward[32], R.J. Ward[21], N. Warrack[57], A.T. Watson[21], M.F. Watson[21], G. Watts[148], B.M. Waugh[95], A.F. Webb[11], C. Weber[29], M.S. Weber[20], S.A. Weber[34], S.M. Weber[61a], Y. Wei[134], A.R. Weidberg[134], J. Weingarten[47], M. Weirich[100], C. Weiser[52], P.S. Wells[36], T. Wenaus[29], B. Wendland[47], T. Wengler[36], S. Wenig[36], N. Wermes[24], M. Wessels[61a], T.D. Weston[20], K. Whalen[131], A.M. Wharton[90], A.S. White[106], A. White[8], M.J. White[1], D. Whiteson[171], B.W. Whitmore[90], W. Wiedenmann[181], C. Wiel[48], M. Wielers[143], N. Wieseotte[100], C. Wiglesworth[40], L.A.M. Wiik-Fuchs[52], H.G. Wilkens[36], L.J. Wilkins[94], D.M. Williams[39], H.H. Williams[136], S. Williams[32], S. Willocq[103], P.J. Windischhofer[134], I. Wingerter-Seez[5], E. Winkels[156], F. Winklmeier[131], B.T. Winter[52], M. Wittgen[153], M. Wobisch[96], A. Wolf[100], R. Wölker[134], J. Wollrath[52], M.W. Wolter[85], H. Wolters[139a,139c], V.W.S. Wong[175], A.F. Wongel[46], N.L. Woods[145], S.D. Worm[46], B.K. Wosiek[85], K.W. Woźniak[85], K. Wraight[57], S.L. Wu[181], X. Wu[54], Y. Wu[60a], J. Wuerzinger[134], T.R. Wyatt[101], B.M. Wynne[50], S. Xella[40], J. Xiang[63c], X. Xiao[106], X. Xie[60a], I. Xiotidis[156], D. Xu[15a], H. Xu[60a], H. Xu[60a], L. Xu[29], R. Xu[136], T. Xu[144], W. Xu[106], Y. Xu[15b], Z. Xu[60b], Z. Xu[153], B. Yabsley[157], S. Yacoob[33a], D.P. Yallup[95], N. Yamaguchi[88], Y. Yamaguchi[165], A. Yamamoto[82], M. Yamatani[163], T. Yamazaki[163], Y. Yamazaki[83], J. Yan[60c], Z. Yan[25], H.J. Yang[60c,60d], H.T. Yang[18], S. Yang[60a], T. Yang[63c], X. Yang[60a], X. Yang[60b,58], Y. Yang[163], Z. Yang[106,60a], W-M. Yao[18], Y.C. Yap[46], H. Ye[15c], J. Ye[42], S. Ye[29], I. Yeletskikh[80], M.R. Yexley[90], E. Yigitbasi[25], P. Yin[39], K. Yorita[179], K. Yoshihara[79], C.J.S. Young[36], C. Young[153], J. Yu[79], R. Yuan[60b,i], X. Yue[61a], M. Zaazoua[35e], B. Zabinski[85], G. Zacharis[10], E. Zaffaroni[54], J. Zahreddine[135], A.M. Zaitsev[123,af], T. Zakareishvili[159b], N. Zakharchuk[34], S. Zambito[36], D. Zanzi[36], S.V. Zeißner[47], C. Zeitnitz[182], G. Zemaityte[134], J.C. Zeng[173], O. Zenin[123], T. Ženiš[28a], D. Zerwas[65], M. Zgubič[134], B. Zhang[15c], D.F. Zhang[15b], G. Zhang[15b], J. Zhang[6], K. Zhang[15a], L. Zhang[15c], L. Zhang[60a], M. Zhang[173], R. Zhang[181], S. Zhang[106], X. Zhang[60c], X. Zhang[60b], Y. Zhang[15a,15d], Z. Zhang[63a], Z. Zhang[65], P. Zhao[49], Y. Zhao[145], Z. Zhao[60a], A. Zhemchugov[80], Z. Zheng[106], D. Zhong[173], B. Zhou[106], C. Zhou[181], H. Zhou[7], M. Zhou[155], N. Zhou[60c], Y. Zhou[7], C.G. Zhu[60b], C. Zhu[15a,15d], H.L. Zhu[60a], H. Zhu[15a], J. Zhu[106], Y. Zhu[60a], X. Zhuang[15a], K. Zhukov[111], V. Zhulanov[122b,122a], D. Zieminska[66], N.I. Zimine[80], S. Zimmermann[52,*], Z. Zinonos[115], M. Ziolkowski[151], L. Živković[16], G. Zobernig[181], A. Zoccoli[23b,23a], K. Zoch[53], T.G. Zorbas[149], R. Zou[37] and L. Zwalinski[36]

[1] *Department of Physics, University of Adelaide, Adelaide; Australia*
[2] *Physics Department, SUNY Albany, Albany NY; United States of America*
[3] *Department of Physics, University of Alberta, Edmonton AB; Canada*
[4] [(a)] *Department of Physics, Ankara University, Ankara;* [(b)] *Istanbul Aydin University, Application and Research Center for Advanced Studies, Istanbul;* [(c)] *Division of Physics, TOBB University of Economics and Technology, Ankara; Turkey*
[5] *LAPP, Univ. Savoie Mont Blanc, CNRS/IN2P3, Annecy; France*
[6] *High Energy Physics Division, Argonne National Laboratory, Argonne IL; United States of America*
[7] *Department of Physics, University of Arizona, Tucson AZ; United States of America*
[8] *Department of Physics, University of Texas at Arlington, Arlington TX; United States of America*
[9] *Physics Department, National and Kapodistrian University of Athens, Athens; Greece*
[10] *Physics Department, National Technical University of Athens, Zografou; Greece*
[11] *Department of Physics, University of Texas at Austin, Austin TX; United States of America*

JHEP07(2021)167

[12] [(a)] Bahcesehir University, Faculty of Engineering and Natural Sciences, Istanbul;[(b)] Istanbul Bilgi University, Faculty of Engineering and Natural Sciences, Istanbul;[(c)] Department of Physics, Bogazici University, Istanbul;[(d)] Department of Physics Engineering, Gaziantep University, Gaziantep; Turkey
[13] Institute of Physics, Azerbaijan Academy of Sciences, Baku; Azerbaijan
[14] Institut de Física d'Altes Energies (IFAE), Barcelona Institute of Science and Technology, Barcelona; Spain
[15] [(a)] Institute of High Energy Physics, Chinese Academy of Sciences, Beijing;[(b)] Physics Department, Tsinghua University, Beijing;[(c)] Department of Physics, Nanjing University, Nanjing;[(d)] University of Chinese Academy of Science (UCAS), Beijing; China
[16] Institute of Physics, University of Belgrade, Belgrade; Serbia
[17] Department for Physics and Technology, University of Bergen, Bergen; Norway
[18] Physics Division, Lawrence Berkeley National Laboratory and University of California, Berkeley CA; United States of America
[19] Institut für Physik, Humboldt Universität zu Berlin, Berlin; Germany
[20] Albert Einstein Center for Fundamental Physics and Laboratory for High Energy Physics, University of Bern, Bern; Switzerland
[21] School of Physics and Astronomy, University of Birmingham, Birmingham; United Kingdom
[22] [(a)] Facultad de Ciencias y Centro de Investigaciónes, Universidad Antonio Nariño, Bogotá;[(b)] Departamento de Física, Universidad Nacional de Colombia, Bogotá, Colombia; Colombia
[23] [(a)] INFN Bologna and Universita' di Bologna, Dipartimento di Fisica;[(b)] INFN Sezione di Bologna; Italy
[24] Physikalisches Institut, Universität Bonn, Bonn; Germany
[25] Department of Physics, Boston University, Boston MA; United States of America
[26] Department of Physics, Brandeis University, Waltham MA; United States of America
[27] [(a)] Transilvania University of Brasov, Brasov;[(b)] Horia Hulubei National Institute of Physics and Nuclear Engineering, Bucharest;[(c)] Department of Physics, Alexandru Ioan Cuza University of Iasi, Iasi;[(d)] National Institute for Research and Development of Isotopic and Molecular Technologies, Physics Department, Cluj-Napoca;[(e)] University Politehnica Bucharest, Bucharest;[(f)] West University in Timisoara, Timisoara; Romania
[28] [(a)] Faculty of Mathematics, Physics and Informatics, Comenius University, Bratislava;[(b)] Department of Subnuclear Physics, Institute of Experimental Physics of the Slovak Academy of Sciences, Kosice; Slovak Republic
[29] Physics Department, Brookhaven National Laboratory, Upton NY; United States of America
[30] Departamento de Física, Universidad de Buenos Aires, Buenos Aires; Argentina
[31] California State University, CA; United States of America
[32] Cavendish Laboratory, University of Cambridge, Cambridge; United Kingdom
[33] [(a)] Department of Physics, University of Cape Town, Cape Town;[(b)] iThemba Labs, Western Cape;[(c)] Department of Mechanical Engineering Science, University of Johannesburg, Johannesburg;[(d)] National Institute of Physics, University of the Philippines Diliman;[(e)] University of South Africa, Department of Physics, Pretoria;[(f)] School of Physics, University of the Witwatersrand, Johannesburg; South Africa
[34] Department of Physics, Carleton University, Ottawa ON; Canada
[35] [(a)] Faculté des Sciences Ain Chock, Réseau Universitaire de Physique des Hautes Energies - Université Hassan II, Casablanca;[(b)] Faculté des Sciences, Université Ibn-Tofail, Kénitra;[(c)] Faculté des Sciences Semlalia, Université Cadi Ayyad, LPHEA-Marrakech;[(d)] LPMR, Faculté des Sciences, Université Mohamed Premier, Oujda;[(e)] Faculté des sciences, Université Mohammed V, Rabat; Morocco
[36] CERN, Geneva; Switzerland
[37] Enrico Fermi Institute, University of Chicago, Chicago IL; United States of America
[38] LPC, Université Clermont Auvergne, CNRS/IN2P3, Clermont-Ferrand; France
[39] Nevis Laboratory, Columbia University, Irvington NY; United States of America

JHEP07(2021)167

[40] Niels Bohr Institute, University of Copenhagen, Copenhagen; Denmark
[41] [(a)] Dipartimento di Fisica, Università della Calabria, Rende;[(b)] INFN Gruppo Collegato di Cosenza, Laboratori Nazionali di Frascati; Italy
[42] Physics Department, Southern Methodist University, Dallas TX; United States of America
[43] Physics Department, University of Texas at Dallas, Richardson TX; United States of America
[44] National Centre for Scientific Research "Demokritos", Agia Paraskevi; Greece
[45] [(a)] Department of Physics, Stockholm University;[(b)] Oskar Klein Centre, Stockholm; Sweden
[46] Deutsches Elektronen-Synchrotron DESY, Hamburg and Zeuthen; Germany
[47] Lehrstuhl für Experimentelle Physik IV, Technische Universität Dortmund, Dortmund; Germany
[48] Institut für Kern- und Teilchenphysik, Technische Universität Dresden, Dresden; Germany
[49] Department of Physics, Duke University, Durham NC; United States of America
[50] SUPA - School of Physics and Astronomy, University of Edinburgh, Edinburgh; United Kingdom
[51] INFN e Laboratori Nazionali di Frascati, Frascati; Italy
[52] Physikalisches Institut, Albert-Ludwigs-Universität Freiburg, Freiburg; Germany
[53] II. Physikalisches Institut, Georg-August-Universität Göttingen, Göttingen; Germany
[54] Département de Physique Nucléaire et Corpusculaire, Université de Genève, Genève; Switzerland
[55] [(a)] Dipartimento di Fisica, Università di Genova, Genova;[(b)] INFN Sezione di Genova; Italy
[56] II. Physikalisches Institut, Justus-Liebig-Universität Giessen, Giessen; Germany
[57] SUPA - School of Physics and Astronomy, University of Glasgow, Glasgow; United Kingdom
[58] LPSC, Université Grenoble Alpes, CNRS/IN2P3, Grenoble INP, Grenoble; France
[59] Laboratory for Particle Physics and Cosmology, Harvard University, Cambridge MA; United States of America
[60] [(a)] Department of Modern Physics and State Key Laboratory of Particle Detection and Electronics, University of Science and Technology of China, Hefei;[(b)] Institute of Frontier and Interdisciplinary Science and Key Laboratory of Particle Physics and Particle Irradiation (MOE), Shandong University, Qingdao;[(c)] School of Physics and Astronomy, Shanghai Jiao Tong University, Key Laboratory for Particle Astrophysics and Cosmology (MOE), SKLPPC, Shanghai;[(d)] Tsung-Dao Lee Institute, Shanghai; China
[61] [(a)] Kirchhoff-Institut für Physik, Ruprecht-Karls-Universität Heidelberg, Heidelberg;[(b)] Physikalisches Institut, Ruprecht-Karls-Universität Heidelberg, Heidelberg; Germany
[62] Faculty of Applied Information Science, Hiroshima Institute of Technology, Hiroshima; Japan
[63] [(a)] Department of Physics, Chinese University of Hong Kong, Shatin, N.T., Hong Kong;[(b)] Department of Physics, University of Hong Kong, Hong Kong;[(c)] Department of Physics and Institute for Advanced Study, Hong Kong University of Science and Technology, Clear Water Bay, Kowloon, Hong Kong; China
[64] Department of Physics, National Tsing Hua University, Hsinchu; Taiwan
[65] IJCLab, Université Paris-Saclay, CNRS/IN2P3, 91405, Orsay; France
[66] Department of Physics, Indiana University, Bloomington IN; United States of America
[67] [(a)] INFN Gruppo Collegato di Udine, Sezione di Trieste, Udine;[(b)] ICTP, Trieste;[(c)] Dipartimento Politecnico di Ingegneria e Architettura, Università di Udine, Udine; Italy
[68] [(a)] INFN Sezione di Lecce;[(b)] Dipartimento di Matematica e Fisica, Università del Salento, Lecce; Italy
[69] [(a)] INFN Sezione di Milano;[(b)] Dipartimento di Fisica, Università di Milano, Milano; Italy
[70] [(a)] INFN Sezione di Napoli;[(b)] Dipartimento di Fisica, Università di Napoli, Napoli; Italy
[71] [(a)] INFN Sezione di Pavia;[(b)] Dipartimento di Fisica, Università di Pavia, Pavia; Italy
[72] [(a)] INFN Sezione di Pisa;[(b)] Dipartimento di Fisica E. Fermi, Università di Pisa, Pisa; Italy
[73] [(a)] INFN Sezione di Roma;[(b)] Dipartimento di Fisica, Sapienza Università di Roma, Roma; Italy
[74] [(a)] INFN Sezione di Roma Tor Vergata;[(b)] Dipartimento di Fisica, Università di Roma Tor Vergata, Roma; Italy
[75] [(a)] INFN Sezione di Roma Tre;[(b)] Dipartimento di Matematica e Fisica, Università Roma Tre, Roma; Italy
[76] [(a)] INFN-TIFPA;[(b)] Università degli Studi di Trento, Trento; Italy

JHEP07(2021)167

[77] Institut für Astro- und Teilchenphysik, Leopold-Franzens-Universität, Innsbruck; Austria
[78] University of Iowa, Iowa City IA; United States of America
[79] Department of Physics and Astronomy, Iowa State University, Ames IA; United States of America
[80] Joint Institute for Nuclear Research, Dubna; Russia
[81] [(a)] Departamento de Engenharia Elétrica, Universidade Federal de Juiz de Fora (UFJF), Juiz de Fora;[(b)] Universidade Federal do Rio De Janeiro COPPE/EE/IF, Rio de Janeiro;[(c)] Instituto de Física, Universidade de São Paulo, São Paulo; Brazil
[82] KEK, High Energy Accelerator Research Organization, Tsukuba; Japan
[83] Graduate School of Science, Kobe University, Kobe; Japan
[84] [(a)] AGH University of Science and Technology, Faculty of Physics and Applied Computer Science, Krakow;[(b)] Marian Smoluchowski Institute of Physics, Jagiellonian University, Krakow; Poland
[85] Institute of Nuclear Physics Polish Academy of Sciences, Krakow; Poland
[86] Faculty of Science, Kyoto University, Kyoto; Japan
[87] Kyoto University of Education, Kyoto; Japan
[88] Research Center for Advanced Particle Physics and Department of Physics, Kyushu University, Fukuoka; Japan
[89] Instituto de Física La Plata, Universidad Nacional de La Plata and CONICET, La Plata; Argentina
[90] Physics Department, Lancaster University, Lancaster; United Kingdom
[91] Oliver Lodge Laboratory, University of Liverpool, Liverpool; United Kingdom
[92] Department of Experimental Particle Physics, Jožef Stefan Institute and Department of Physics, University of Ljubljana, Ljubljana; Slovenia
[93] School of Physics and Astronomy, Queen Mary University of London, London; United Kingdom
[94] Department of Physics, Royal Holloway University of London, Egham; United Kingdom
[95] Department of Physics and Astronomy, University College London, London; United Kingdom
[96] Louisiana Tech University, Ruston LA; United States of America
[97] Fysiska institutionen, Lunds universitet, Lund; Sweden
[98] Centre de Calcul de l'Institut National de Physique Nucléaire et de Physique des Particules (IN2P3), Villeurbanne; France
[99] Departamento de Física Teorica C-15 and CIAFF, Universidad Autónoma de Madrid, Madrid; Spain
[100] Institut für Physik, Universität Mainz, Mainz; Germany
[101] School of Physics and Astronomy, University of Manchester, Manchester; United Kingdom
[102] CPPM, Aix-Marseille Université, CNRS/IN2P3, Marseille; France
[103] Department of Physics, University of Massachusetts, Amherst MA; United States of America
[104] Department of Physics, McGill University, Montreal QC; Canada
[105] School of Physics, University of Melbourne, Victoria; Australia
[106] Department of Physics, University of Michigan, Ann Arbor MI; United States of America
[107] Department of Physics and Astronomy, Michigan State University, East Lansing MI; United States of America
[108] B.I. Stepanov Institute of Physics, National Academy of Sciences of Belarus, Minsk; Belarus
[109] Research Institute for Nuclear Problems of Byelorussian State University, Minsk; Belarus
[110] Group of Particle Physics, University of Montreal, Montreal QC; Canada
[111] P.N. Lebedev Physical Institute of the Russian Academy of Sciences, Moscow; Russia
[112] National Research Nuclear University MEPhI, Moscow; Russia
[113] D.V. Skobeltsyn Institute of Nuclear Physics, M.V. Lomonosov Moscow State University, Moscow; Russia
[114] Fakultät für Physik, Ludwig-Maximilians-Universität München, München; Germany
[115] Max-Planck-Institut für Physik (Werner-Heisenberg-Institut), München; Germany
[116] Nagasaki Institute of Applied Science, Nagasaki; Japan
[117] Graduate School of Science and Kobayashi-Maskawa Institute, Nagoya University, Nagoya; Japan
[118] Department of Physics and Astronomy, University of New Mexico, Albuquerque NM; United States of America

JHEP07(2021)167

[119] *Institute for Mathematics, Astrophysics and Particle Physics, Radboud University/Nikhef, Nijmegen; Netherlands*
[120] *Nikhef National Institute for Subatomic Physics and University of Amsterdam, Amsterdam; Netherlands*
[121] *Department of Physics, Northern Illinois University, DeKalb IL; United States of America*
[122] [(a)] *Budker Institute of Nuclear Physics and NSU, SB RAS, Novosibirsk;* [(b)] *Novosibirsk State University Novosibirsk; Russia*
[123] *Institute for High Energy Physics of the National Research Centre Kurchatov Institute, Protvino; Russia*
[124] *Institute for Theoretical and Experimental Physics named by A.I. Alikhanov of National Research Centre "Kurchatov Institute", Moscow; Russia*
[125] *Department of Physics, New York University, New York NY; United States of America*
[126] *Ochanomizu University, Otsuka, Bunkyo-ku, Tokyo; Japan*
[127] *Ohio State University, Columbus OH; United States of America*
[128] *Homer L. Dodge Department of Physics and Astronomy, University of Oklahoma, Norman OK; United States of America*
[129] *Department of Physics, Oklahoma State University, Stillwater OK; United States of America*
[130] *Palacký University, Joint Laboratory of Optics, Olomouc; Czech Republic*
[131] *Institute for Fundamental Science, University of Oregon, Eugene, OR; United States of America*
[132] *Graduate School of Science, Osaka University, Osaka; Japan*
[133] *Department of Physics, University of Oslo, Oslo; Norway*
[134] *Department of Physics, Oxford University, Oxford; United Kingdom*
[135] *LPNHE, Sorbonne Université, Université de Paris, CNRS/IN2P3, Paris; France*
[136] *Department of Physics, University of Pennsylvania, Philadelphia PA; United States of America*
[137] *Konstantinov Nuclear Physics Institute of National Research Centre "Kurchatov Institute", PNPI, St. Petersburg; Russia*
[138] *Department of Physics and Astronomy, University of Pittsburgh, Pittsburgh PA; United States of America*
[139] [(a)] *Laboratório de Instrumentação e Física Experimental de Partículas - LIP, Lisboa;* [(b)] *Departamento de Física, Faculdade de Ciências, Universidade de Lisboa, Lisboa;* [(c)] *Departamento de Física, Universidade de Coimbra, Coimbra;* [(d)] *Centro de Física Nuclear da Universidade de Lisboa, Lisboa;* [(e)] *Departamento de Física, Universidade do Minho, Braga;* [(f)] *Departamento de Física Teórica y del Cosmos, Universidad de Granada, Granada (Spain);* [(g)] *Dep Física and CEFITEC of Faculdade de Ciências e Tecnologia, Universidade Nova de Lisboa, Caparica;* [(h)] *Instituto Superior Técnico, Universidade de Lisboa, Lisboa; Portugal*
[140] *Institute of Physics of the Czech Academy of Sciences, Prague; Czech Republic*
[141] *Czech Technical University in Prague, Prague; Czech Republic*
[142] *Charles University, Faculty of Mathematics and Physics, Prague; Czech Republic*
[143] *Particle Physics Department, Rutherford Appleton Laboratory, Didcot; United Kingdom*
[144] *IRFU, CEA, Université Paris-Saclay, Gif-sur-Yvette; France*
[145] *Santa Cruz Institute for Particle Physics, University of California Santa Cruz, Santa Cruz CA; United States of America*
[146] [(a)] *Departamento de Física, Pontificia Universidad Católica de Chile, Santiago;* [(b)] *Universidad Andres Bello, Department of Physics, Santiago;* [(c)] *Instituto de Alta Investigación, Universidad de Tarapacá, Arica;* [(d)] *Departamento de Física, Universidad Técnica Federico Santa María, Valparaíso; Chile*
[147] *Universidade Federal de São João del Rei (UFSJ), São João del Rei; Brazil*
[148] *Department of Physics, University of Washington, Seattle WA; United States of America*
[149] *Department of Physics and Astronomy, University of Sheffield, Sheffield; United Kingdom*
[150] *Department of Physics, Shinshu University, Nagano; Japan*
[151] *Department Physik, Universität Siegen, Siegen; Germany*
[152] *Department of Physics, Simon Fraser University, Burnaby BC; Canada*

JHEP07(2021)167

[153] SLAC National Accelerator Laboratory, Stanford CA; United States of America
[154] Department of Physics, Royal Institute of Technology, Stockholm; Sweden
[155] Departments of Physics and Astronomy, Stony Brook University, Stony Brook NY; United States of America
[156] Department of Physics and Astronomy, University of Sussex, Brighton; United Kingdom
[157] School of Physics, University of Sydney, Sydney; Australia
[158] Institute of Physics, Academia Sinica, Taipei; Taiwan
[159] [(a)] E. Andronikashvili Institute of Physics, Iv. Javakhishvili Tbilisi State University, Tbilisi;[(b)] High Energy Physics Institute, Tbilisi State University, Tbilisi; Georgia
[160] Department of Physics, Technion, Israel Institute of Technology, Haifa; Israel
[161] Raymond and Beverly Sackler School of Physics and Astronomy, Tel Aviv University, Tel Aviv; Israel
[162] Department of Physics, Aristotle University of Thessaloniki, Thessaloniki; Greece
[163] International Center for Elementary Particle Physics and Department of Physics, University of Tokyo, Tokyo; Japan
[164] Graduate School of Science and Technology, Tokyo Metropolitan University, Tokyo; Japan
[165] Department of Physics, Tokyo Institute of Technology, Tokyo; Japan
[166] Tomsk State University, Tomsk; Russia
[167] Department of Physics, University of Toronto, Toronto ON; Canada
[168] [(a)] TRIUMF, Vancouver BC;[(b)] Department of Physics and Astronomy, York University, Toronto ON; Canada
[169] Division of Physics and Tomonaga Center for the History of the Universe, Faculty of Pure and Applied Sciences, University of Tsukuba, Tsukuba; Japan
[170] Department of Physics and Astronomy, Tufts University, Medford MA; United States of America
[171] Department of Physics and Astronomy, University of California Irvine, Irvine CA; United States of America
[172] Department of Physics and Astronomy, University of Uppsala, Uppsala; Sweden
[173] Department of Physics, University of Illinois, Urbana IL; United States of America
[174] Instituto de Física Corpuscular (IFIC), Centro Mixto Universidad de Valencia - CSIC, Valencia; Spain
[175] Department of Physics, University of British Columbia, Vancouver BC; Canada
[176] Department of Physics and Astronomy, University of Victoria, Victoria BC; Canada
[177] Fakultät für Physik und Astronomie, Julius-Maximilians-Universität Würzburg, Würzburg; Germany
[178] Department of Physics, University of Warwick, Coventry; United Kingdom
[179] Waseda University, Tokyo; Japan
[180] Department of Particle Physics and Astrophysics, Weizmann Institute of Science, Rehovot; Israel
[181] Department of Physics, University of Wisconsin, Madison WI; United States of America
[182] Fakultät für Mathematik und Naturwissenschaften, Fachgruppe Physik, Bergische Universität Wuppertal, Wuppertal; Germany
[183] Department of Physics, Yale University, New Haven CT; United States of America

[a] Also at Borough of Manhattan Community College, City University of New York, New York NY; United States of America
[b] Also at Center for High Energy Physics, Peking University; China
[c] Also at Centro Studi e Ricerche Enrico Fermi; Italy
[d] Also at CERN, Geneva; Switzerland
[e] Also at CPPM, Aix-Marseille Université, CNRS/IN2P3, Marseille; France
[f] Also at Département de Physique Nucléaire et Corpusculaire, Université de Genève, Genève; Switzerland
[g] Also at Departament de Fisica de la Universitat Autonoma de Barcelona, Barcelona; Spain
[h] Also at Department of Financial and Management Engineering, University of the Aegean, Chios; Greece

JHEP07(2021)167

[i] Also at Department of Physics and Astronomy, Michigan State University, East Lansing MI; United States of America
[j] Also at Department of Physics and Astronomy, University of Louisville, Louisville, KY; United States of America
[k] Also at Department of Physics, Ben Gurion University of the Negev, Beer Sheva; Israel
[l] Also at Department of Physics, California State University, East Bay; United States of America
[m] Also at Department of Physics, California State University, Fresno; United States of America
[n] Also at Department of Physics, California State University, Sacramento; United States of America
[o] Also at Department of Physics, King's College London, London; United Kingdom
[p] Also at Department of Physics, St. Petersburg State Polytechnical University, St. Petersburg; Russia
[q] Also at Department of Physics, University of Fribourg, Fribourg; Switzerland
[r] Also at Dipartimento di Matematica, Informatica e Fisica, Università di Udine, Udine; Italy
[s] Also at Faculty of Physics, M.V. Lomonosov Moscow State University, Moscow; Russia
[t] Also at Giresun University, Faculty of Engineering, Giresun; Turkey
[u] Also at Graduate School of Science, Osaka University, Osaka; Japan
[v] Also at Hellenic Open University, Patras; Greece
[w] Also at Institucio Catalana de Recerca i Estudis Avancats, ICREA, Barcelona; Spain
[x] Also at Institut für Experimentalphysik, Universität Hamburg, Hamburg; Germany
[y] Also at Institute for Nuclear Research and Nuclear Energy (INRNE) of the Bulgarian Academy of Sciences, Sofia; Bulgaria
[z] Also at Institute for Particle and Nuclear Physics, Wigner Research Centre for Physics, Budapest; Hungary
[aa] Also at Institute of Particle Physics (IPP); Canada
[ab] Also at Institute of Physics, Azerbaijan Academy of Sciences, Baku; Azerbaijan
[ac] Also at Instituto de Fisica Teorica, IFT-UAM/CSIC, Madrid; Spain
[ad] Also at Istanbul University, Dept. of Physics, Istanbul; Turkey
[ae] Also at Joint Institute for Nuclear Research, Dubna; Russia
[af] Also at Moscow Institute of Physics and Technology State University, Dolgoprudny; Russia
[ag] Also at National Research Nuclear University MEPhI, Moscow; Russia
[ah] Also at Physics Department, An-Najah National University, Nablus; Palestine
[ai] Also at Physikalisches Institut, Albert-Ludwigs-Universität Freiburg, Freiburg; Germany
[aj] Also at The City College of New York, New York NY; United States of America
[ak] Also at TRIUMF, Vancouver BC; Canada
[al] Also at Universita di Napoli Parthenope, Napoli; Italy
[am] Also at University of Chinese Academy of Sciences (UCAS), Beijing; China
[*] Deceased

JHEP07(2021)167